ENERGY LABORATORY

MASSACHUSETTS INSTITUTE
OF TECHNOLOGY

OPTIMIZATION OF THE AXIAL POWER SHAPE IN PRESSURIZED WATER REACTORS

by
M.A. Malik
A. Kamal
M.J. Driscoll
D.D. Lanning

DOE Contract No. DE-AC02-79ET34022 (Nuclear Engineering Department Report No. MITNE-247, Energy Laboratory Report MIT-EL-81-037), November, 1981

DOE/ET/34022-2
MITNE-247
MIT-EL-81-037

OPTIMIZATION OF THE AXIAL POWER SHAPE IN PRESSURIZED WATER REACTORS

by
M.A. Malik
A. Kamal
M.J. Driscoll
D.D. Lanning

DOE Contract No. DE-AC02-79ET34022 (Nuclear Engineering Department Report No. MITNE-247, Energy Laboratory Report MIT-EL-81-037), November, 1981

DOE/ET/34022-2

OPTIMIZATION OF THE AXIAL POWER SHAPE IN PRESSURIZED WATER REACTORS

by

M.A. Malik
A. Kamal
M.J. Driscoll
D.D. Lanning

A Principal Topical Report for FY 1981

Department of Nuclear Engineering
and
Energy Laboratory
MASSACHUSETTS INSTITUTE OF TECHNOLOGY
Cambridge, Massachusetts 02139

Sponsored by

U.S. Department of Energy
Division of Energy Technology
Under Contract No. DE-AC02-79ET34022

NOTICE

Printed in the United States of America

Available from

National Technical Information Service
U.S. Department of Commerce
5285 Port Royal Road
Springfield, VA 22152

Distribution

R. Crowther
Project Manager
General Electric Company
175 Curtner Company
San Jose, California 95125

Dr. Peter M. Lang, Chief
LWR Branch
Division of Nuclear Power Development
US Dept. of Energy, Mail Stop B-107
Washington, D.C. 20545 (5 copies)

N.L. Shapiro
Manager, Advanced Design Projects
Combustion Engineering, Inc.
1000 Prospect Hill Road
Windsor, CT 06095

W.L. Orr
Manager of Product Development Support
Nuclear Fuel Division
Westinghouse Electric Corp.
P.O. Box 355
Pittsburgh, PA 15230

Dr. Richard B. Stout
Nuclear Fuels Engineering Dept.
Exxon Nuclear
2101 Horn Rapids Road
Richland, WA 99352

V. Uotinen
Project Manager
The Babcock & Wilcox Co.
P.O. Box 1260
Lynchburg, VA 24505

ABSTRACT

Analytical and numerical methods have been applied to find the optimum axial power profile in a PWR with respect to uranium utilization. The preferred shape was found to have a large central region of uniform power density, with a roughly cosinusoidal profile near the ends of the assembly. Reactivity and fissile enrichment distributions which yield the optimum profile were determined, and a 3-region design was developed which gives essentially the same power profile as the continuously varying optimum composition.

State of the art computational methods, LEOPARD and PDQ-7, were used to evaluate the beginning-of-life and burnup history behavior of a series of three-zone assembly designs, all of which had a large central zone followed by a shorter region of higher enrichment, and with a still thinner blanket of depleted uranium fuel pellets at the outer periphery. It was found that if annular fuel pellets were used in the higher enrichment zone, a design was created which not only had the best uranium savings (2.8% more energy from the same amount of natural uranium, compared to a conventional, uniform, unblanketed design), but also had a power shape with a lower peak-to-average power ratio (by 16.5%) than the reference case, and which held its power shape very nearly constant over life. This contrasted with the designs without part length annular fuel, which tended to burn into an end-peaked power distribution, and with blanket-only designs, which had a poorer peak-to-average power ratio than the reference unblanketed case.

ACKNOWLEDGEMENTS

The work presented in this report has been performed primarily by the principal author, Mushtaq A. Malik, who has submitted substantially the same report in partial fulfillment of the requirements for the S.M. degree in Nuclear Engineering at M.I.T.

The present work was supported by a Department of Energy (DOE) contract administered through the M.I.T. Energy Laboratory. Computer calculations were carried out at the M.I.T. Information Processing Center and the Laboratory for Nuclear Science.

TABLE OF CONTENTS

TABLE OF CONTENTS (continued)

TABLE OF CONTENTS (continued)

LIST OF FIGURES

LIST OF FIGURES (continued)

LIST OF TABLES

Chapter 1

INTRODUCTION

1.1 Foreword

The majority of nuclear reactors in operation and under construction in the United States and worldwide are light water reactors (LWRs). These reactors have been developed to an advanced state as a result of many years of experience and commercial competition. At present LWRs operate on the once through uranium cycle, although it was originally envisioned that they would be employed in a recycle mode in which plutonium and residual uranium would be recovered through reprocessing and recycled to reduce the requirements for mined uranium and separative work. This strategy was felt to be a natural precursor to the development and eventual deployment of fast breeder reactors. An initial source of breeder fuel would then be available in the form of plutonium recovered from LWRs.

In late 1976 an administrative decision to defer the commercial use of plutonium as power reactor fuel in the United States was announced. This in turn provided the incentive to perform an evaluation of the improvement in uranium utilization which can be obtained by incorporating various design modifications in the current generation of LWRs operating in a once-through fueling mode. During the past four years a wide range of design and fuel modifications have been identified and analyzed by a broadly based group of researchers worldwide (I-1, N-1). Methods investigated at M.I.T. are summarized in Table 1.1.

Of particular interest here is the use of axial blankets

and axial power shaping in pressurized water reactors (PWRs), one reason being that in the post-INFCE era when reinstitution of the commitment to LWR recycle appears imminent, this modification should be an equally attractive means to conserve uranium in the recycle mode

1.2 Background and Previous Work

Fuel utilization is very sensitive to neutron losses. In a LWR the combination of axial and radial leakage can account for as much as five percent of total neutron production. Accordingly some years ago, the use of axial blankets was proposed to reduce leakage in BWRs. The benefits of this modification were subsequently demonstrated and axial blankets have now been incorporated in newer BWR core designs

It is only lately, however, that comparable attention has been focussed on the PWR. The simplest realization of the axial blanket involves replacing the top and bottom of the enriched fuel column with low enriched pellets while increasing the U-235 enrichment in the central pellets in the fuel column. This repositioning of the initial fissile inventory decreases the neutron leakage and increases power in the central portion of the fuel rod

TABLE 1.1

Selected Results for Uranium Conservation Tactics

For PWRs on a Once-Through Fuel Cycle

	OPTION	$^{nat}U_3O_8$ SAVINGS	COMMENT
1.	Increasing burnup and number of batches	∿15%	5 batch core, B = 50,000 MWD/MT
2.	Radial blankets of natural uranium	≤0	Spent fuel is a better blanket
3.	Thorium additions to fixed lattice	≤0	Small savings might be possible if reconstitution is practicable
4.	Axial blankets of depleted uranium	∿2%	Axial power peaking limits this option
5.	Low-leakage fuel management	∿3%	Burnable poison probably needed to hold down fresh fuel
6.	Re-optimizing lattice H/U	∿2%	For high burnup cores, very design specific
7.	Continuous mechanical spectral shift	10-15%	Impractical from an engineering standpoint?
8.	End-of-cycle pin pulling and bundle reconstitution	≤0	Hypothesized savings tend to vanish in consistent comparisons
9.	Mid-cycle pin pulling and bundle reconstitution	∿10%	Probably uneconomical due to extra refueling shutdown; potential T/H problems
10.	Using quarter-size fuel assemblies	0.7%	Savings may be larger if full advantage of fuel management flexibility is taken; costs may outweigh savings
11.	Optimum power shaping using burnable poison	1-4%	Some ambiguity in such comparisons because acceptable reload patterns may differ; quantification of residual poison penalties is important
12.	Annular fuel	∿0	No inherent neutronic advantages; may facilitate other options
13.	Routine pre-planned coastdown for economic optimum interval	∿7%	Results are sensitive to capacity factor during normal operation and coastdown; savings can be doubled by coastdown to economic breakeven

Previous work at M.I.T. (F-1, K-1, S-1), and by many others elsewhere (M-3, C-5, R-2), indicated that improvements in axial fuel management could result in ore savings in LWRs. An analysis by the Babcock and Wilcox Company (H-4) indicates that uranium utilization improvements of up to 4% can be achieved using 9-inch natural uranium blankets at both ends of the core. Since the power density in the blanket region is lower than it would be in the fuel it displaces in an unblanketed core, the power density of the enriched fuel region must increase. This axial power peaking increase, inherent with retrofittable axial blanket designs, reduces the core DNBR and other thermal margins. For example, the beginning of life axial peak power was found to increase by 12.5% for a 10-inch natural uranium blanket design, and this power increase translated into a 22% reduction in DNBR (H-4), which may have adverse effects on the safety analysis of those events which are strongly dependent on local power density.

These circumstances naturally lead one to inquire whether there are ways to alleviate the power peaking problem while retaining the advantage of blanketing the core; and, more generally, to answer the question as to what axial distribution of fuel enrichment is optimal with respect to uranium utilization.

1.3 Research Objectives

The use of natural or depleted uranium blankets improves uranium utilization by making more efficient use of neutrons which would otherwise leak from the core, but this improvement is achieved at the expense of increased axial power peaking. One obvious technique to reduce the power peak is axial enrichment zoning. Reduction of power peaking in this manner has the potential for improving core operating margins, which in turn can be traded off to realize further ore savings. Thus the main objective of the present work has been to improve axial power shaping in blanketed PWR cores. The program established in pursuit of this general objective had the following specific subtasks:

1. Determination of an optimum power shape through analytical methods.
2. Determination of reactivity and enrichment profiles which would give this optimum power shape.
3. Investigation of enrichment zones at beginning-of-cycle which will give this target reactivity profile.
4. Verification of the suitability of candidate zoning over assembly burnup lifetime using the PDQ-7 depletion code, and finally,
5. Investigation of the use of an annular fuel region to remedy some of the shortcomings evidenced in the preceding stages.

1.4 Organization of this Report

The work reported here is organized as follows.

Chapter Two provides an outline of various computer codes and analytical models used in this research. A simple algorithm developed to determine the optimum power profile is described.

In Chapter Three the reference case is analyzed: an assembly typical of current unblanketed PWRs. This case will then serve as the basis for comparison with all subsequent modifications. Various axially-zoned cases are described and analyzed. Test case depletion results are compared with the reference case.

In Chapter Four the enrichment zone configuration is improved by using annular fuel. Thermal margins and ore requirements of these cases, relative to the reference case, are reported and discussed.

Finally, in Chapter Five, the present work is summarized, the main conclusions are presented and recommendations for future work are made.

Various appendices follow to provide detail supporting the work reported in the main text.

CHAPTER 2

ANALYTICAL AND NUMERICAL METHODS

2.1 Introduction

The design and analysis of a nuclear reactor requires the accurate determination of reaction rates and isotopic distributions at different locations in the reactor throughout its operating life. The development of increasingly sophisticated and powerful computer programs has simplified the exceedingly complex problems which arise as a result of the dependence of nuclear cross sections on material compositions, dimensions, temperatures and thermal-hydraulic parameters.

Diffusion-depletion programs are often used to obtain the neutron flux and material distributions in a reactor as a function of time. The calculations are typically performed in two steps. First, the neutron flux distribution for neutrons in several energy groups is obtained at discrete spatial mesh points in the reactor. The spatial flux is combined with the material inventory and nuclear cross sections to obtain the power distribution. Once the spatial fluxes and power distributions are found, the next step is to simulate reactor operation during a specified time interval. Using the power, normalized flux and spectrum-averaged cross sections from the spatial calculation, the differential equations describing the time behavior of the nuclide concentrations are solved for the time interval. The solution

yields a new distribution of nuclide concentrations in the reactor, which are then used in the generation of few group macroscopic cross sections for the next spatial calculation.

The computer programs used in this present research have been tested and used by national laboratories, vendors, and utilities for fuel management analysis (A-1). A brief description of these codes will be given in this chapter.

Since computational time and cost constraints set practical limits on the number of solutions which can be investigated (and since a pure trial and error approach might overlook a conceptually better configuration), instead of computer codes, simple analytical models were used to search for an optimum power profile. Necessary details of these simple models are also included in this chapter.

2.2 Computer Codes Used

The present work relied mainly on the LEOPARD, CHIMP and PDQ-7 codes. In the sections which follow, brief descriptions of these codes are given. A general discussion of computer methods for reactor analysis is given in reference (A-2). This reference describes each of these codes in more detail, and it also describes other codes which perform the same functions. Detailed manuals for each code are also referenced, in which instructions for implementation can be found.

2.2.1 The LEOPARD code

The LEOPARD (B-1) program develops few (2 or 4) group constants for LWR unit cells or supercells (cell plus extra region) using MUFT (B-2) as a subprogram in the fast region (above 0.625 ev) and SOFOCATE (A-3) as a subprogram in the thermal region. In addition, the code can make a point depletion calculation, recomputing the spectrum before each discrete burnup step.

The EPRI version of LEOPARD was used in the present work. Its microscopic cross section library was derived from the Evaluated Nuclear Data File version B-IV (ENDF/B-IV) using the SPOTS code (B-1). The ETOM and FLANGE programs process this basic data into the multigroup master data required by MUFT (54 groups) and SOFOCATE (172 groups).

MUFT solves the one-dimensional steady state transport equation assuming only linear anisotropic scattering (the P1 approximation), approximating the spatial dependence by a single spatial mode expressed in terms of an equivalent bare core buckling B^2 (the B1 approximation), treating elastic scattering by a continuous slowing down model (Greuling-Goertzel Model) and inelastic scattering by means of a multigroup transfer matrix. Cross sections for the heavy nuclides at resonance energies are treated by assuming only hydrogen moderation, with no Doppler correction. SOFOCATE handles the thermal region using the buckling treatment to characterize leakage, the P1 approximation, and the Wigner-

Wilkins (proton gas) spectral methodology. This model yields the correct 1/E behavior at high energies and accounts for absorption heating and leakage cooling effects, and also for flux depression at thermal resonances. Both MUFT and SOFOCATE execute homogeneous unit cell calculations. This approximation is not valid when the dimensions of the unit cell are greater than the mean free path of the neutrons. Thus heterogeneity is introduced through the use of fast advantage factors, thermal disadvantage factors and an iteratively adjusted resonance self shielding factor. The fast advantage factor correction is made through application of a prescription derived by collision probability analysis. The thermal disadvantage factor is calculated for each thermal group using the well-known ABH method.

One option of the LEOPARD code utilizes the mixed number density (MND) thermal activation model (B-4). This model uses a boundary condition of neutron activation continuity rather than flux continuity over an energy interval. The MND boundary condition corrects for the discontinuity in thermal reaction rates due to a discontinuity in microscopic cross sections at material interfaces.

The extra region is used only when performing super-cell calculations. Its function is to take into account structural materials, control rod sheaths, water gaps between assemblies, etc. The input supplied by the user consists of lattice dimensions, the composition of each region, fuel,

moderator and clad temperatures (used in calculating the Doppler contribution to the U-238 resonance integral, the power, the heavy metal loading, the volume, the burnup steps and control poison concentrations.

LEOPARD also performs zero dimensional depletion calculations. Core spatial effects are neglected, but the user may input a buckling value to account for leakage. The spectrum is calculated at the beginning of each depletion time step; the spectrum-averaged cross section and group fluxes are then used to solve the depletion equation (which determines the new isotopic concentrations). This process is repeated for all time steps.

2.2.2. The CHIMP code

The CHIMP code was developed by Yankee Atomic Electric Company to handle the large amount of data manipulation involved in linking LEOPARD to other neutronic codes. The large number of flux weighted microscopic cross sections produced by LEOPARD at each time step are processed by the CHIMP code to prepare microscopic and macroscopic tables for the fueled region of PDQ-7. The isotopes whose cross sections are fairly invariant with burnup are assigned to "master table sets" while the rest are included in "interpolating table sets."

The basic input for CHIMP is punched data from LEOPARD. (When running LEOPARD, the user has the option to obtain either punched volume-weighted number densities, super-cell

macroscopic cross sections, microscopic cross sections, or any combination depending upon the option chosen in columns 30 and 33 of the LEOPARD option card.)

2.2.3 The PDQ code

The "PDQ" package includes both PDQ-7 and HARMONY. PDQ-7 solves the few group diffusion equations, and HARMONY performs the depletion calculation using an interpolation scheme to account for cross section variation.

The PDQ code can solve the diffusion-depletion problem in one, two or three dimensions for rectangular, cylindrical, spherical and hexagonal geometries. Up to five neutron energy groups can be handled by this program. Zero current or zero flux boundary conditions are admissible.

PDQ-7 solves the multigroup diffusion equation by discretizing the energy and spatial variables. The one-dimensional group equations are solved by Gauss elimination, and the two-dimensional group equations are solved by using a single line cyclic Chebyshev semi-iterative technique. The cross section data manipulation and the depletion calculations utilize the HARMONY part of PDQ. The depletion equations to be solved are specified by the user and the cross section tables are obtained from the LEOPARD code after being processed by the CHIMP code. The neutron flux used in the solution of the depletion equations is normalized to a specified power level at the beginning of the time interval.

The dependence of the cross sections on nuclide concentration is dealt with through the use of interpolating tables by fitting LEOPARD output to a polynomial of specified order. At the end of each depletion time step, PDQ-7 solves for the spatial flux shape, and these values of the flux are used in the following time step. Options for point and block depletion are available.

2.3 Analytical Models

Nuclear fuel management problems are greatly simplified by judicious approximations which permit the development of equations that quantitatively describe the relationships that exist between system variables or parameters. This section is concerned with the simple analytical models used in the course of the present work.

2.3.1 The linear reactivity model (S-1)

The basic assumption of this model is that reactivity, ρ, is a linear function of burnup, B, that is:

$$\rho = \rho_o - AB \qquad (2.1)$$

where ρ_o is the initial reactivity of undepleted fuel at full power and A is the slope of the reactivity vs. burnup curve.

It is worth noting that reactivity, $\rho = \frac{k-1}{k}$, as a function of burnup is more linear than is the effective multiplication factor, k. We can therefore write a linear relation between reactivity and burnup at each point:

$$\rho(z) = \rho_o(z) - AB(z) \tag{2.2}$$

The local and average burnup are related by

$$B(z) = 2b\bar{B}f(z) , \tag{2.3}$$

where $f(z) \equiv$ relative power per unit length (which is assumed to be directly proportional to the neutron source strength); subjected to the normalization:

$$\int_{-b}^{b} f(z)dz = 1.0 \tag{2.4}$$

Following Reference (S-1), power weighting is applied to find system reactivity, which is equated to leakage reactivity at end-of-cycle. Hence

$$\rho_L = \bar{\rho}_o - 2bAB \int_{-b}^{b} f^2(z)dz \tag{2.5}$$

In this relation the initial reactivity is:

$$\bar{\rho}_o = \int_{-b}^{b} f(z)\rho_o(z)dz \tag{2.6}$$

Solving for average assembly burnup,

$$\bar{B} = \frac{\bar{\rho}_o - \rho_L}{2bA \int_{-b}^{b} f^2(z)dz} \tag{2.7}$$

This equation will serve to define the objective function, $\overline{B}$, in an optimization process which will be described in the sections which follow.

2.3.2 Group and one-half model

Two group theory requires the solution of the following coupled differential equations:

fast group (above ~ 0.6 ev)

$$-D_1\nabla^2\phi_1 + \Sigma_{a1}\phi_1 + \Sigma_{12}\phi_2 - \frac{1}{k}(\nu\Sigma_{f1}\phi_1 + \nu\Sigma_{f2}\phi_2) = 0 \qquad (2.8)$$

leakage | absorption | down-scatter | fission source

thermal group

$$-D_2\nabla^2\phi_2 + \Sigma_{a2}\phi_2 - \Sigma_{12}\phi_1 = 0 \qquad (2.9)$$

leakage | absorption | in-scatter

In the above equations Σ_{12} is the macroscopic down-scatter cross section from group one to group two.

The group and one-half model, in which thermal leakage is neglected ($\nabla^2\phi_2 = 0$) is a good approximation, since thermal leakage is an order of magnitude smaller than fast leakage. With this approximation the two equations can be condensed into a single equation in the fast flux, which is considerably easier to solve.

In a two group formulation, the thermal power in a region can be written as

$$q = \kappa\Sigma_{f1}\phi_1 + \kappa\Sigma_{f2}\phi_2 \tag{2.10}$$

where κ is the energy released per fission.

Using the group and one-half model approximation $\Sigma_{12}\phi_1 = \Sigma_{a2}\phi_2$, and Eq.(2.10),

$$q = \kappa \left[\Sigma_{f1} + \frac{\Sigma_{f2}\Sigma_{12}}{\Sigma_{a2}}\right] \phi_1 \tag{2.11}$$

The two group value of k_∞ is

$$k_\infty = \frac{\nu\Sigma_{f1}}{\Sigma_{a1} + \Sigma_{12}} + \frac{\Sigma_{12}}{\Sigma_{a1} + \Sigma_{12}} \frac{\nu\Sigma_{f2}}{\Sigma_{a2}} \tag{2.12}$$

Thus the power can be written as

$$q = \frac{\kappa}{\nu} (\Sigma_{a1} + \Sigma_{12}) k_\infty\phi_1 \tag{2.13}$$

Assuming that $\frac{\kappa}{\nu} (\Sigma_{a1} + \Sigma_{12})$ is constant it follows that

$$f(z) \propto q(z) \propto k_\infty\phi_1(z) , \tag{2.14}$$

and using

$$k_\infty = \frac{1}{1-\rho} , \tag{2.15}$$

one finds:

$$f(z) \propto \frac{\phi_1(z)}{1 - \rho(z)} \tag{2.16}$$

This is one prescription which will be put to good use shortly in the determination of an enrichment profile consistent with an optimum power profile.

2.4 Optimum Power Profile

Discharge burnup is a function of the axial power profile through Eq.(2.7). If it were not for leakage, $\bar{B}$ would be maximized by making f(z) uniform over the entire length of a fuel assembly. In the presence of leakage, however, reduced power near the periphery would be preferable. Thus there is an inherent trade-off which leads to an optimum f(z). To determine this shape an analytical expression is required for the leakage, namely,

$$\rho_L = \int_{-b}^{b} f(z)J(z)dz \tag{2.17}$$

where J(z) is the fraction of neutrons born at z which leak out of either end of the assembly.

Using a one-group diffusion kernel:

$$J(z) = \frac{1}{2}\left[e^{-(b-z)/M} + e^{-(b+z)/M}\right] \tag{2.18}$$

in which M ≡ migration length (≃ 7.5 cm in a PWR).

A small computer program has been written to implement Eq.(2.7) and to find the best f(z) by an iterative process. Figure 2.1 displays a flow chart of this iterative methodology. The core is divided into a number of evenly distributed mesh points in the axial direction. A flat power profile is used as the initial input, and after making a local change in the power profile the global effect on burnup is noted for each mesh point. In the next step the profile is modified at each point according to the corresponding partial changes computed in the previous step. This process is repeated until no further increase in discharge burnup is found. An optimum power profile determined in this manner is shown in Figure 2.2. Note the large flat central zone and the roughly cosinusoidal decrease at the end of the core. The burnup for this optimum shape is 15.5% greater than the burnup associated with a cosine power shape, and 3.6% higher than the burnup generated by a flat power shape. The listing of the program and a sample output are included in Appendix A.

The next step is to determine reactivity and enrichment profiles which would give this optimum power shape. For this purpose the fast flux kernel is used to compute the fast flux shape:

$$\phi_1(z) = \lambda \int_{-b}^{b} G(z|\xi)\ f(\xi)d\xi \qquad (2.19)$$

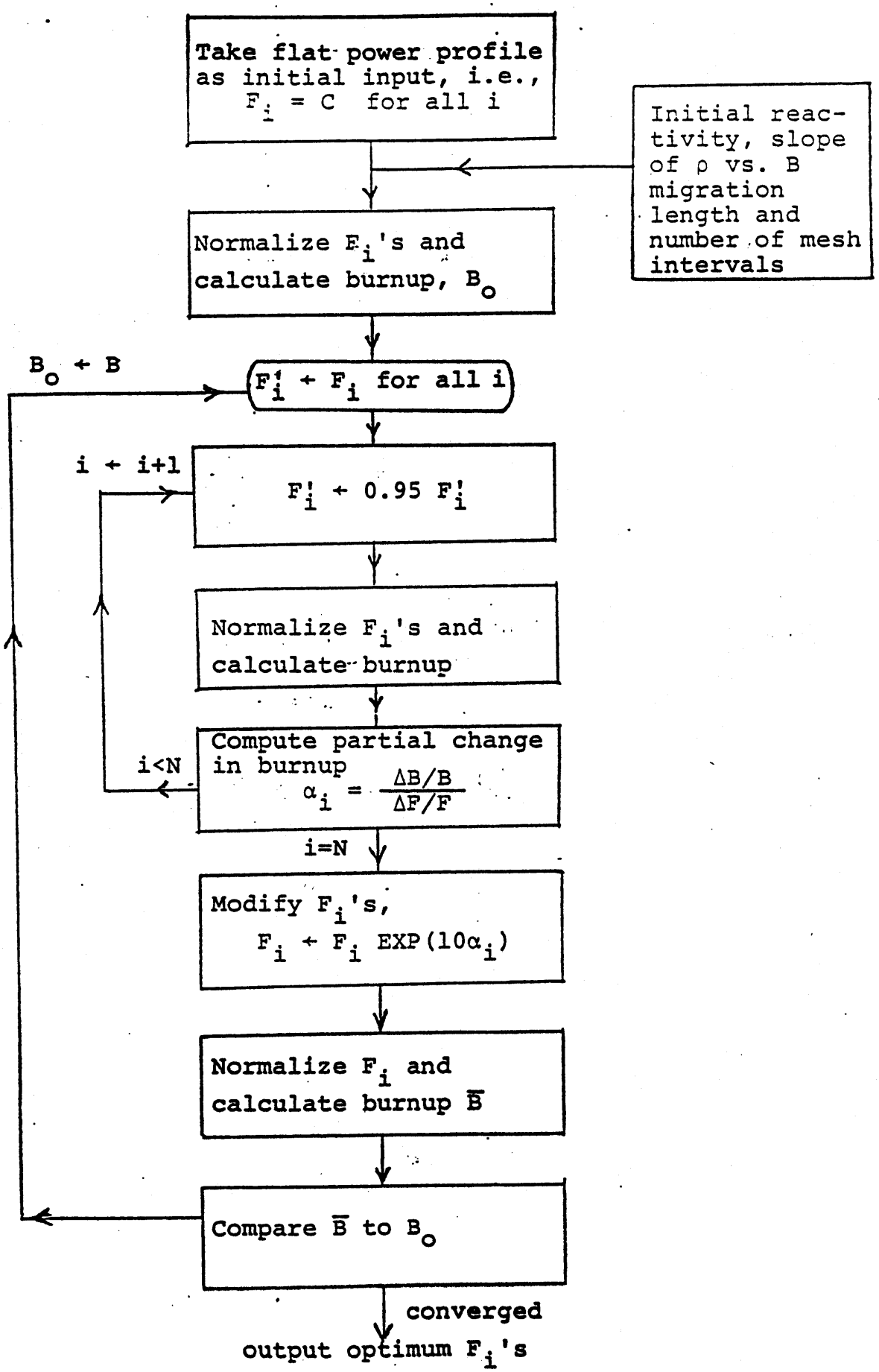

Figure 2.1 Flowchart for Computer Code Methodology

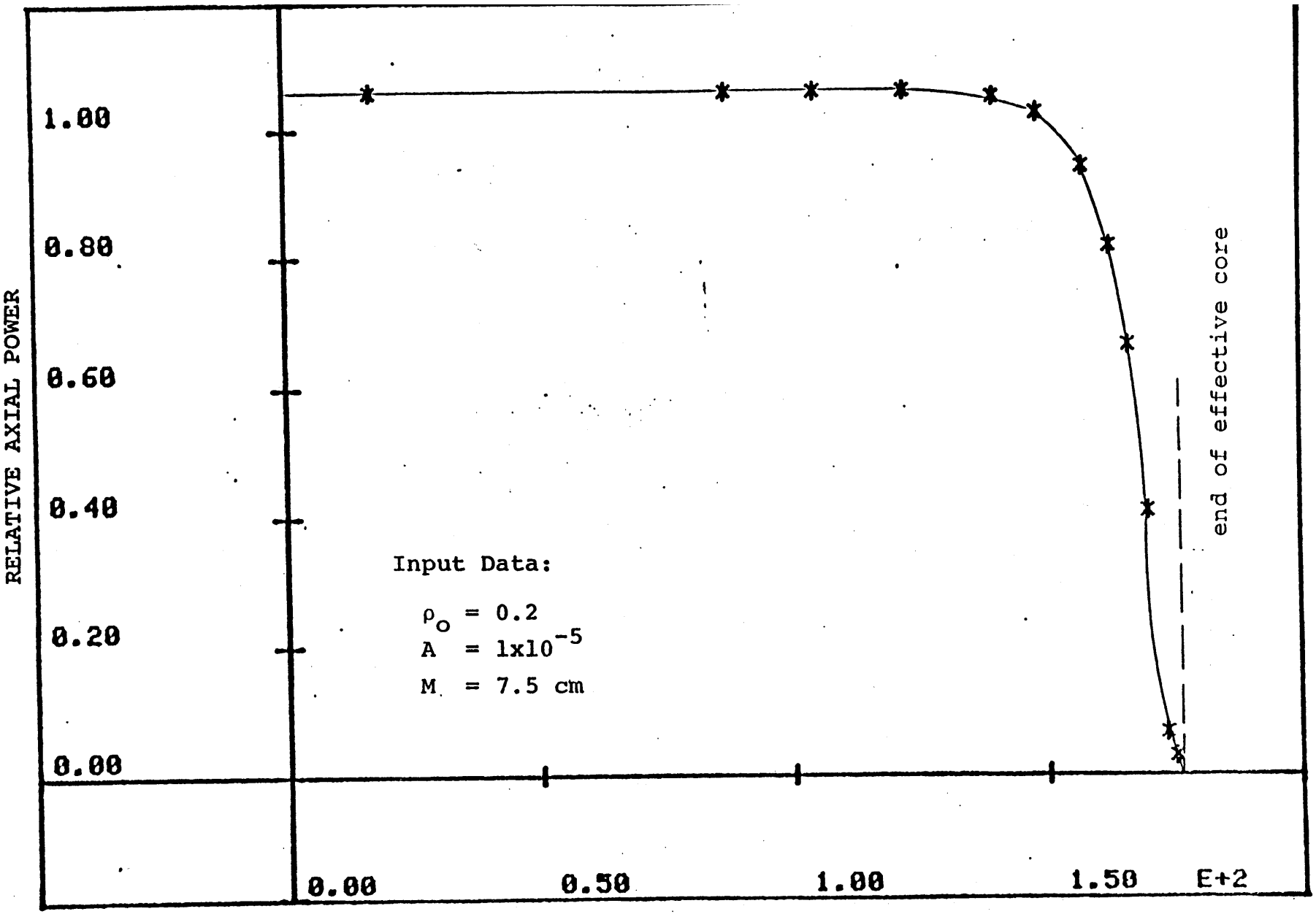

Figure 2.2 Optimum Axial Power Profile

in which

$$G(z|\xi) = \frac{M}{2D} e^{-|z-\xi|/M} \tag{2.20}$$

is a fast flux kernel and gives the flux at z per unit source at ξ. Using this fast flux in the "group and one-half model" result, Eq.(2.16), $\rho(z)$, the reactivity profile, has been found.

Finally, reactivity and enrichment are approximately linearly related:

$$\rho(z) \simeq 0.1 \left[X(z) - 1\right] \tag{2.21}$$

which gives the corresponding optimum enrichment profile. Optimum reactivity and enrichment profiles are shown in Figure 2.3. The enrichment profile shows that in the central region (more than 75% of the axial length of the fuel assembly) a uniform enrichment is needed, but in the rest of the region, near the periphery, a continuously varying distribution of fissile material is required. Thus an optimum shape can be achieved asymptotically as the number of core regions of different enrichment is increased. But, in fact, from an analytical example discussed in the following section it will become clear that only a few zones of different enrichment can give a solution very close to the optimum solution.

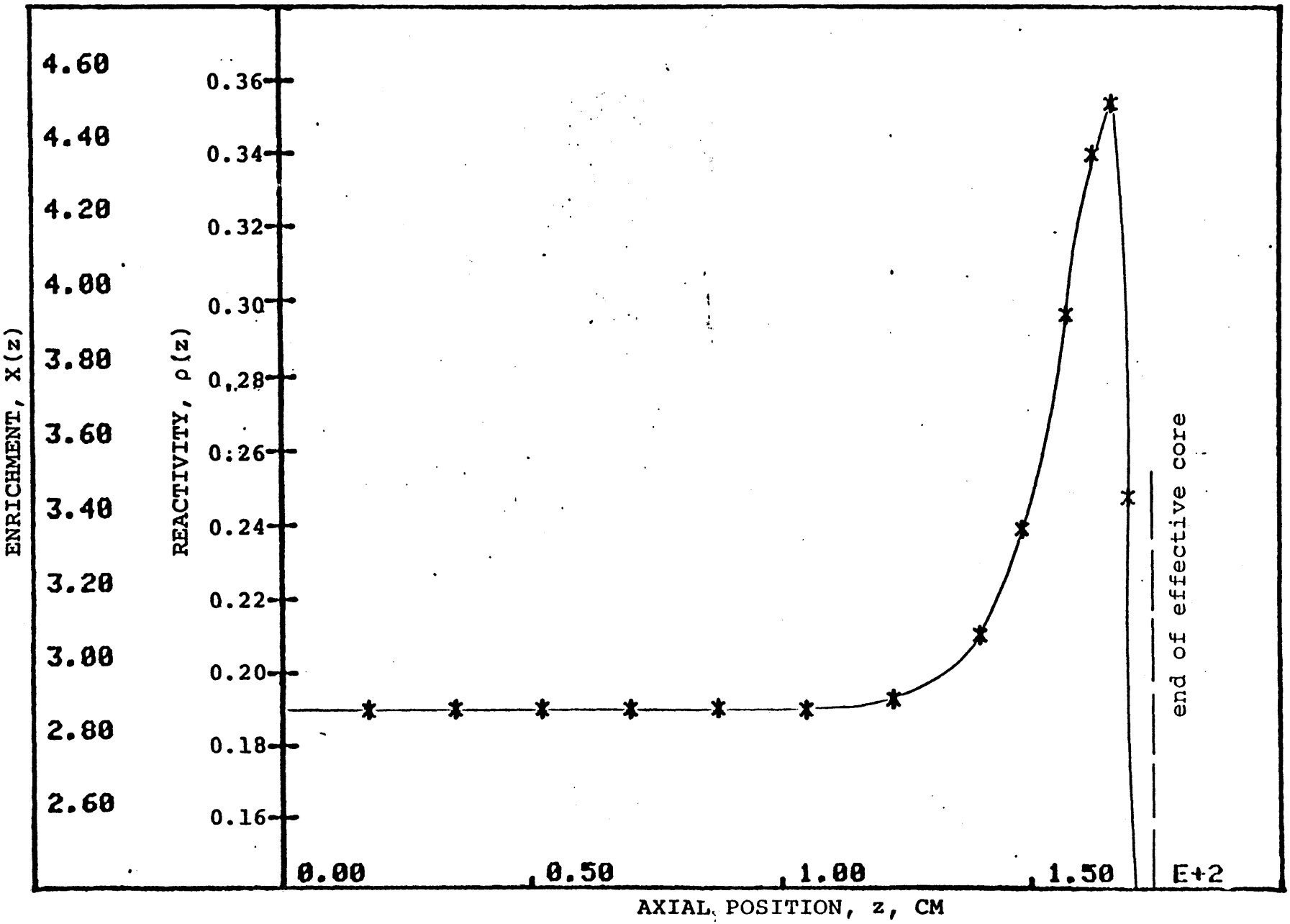

Figure 2.3 Reactivity and Enrichment Profiles Corresponding to an Optimum Power Profile

2.5 Analytical Example

By substituting uniform and cosine power shapes into Eq.(2.17), it can be shown that the leakage generated by the cosine power shape is almost a factor of ten less than that associated with a uniform power shape (see Table 2.1). But since the minimization of leakage, ρ_L, conflicts with the minimization of the axial power profile index, $\int_{-b}^{b} f^2(z)dz$, the pure cosine shape is not optimum with respect to burnup. Examination of the kernel equation, Eq.(2.18), indicates that the leakage effect is most prominent in the last few migration lengths; that is, most of the neutron loss originates in fuel regions within two or three migration lengths of the periphery. Following this line of reasoning, a flat power profile having a cosine shape near the ends was examined, as shown in Figure 2.4.

The optimum value of 'a,' the length of the region having a cosine shape, was found by substituting this shape into Eq.(2.17) and Eq.(2.7). For representative parameters the value of 'a' was found to be 23 cm, giving a burnup only 0.017% less than the value using the "exact" optimum power profile found numerically. Important features of this example have been shown in Table 2.2, and further details are presented in Appendix B. The optimum power profile found numerically and the optimum case of this analytical example are compared in Figure 2.5.

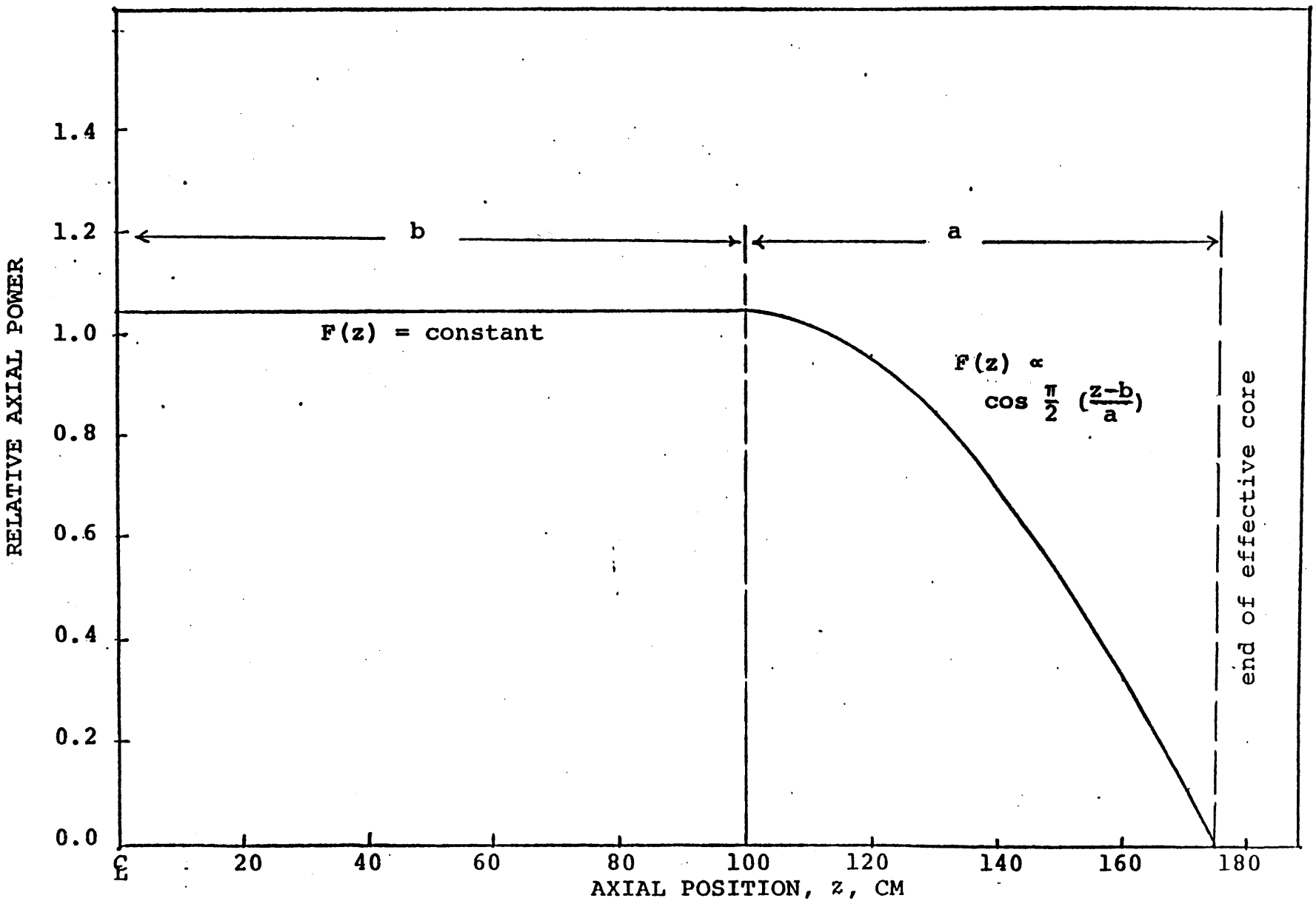

Figure 2.4 Flat Power Profile Having Cosine Shape Near Its Ends

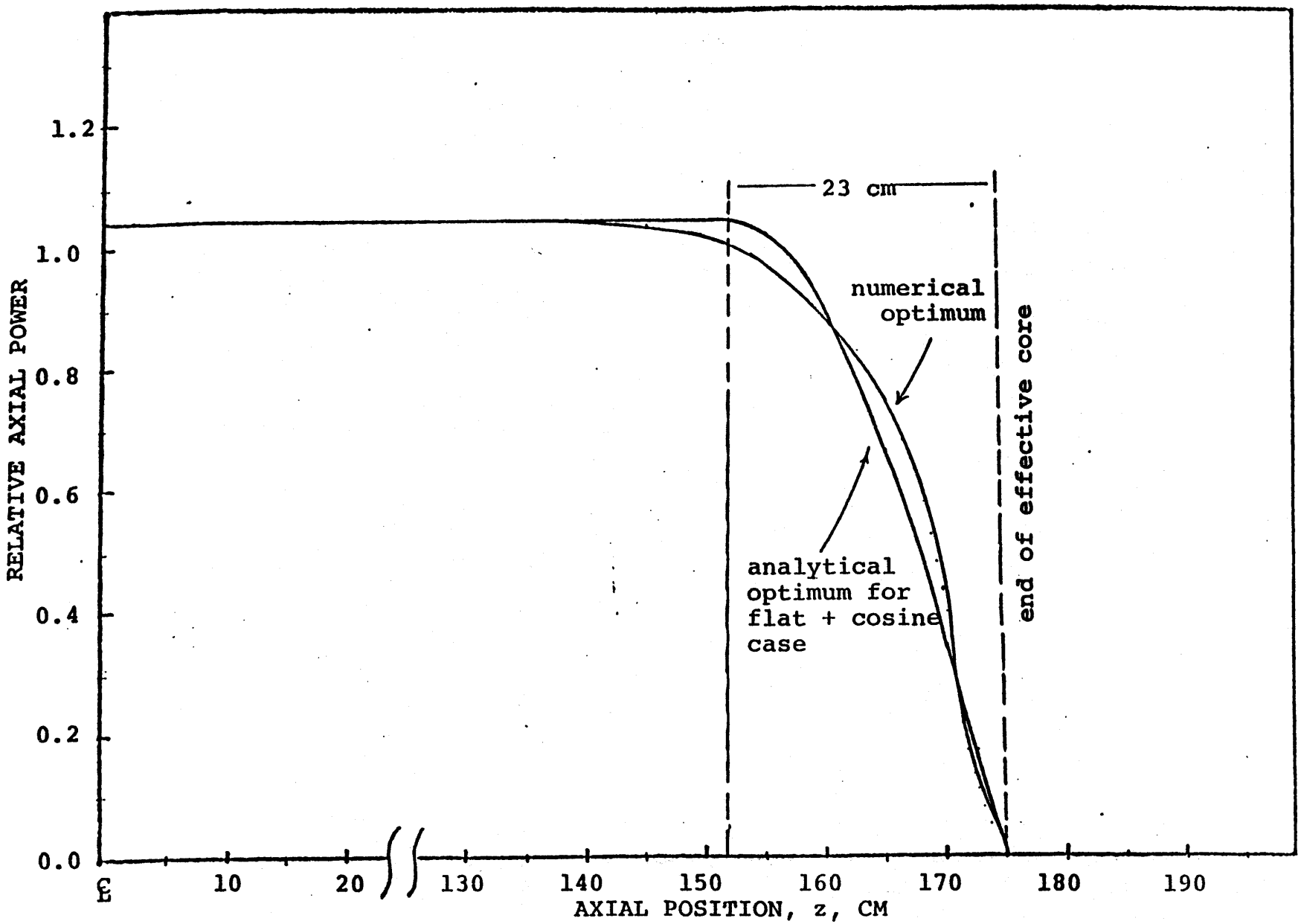

Figure 2.5 Analytical (for Flat + Cosine Shape) and Numerical Optimum Power Profiles

Table 2.1

Effects of Power Shape on Leakage Reactivity

Power Shape	Equation for Power Shape	Leakage Reactivity*
Flat	$F(z) = \text{constant}$	$\frac{M}{2b} = 0.0214$
Cosine	$F(z) \propto \cos\left(\frac{\pi z}{2b}\right)$	$\frac{1}{2}\left(\frac{\pi M}{2b}\right)^2 = 0.0022$
Flat + Cosine**	$F(z) \propto \cos\frac{\pi}{2}\left(\frac{z-b}{a}\right)$	$\frac{\frac{\pi}{a} - \frac{2}{M}\,\mathrm{EXP}\left(\frac{-a}{M}\right)}{4\left[\left(\frac{1}{M}\right)^2+\left(\frac{\pi}{2a}\right)^2\right]\left(\frac{2a}{\pi}+b\right)} + \frac{\mathrm{EXP}\left(\frac{-a}{M}\right)}{\frac{2}{M}\left(\frac{2a}{\pi}+b\right)}$

* For representative parameter values, M=7.5 cm, b=175.0 cm.

** This shape is flat except for a distance 'a' from each end of the assembly, in which it assumes a cosine shape.

Table 2.2

Features of Analytical Example

Step in Analysis	Governing Relations
Equation for flat + cosine shape was expressed as	$f(z) = \kappa$ for flat $f(z) = \kappa \cos \frac{\pi}{2}\left(\frac{z-b}{a}\right)$ for cosine
Normalization condition was imposed to find constant κ	$\int_{-(b+a)}^{b+a} f(z)dz = 1 \quad ; \quad \kappa = \frac{1}{2\left(\frac{2a}{\pi}+b\right)}$
One group diffusion kernel was used to calculate leakage reactivity, ρ_L	$\rho_L = \int_{-(b+a)}^{b+a} f(z)J(z)dz$
	$J(z) = \frac{1}{2}\left[\mathrm{EXP}\left(\frac{-b+z}{M}\right) + \mathrm{EXP}\left(\frac{-b-z}{M}\right)\right]$
	$\rho_L = \frac{\frac{\kappa}{2}}{\left(\frac{1}{M}\right)^2 + \left(\frac{\pi}{2a}\right)^2}\left[\frac{\pi}{2a} - \frac{2}{M}\,\mathrm{EXP}\left(\frac{-a}{M}\right)\right]$
	$+ \quad M\kappa\ \mathrm{EXP}\left(\frac{-a}{M}\right)$
Linear reactivity model was applied to calculate burnup	$\bar{B} = \frac{\rho_o - \rho_L}{2ba\int_{-(b+a)}^{(b+a)} f^2(z)dz}$
Optimum length of the region having a cosine shape was found	Value of a, the cosine shape length, was varied and the value of a which gave maximum burnup was identified

2.6 Chapter Summary

In this chapter analytical and numerical methods used in the present research have been outlined. The first part of the chapter briefly describes the LEOPARD, CHIMP and PDQ-7 codes. The next section dealt with the simple analytical models used; namely, "the linear reactivity model" and "the group and one-half" model. Finally, a simple algorithm has been developed which enables the user to find an optimum power profile by an iterative process embodied in a simple computer program. A purely analytical result for a flat power shape with cosine ends has also been presented.

CHAPTER 3

AXIAL FUEL ASSEMBLY DESIGN

3.1 Introduction

In the previous chapter a simple algorithm was developed to determine the optimum axial power profile. From the corresponding axial distribution of fuel enrichment (see Figure 2.3) it is clear that the optimum assembly can be approximated as a three zone configuration: a central zone of constant power density, a region of higher enrichment, and an outer region of low enrichment (i.e., blanket).

In this chapter the axial fuel zoning which yields a near-optimum power profile at the beginning-of-cycle will be investigated using static diffusion theory calculations. This will be followed by depletion (burnup) analysis of the most promising option for comparison with the reference case. The modified assembly designs which will be analyzed do not involve any changes in the fuel rods apart from zoned loading in the fueled region; the total effective fuel length, pellet radius, etc., are all kept constant.

3.2 The Reference Case

A one dimensional (axial) model of one half of a typical PWR reload assembly was used as the reference case. This case is of basic importance to this work since all the modified designs investigated in this study are based on this model. This configuration has 175 cm of uranium dioxide fuel, with a beginning of life (BOL) U-235 enrichment of

3.0%. The assembly was based on that of the Maine Yankee PWR.* Half-core symmetry (axially) was used, and the radial leakage was approximated by a "DB^2" term added to the macroscopic absorption cross section.

The unfueled region's structure was composed of a 50% stainless steel, 50% borated water mixture. The length assigned to this region was 50 centimeters. In the fuel region one mesh point per centimeter was employed and in the structure one mesh point every five centimeters was used.

3.3 Axial Enrichment Zoning: BOL Studies

As previously noted, the use of axial blankets improves uranium utilization, but this is achieved at the expense of increased axial power peaking. Enrichment zoning of the fuel assembly is investigated here as a means to reduce the power peaking and to improve core operating margins.

Three modified assembly designs which differ in enrichment zoning have been analyzed. It is important for meaningful comparison between the reference and test cases that all cases should be consistent. Hence the test cases have been adjusted such that the quantity of U_3O_8 (i.e., natural uranium) utilized is the same. Since all other dimensions are the same, the length of each zone can be used as a weighting factor for this purpose, i.e.,

$$\left(\frac{X_p - X_w}{X_F - X_w}\right) L = \left(\frac{X_{p_1} - X_w}{X_F - X_w}\right) L_1 + \left(\frac{X_{p_2} - X_w}{X_F - X_w}\right) L_2 + \left(\frac{X_{p_3} - X_w}{X_F - X_w}\right) L_3 \quad (3.1)$$

* See References (S-1) and (K-1) for details.

and

$$L = L_1 + L_2 + L_3 \tag{3.2}$$

which implies that

$$X_p L = X_{p_1} L_1 + X_{p_2} L_2 + X_{p_3} L_3 \tag{3.3}$$

L_1, L_2 and L_3 are the lengths of the different zones, and X_{p_1}, X_{p_2} and X_{p_3} are the corresponding enrichments of these zones.

The cases analyzed are shown in Figure 3.1

Case 1 consists of a 118 cm central core region of 2.8 w/o U-235; a 47 cm core region of 4.1 w/o U-235 and 10 cm of depleted uranium (0.2 w/o U-235) blanket.

Case 2 consists of a 139 cm central core region of 2.9 w/o U-235, a 26 cm core region of 4.44 w/o U-235 and 10 cm of natural uranium blanket.

Case 3 consists of a 128 cm core region of 2.9 w/o U-235, a 37 cm core region of 4.1 w/o U-235 and 10 cm of depleted uranium (0.2 w/o U-235) blanket.

Static LEOPARD runs were used, changing only the enrichment, to generate two group sets of super cell cross sections. These cross sections were used in the PDQ-7 code to obtain the power edit at each mesh point for these cases.

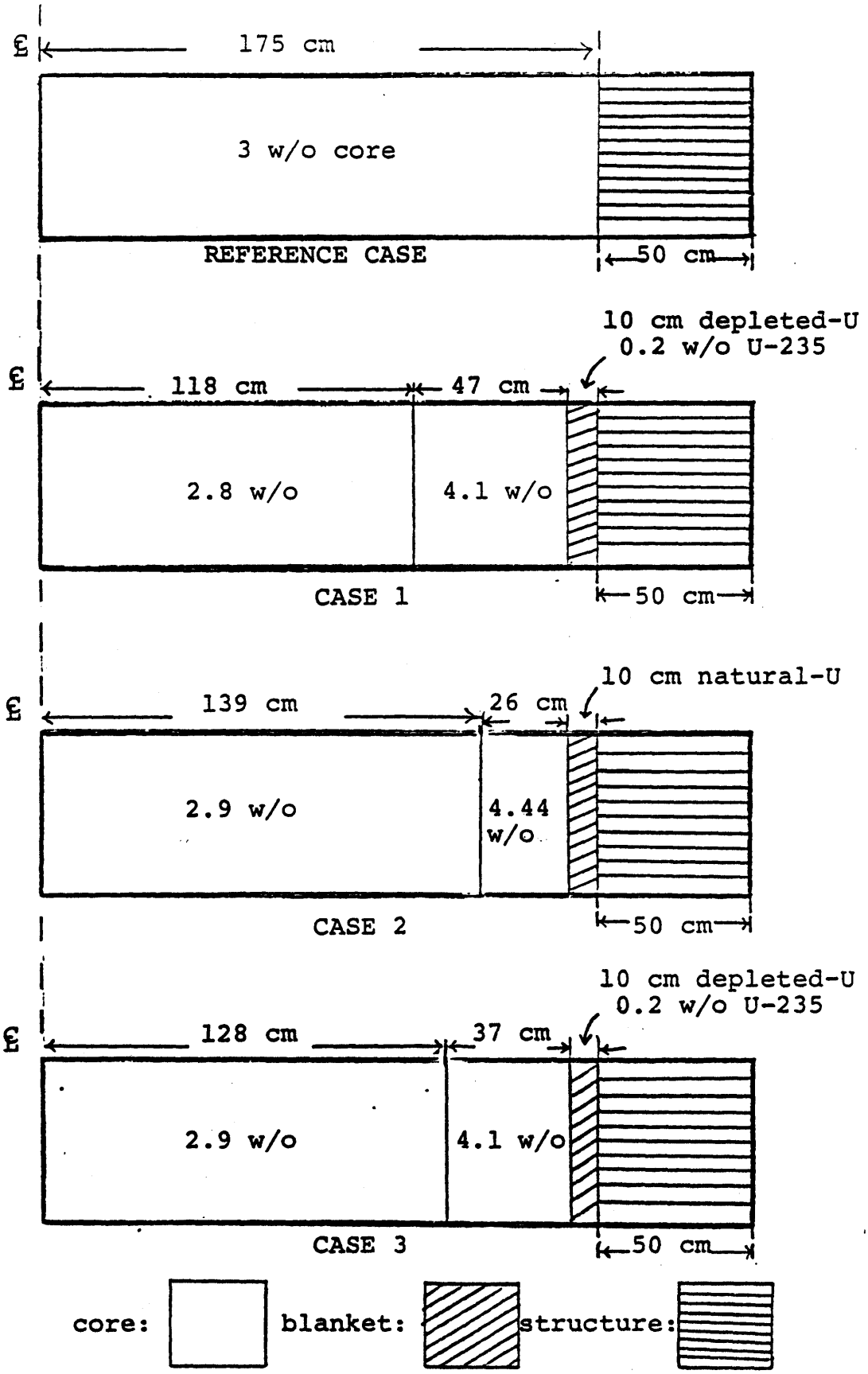

Figure 3.1 Cases Considered to Optimize Axial Power Profile Via Enrichment Zoning

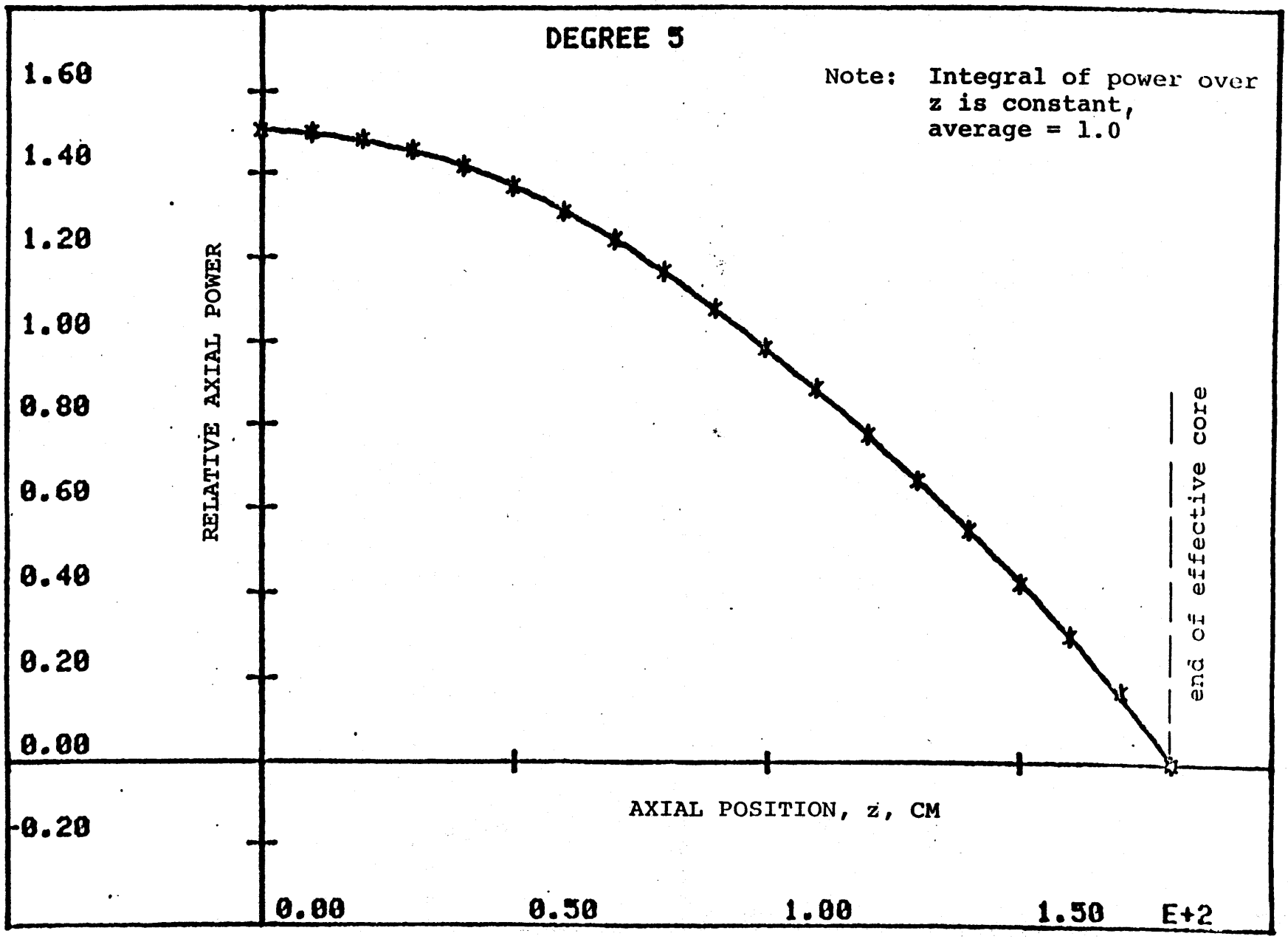

Figure 3.2 Axial Power Profile (BOL) for Reference Case

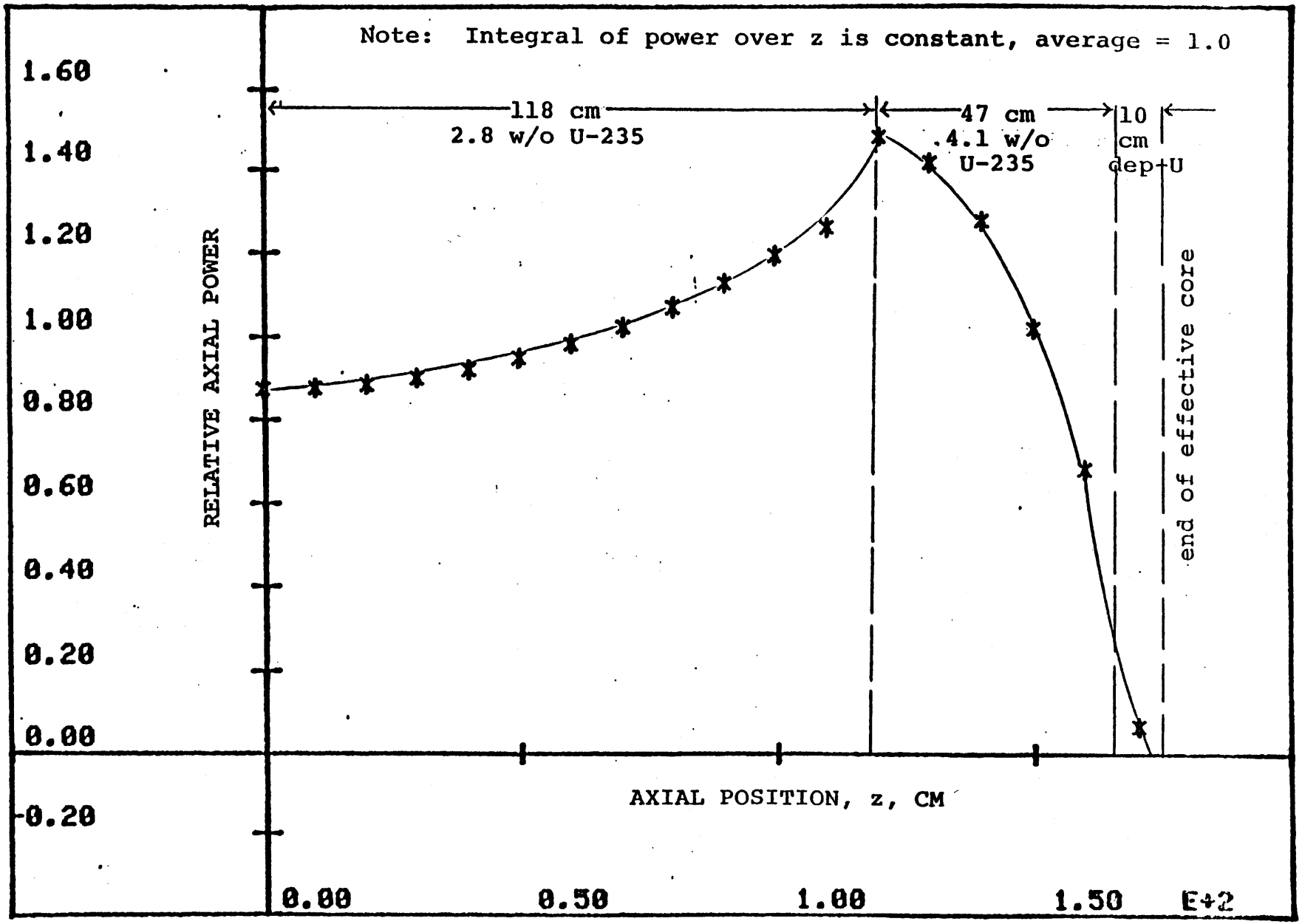

Figure 3.3 Axial Power Profile (BOL) for Case 1

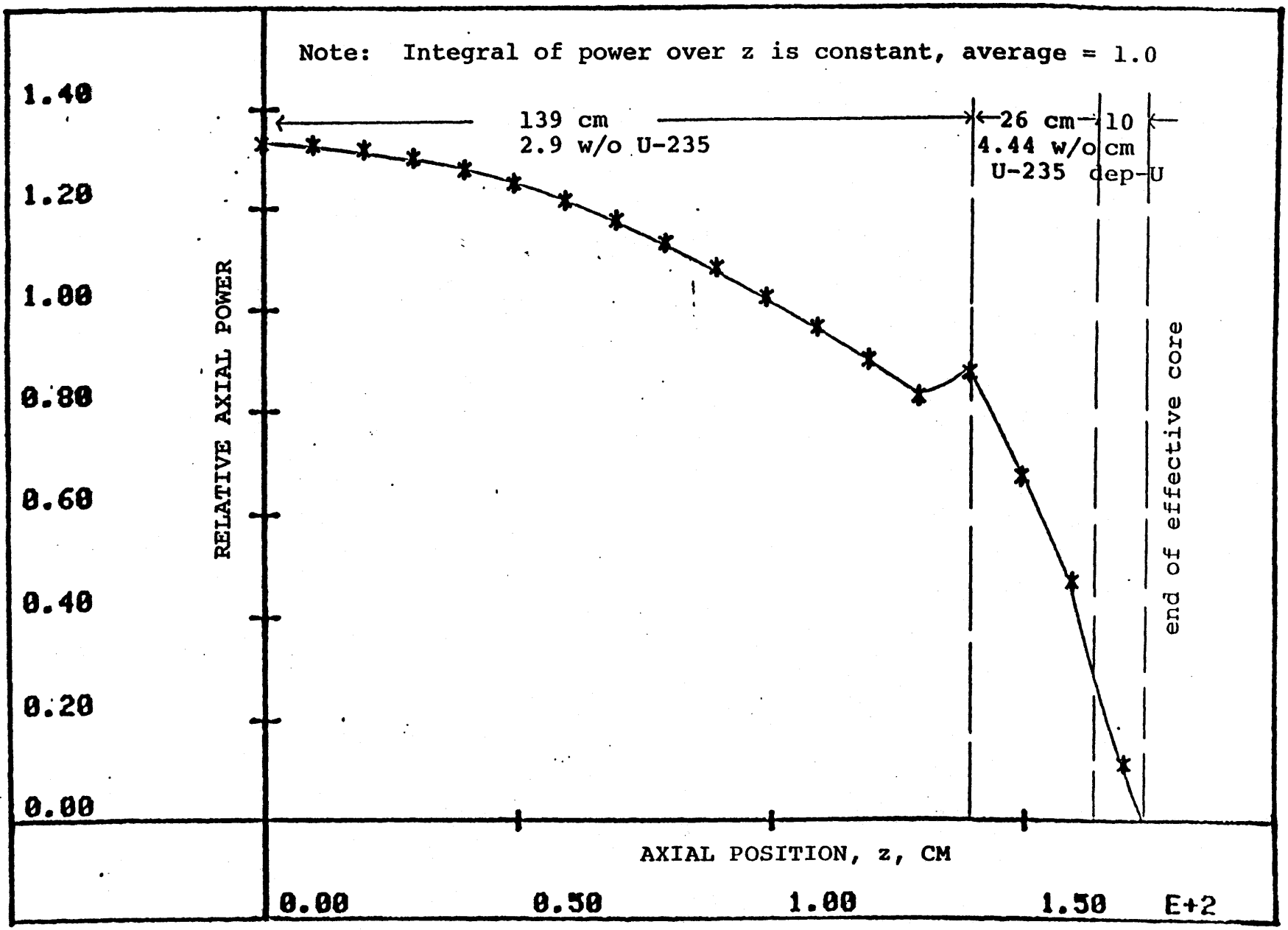

Figure 3.4 Axial Power Profile (BOL) for Case 2

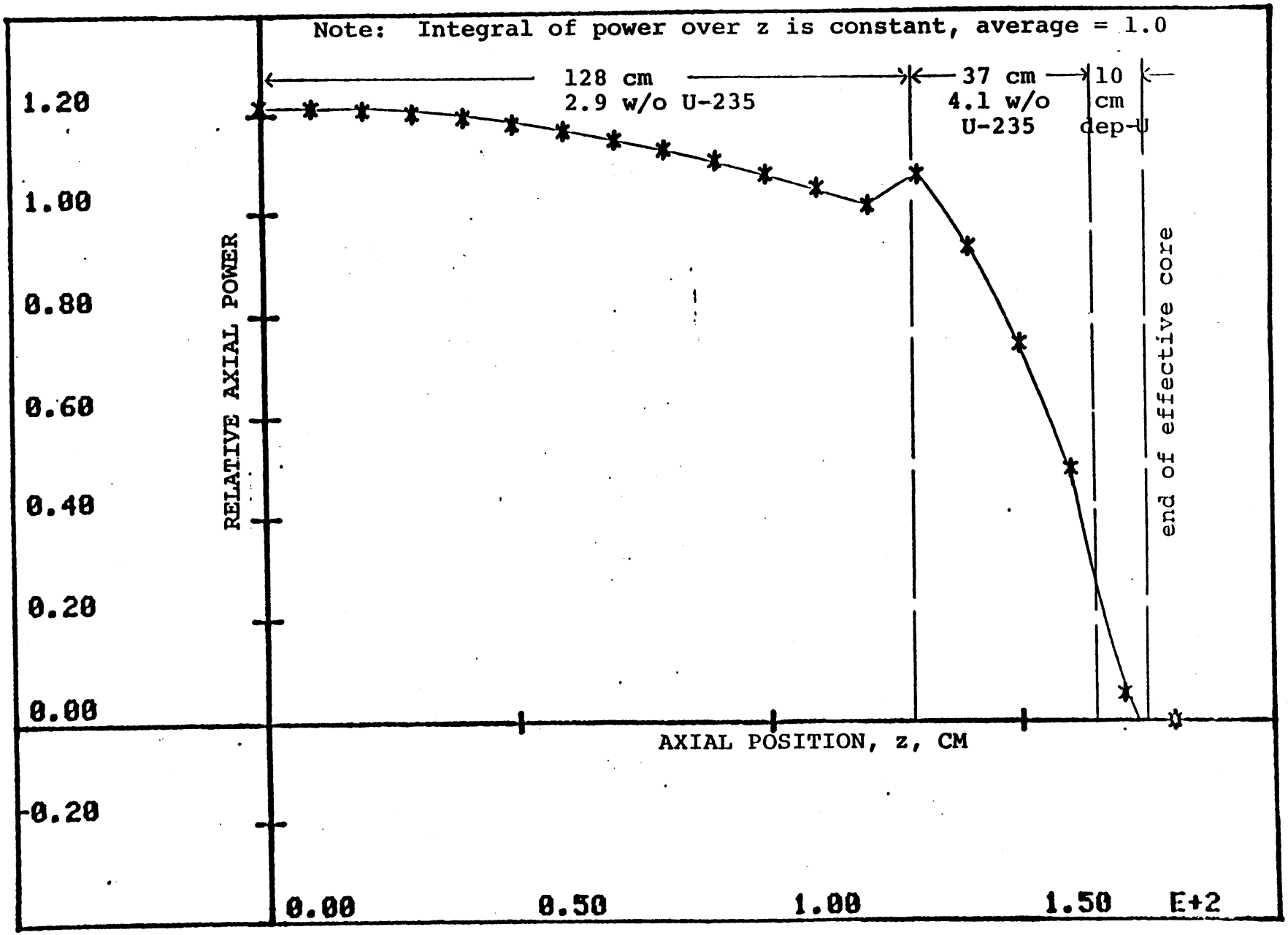

Figure 3.5 Axial Power Profile (BOL) for Case 3

The beginning-of-life power profiles of these cases are shown in Figures 3.3, 3.4 and 3.5.

It is clear from these figures that the BOL power profile for the case 3 configuration is very close to the optimum power profile developed in Chapter 2. Hence this case will be examined further in the next section using PDQ-7 depletion analyses.

3.4 Depletion Results

This section describes the results of PDQ-7 depletion runs for three cases with different configurations. LEOPARD was used to calculate isotopic concentrations and spectrum-averaged cross sections at various depletion time steps. Comparison of the output of LEOPARD depletion cases having different-sized depletion steps (but with the same initial enrichment) showed that the ultimate value predicted for the discharge burnup was affected by as much as 1.0% when, for example, the depletion step was changed from 4000 (MWD/MT) to 5000 (MWD/MT). Thus care was taken to specify identical depletion steps for all cases. This output from LEOPARD was processed by the CHIMP code to prepare cross section tables for PDQ-7.

PDQ-7 depletion was carried out at constant total bundle power. Three time steps were used in the initial 1500 effective-full-power-hours (efph), and thereafter one time step per 1500 efph was used.

Before presenting the results for the depletion runs, some quantities need to be defined.

The reactivity, ρ, of the system is defined as

$$\rho = 1 - \frac{1}{k} \tag{3.4}$$

where k is the effective multiplication factor of the system.

The effect of neutron leakage from the core can be characterized as a decrement in system reactivity:

$$\rho_L = \frac{A_{ex\text{-}core}}{A_{total} k_{sys}} = \frac{A_{ex\text{-}core}}{F_{total}} \tag{3.5}$$

where ρ_L is leakage reactivity, $A_{ex\text{-}core}$ is the total absorption in non-core material, A_{total} is the total absorption in the reactor (core + non-core material), k_{sys} is the system multiplication factor and F_{total} is the total neutron production in the reactor.

3.4.1 Reference case depletion

The configuration of the reference case, the model used to describe a typical currently used PWR assembly, has already been described in this chapter (see Figure 3.1). Table 3.1 shows the values of ρ_{eff}, k_{eff}, ρ_L and the axial peak-to-average power ratio in the assembly as a function of time (in hours) at effective full power.

Figure 3.6 shows the graphical representation of the variation of reactivity, ρ, as a function of efph, using the

Table 3.1

Reference Case Burnup Results

Time (hours at full power)	ρ_{eff}	k_{eff}	ρ_L	Peak-to-Average Power Ratio
0	0.24776	1.32936	0.00316	1.502
125	0.22027	1.28249	0.00434	1.331
800	0.21026	1.26624	0.00453	1.317
1500	0.20285	1.25447	0.00514	1.229
3000	0.18604	1.22856	0.00661	1.148
4500	0.16837	1.20246	0.00751	1.128
6000	0.15022	1.17677	0.00850	1.121
7500	0.13165	1.15161	0.00929	1.112
9000	0.11277	1.12710	0.01003	1.102
10500	0.09344	1.10307	0.01080	1.101
12000	0.07371	1.07958	0.01144	1.091
13500	0.05334	1.05634	0.01226	1.097
15000	0.03228	1.03336	0.01291	1.090
16500	0.01048	1.01059	0.01374	1.096
18000	-0.01224	0.98790	0.01445	1.092
19500	-0.03498	0.96620	0.01486	1.073
21000	-0.05663	0.94641	0.01491	1.041
22500	-0.07821	0.92746	0.01545	1.045
24000	-0.09925	0.90971	0.01552	1.040
25500	-0.12019	0.89270	0.01599	1.032
27000	-0.14100	0.87642	0.01625	1.031
28500	-0.16163	0.86086	0.01658	1.029
30000	-0.18202	0.84600	0.01686	1.029

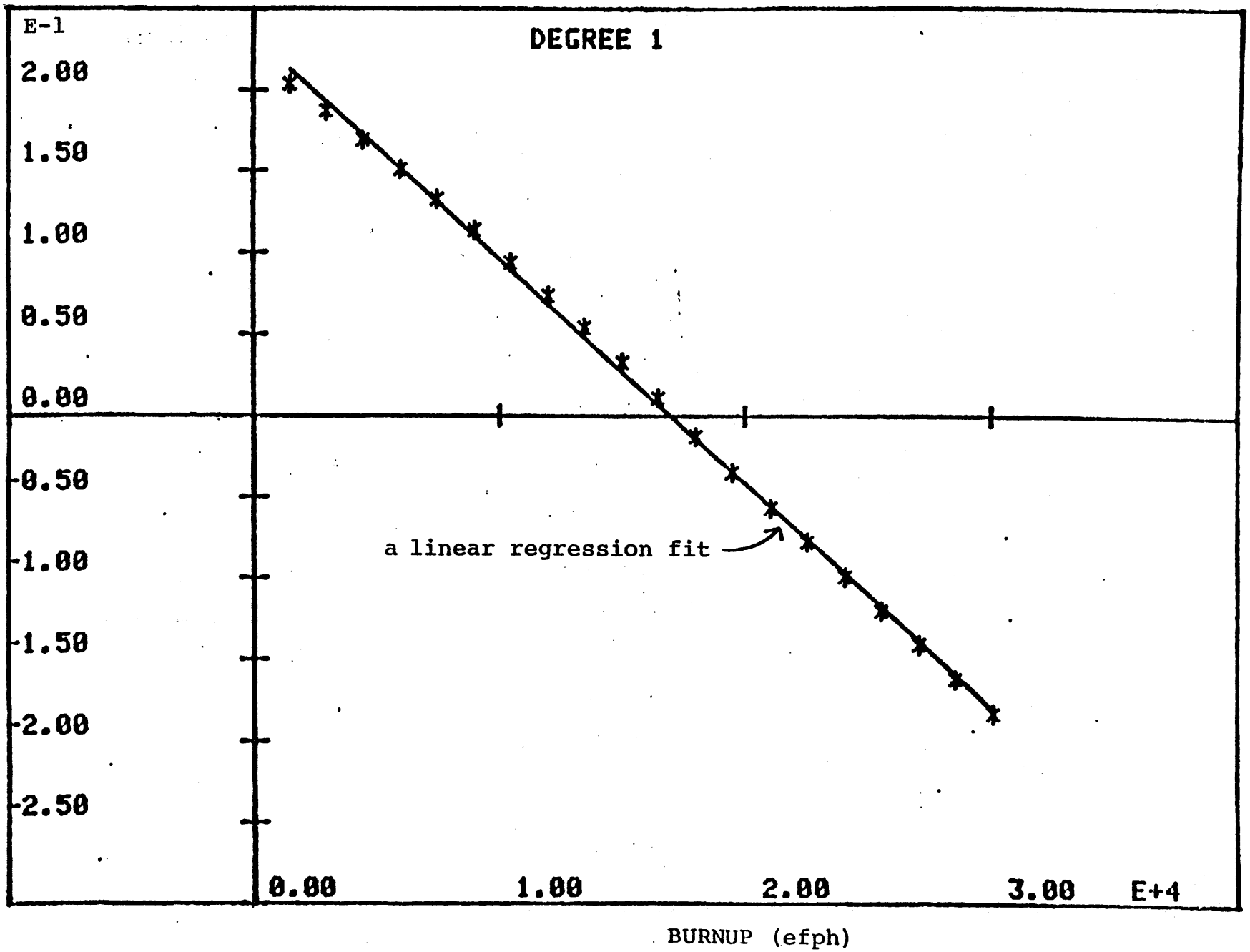

Figure 3.6 Reactivity as a Function of Burnup for the Reference Case

data from Table 3.1. A straight line fit was done on the data using a linear regression method. The correlation coefficient (K-2), which is a criterion for goodness-of-fit, was 0.9977, which shows that the "linearity" is excellent. In this fit the first three sets of values of ρ and efph were not used. They were omitted to allow sufficient time for the initial reactivity drop, due to equilibrium fission product saturation (xenon, samarium) to occur. The intercept on the efph axis, i.e., at ρ=0, was found to be 16945.5, which corresponds to a discharge time of 25418.25 efph (for a 3-batch core and equal batch power sharing). The values of reactivity vs. burnup for this reference case were also submitted to the ALARM code (S-1) under conditions of no radial leakage and equal power sharing. The results indicated that the spent fuel is discharged after 25418.0 hours of irradiation at full power, in good agreement with the results of the simple linear reactivity model.

The variation of the leakage probability of the fueled region with efph is shown in Figure 3.8. This should be looked at in conjunction with Figure 3.7, which shows the normalized axial power profiles at different burnups.

3.4.2 Blanket case depletion

The depletion results of the blanket-only case are important in this study for subsequent comparisons with the other modified assembly designs which have been investigated. In this case 165 cm of 3.1697 w/o U-235 occupied the central

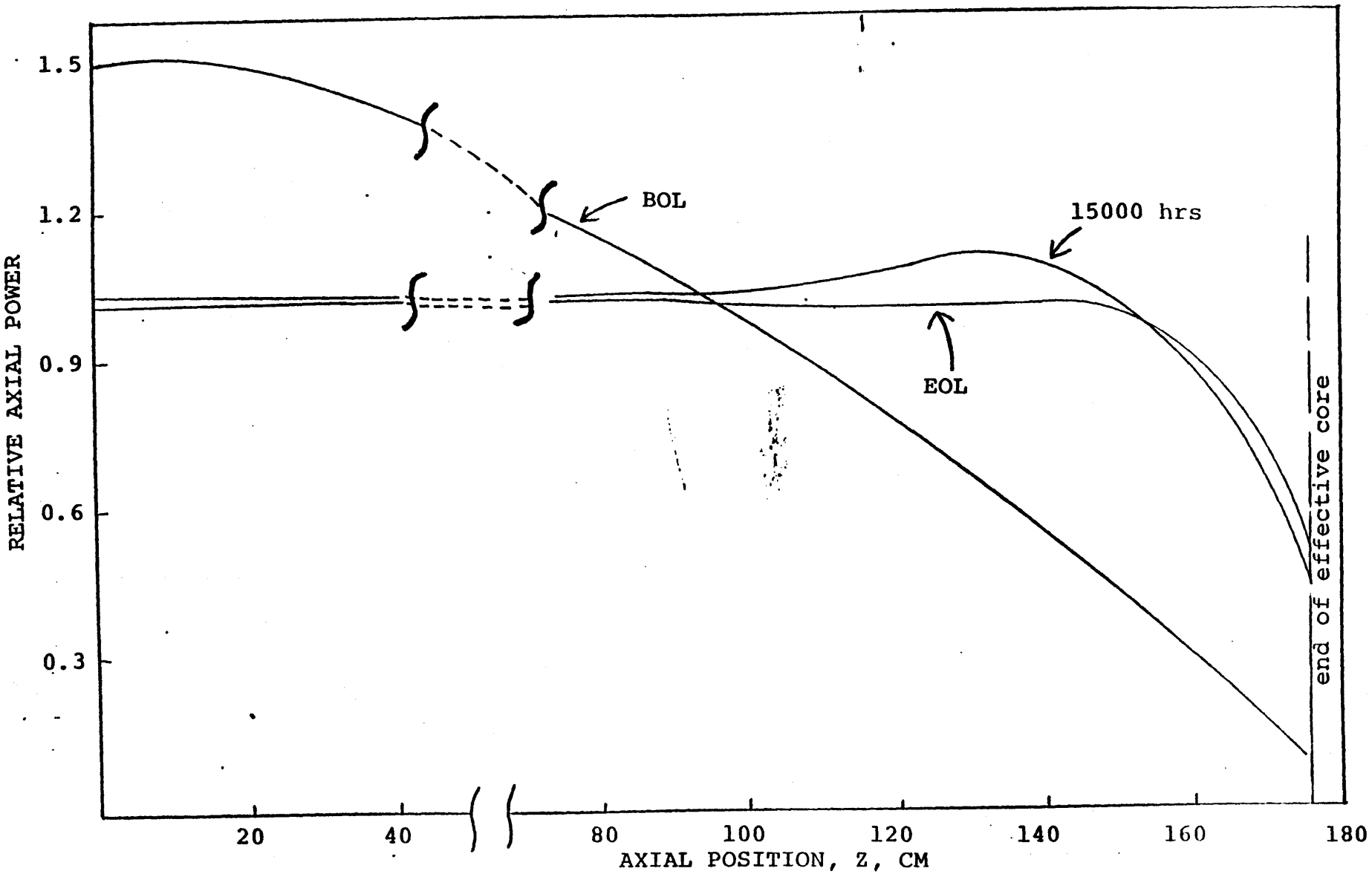

Figure 3.7 Axial Power Profiles for Reference Case

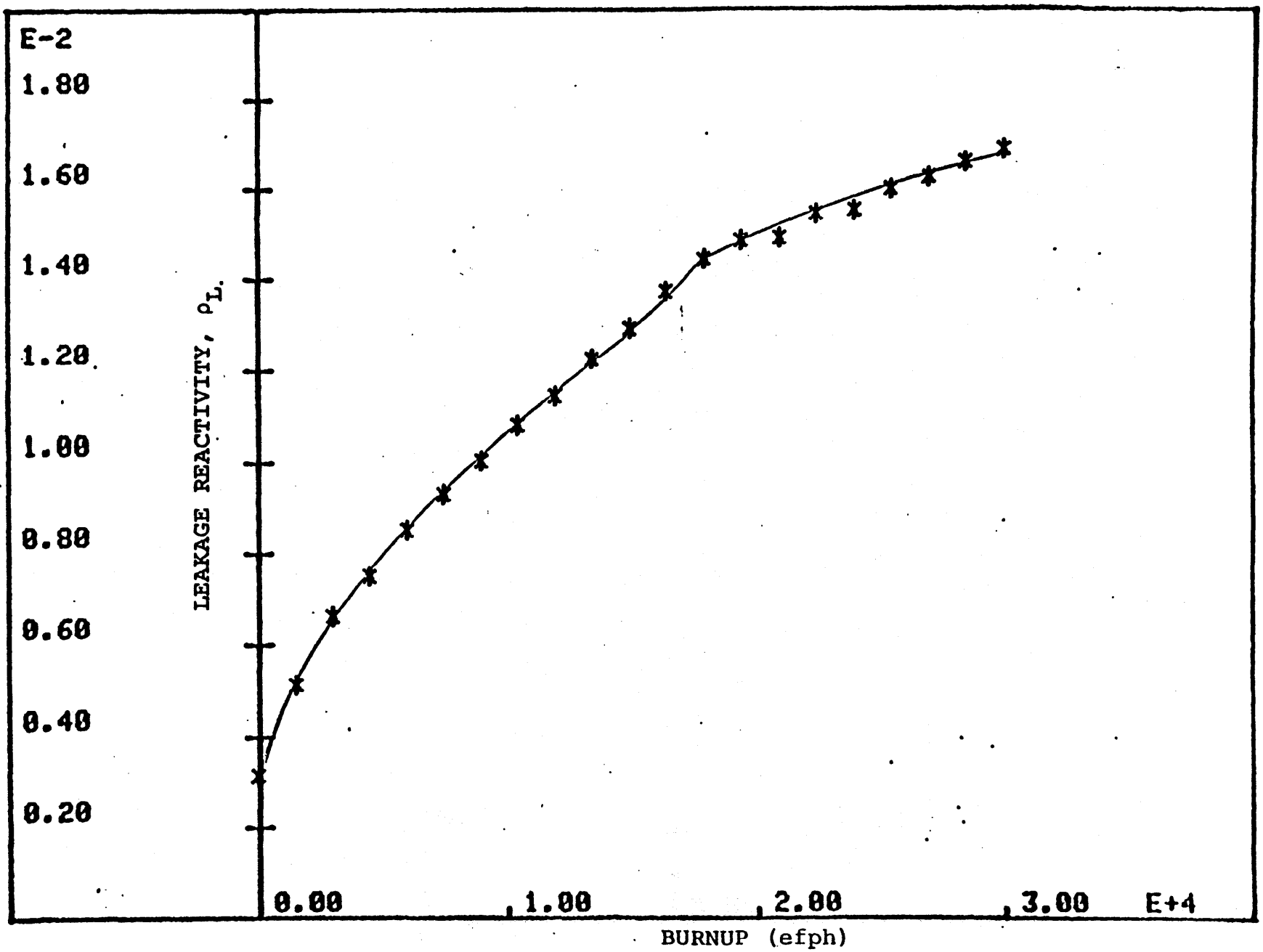

Figure 3.8 Leakage Reactivity, ρ_L , vs. Burnup (efph) for the Reference Case

core region, while the last 10 cm of core were replaced with depleted uranium (0.2 w/o U-235). This blanketed case and the reference case have the same feed-to-product ratio (F/p). The values of ρ_{eff} , k_{eff} , ρ_L and the axial peak-to-average power ratio, all as a function of efph, from the PDQ-7 depletion run are listed in Table 3.2.

The BOL k_{eff} for this case is 0.84% higher than that for the reference case. This is the combined effect of increased neutron importance in the central region and the small benefit of reduced neutron leakage, both caused by the redistribution of the U-235 from ends to central region. A linear regression straight-line fit to the reactivity, ρ, as a function of efph was performed (which is shown in Figure 3.9) in the same manner as for the reference case. The correlation coefficient was 0.99896. The value of discharge efph for a 3-batch core (again predicted by computing the ρ=0 intercept) was computed to be 26025. The values of reactivity vs. burnup for this case were also submitted to the ALARM code. The results indicated that the fuel assembly in this case is discharged at 26025 efph. This is 2.4% higher than the discharge time for the reference case. However, the BOL peak-to-average power ratio for this case is 4.4% higher than that in the reference case. Axial power shapes at BOL and at selected burnups are shown in Figure 3.10. The axial power peaking increase reduces the core DNBR and other thermal margins. In the next case examined, axial enrichment zoning has

Table 3.2

Depleted Uranium Blanket Assembly Burnup Results
(3.1697 w/o Core Region)

Time (hours at full power)	ρ_{eff}	k_{eff}	ρ_L	Peak-to-Average Power Ratio
0	0.25403	1.34054	0.00164	1.568
125	0.22666	1.29309	0.00212	1.402
800	0.21643	1.27621	0.00226	1.380
1500	0.20888	1.26404	0.00257	1.294
3000	0.19184	1.23738	0.00338	1.199
4500	0.17401	1.21066	0.00397	1.178
6000	0.15583	1.18459	0.00458	1.168
7500	0.13722	1.15904	0.00515	1.161
9000	0.11842	1.13433	0.00565	1.147
10500	0.09894	1.10980	0.00629	1.152
12000	0.07913	1.08593	0.00675	1.136
13500	0.05854	1.06219	0.00743	1.146
15000	0.03753	1.03899	0.00788	1.129
16500	0.01538	1.01562	0.00868	1.152
18000	-0.00738	0.99267	0.00914	1.131
19500	-0.02929	0.97154	0.00943	1.100
21000	-0.05088	0.95159	0.00986	1.092
22500	-0.07214	0.93271	0.01018	1.077
24000	-0.09322	0.91473	0.01060	1.074
25500	-0.11426	0.89745	0.01103	1.072
27000	-0.13524	0.88087	0.01146	1.070
28500	-0.15608	0.86499	0.01190	1.067
30000	-0.17670	0.84984	0.01239	1.068

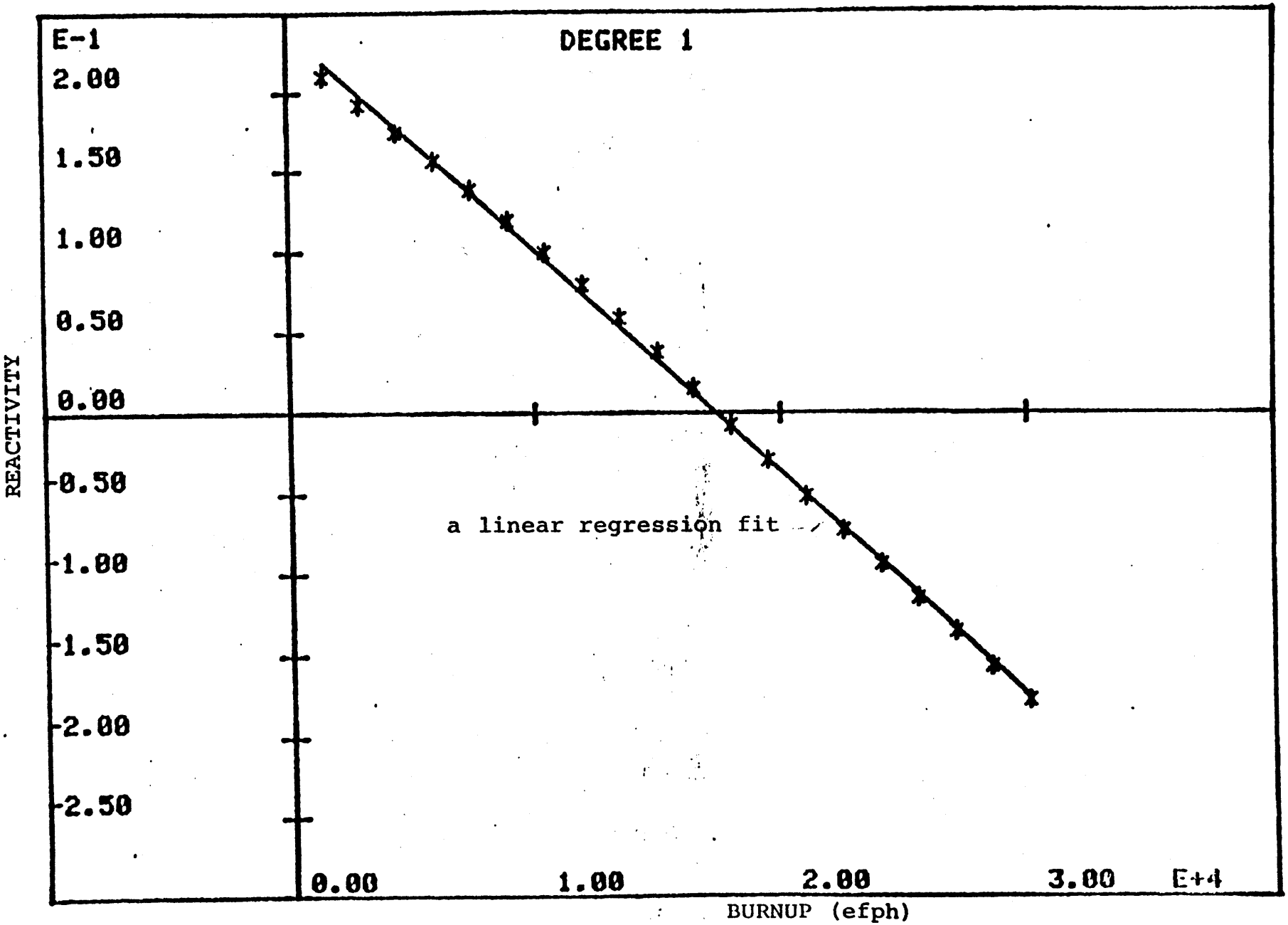

Figure 3.9 Reactivity as a Function of Burnup for the Blanketed Case

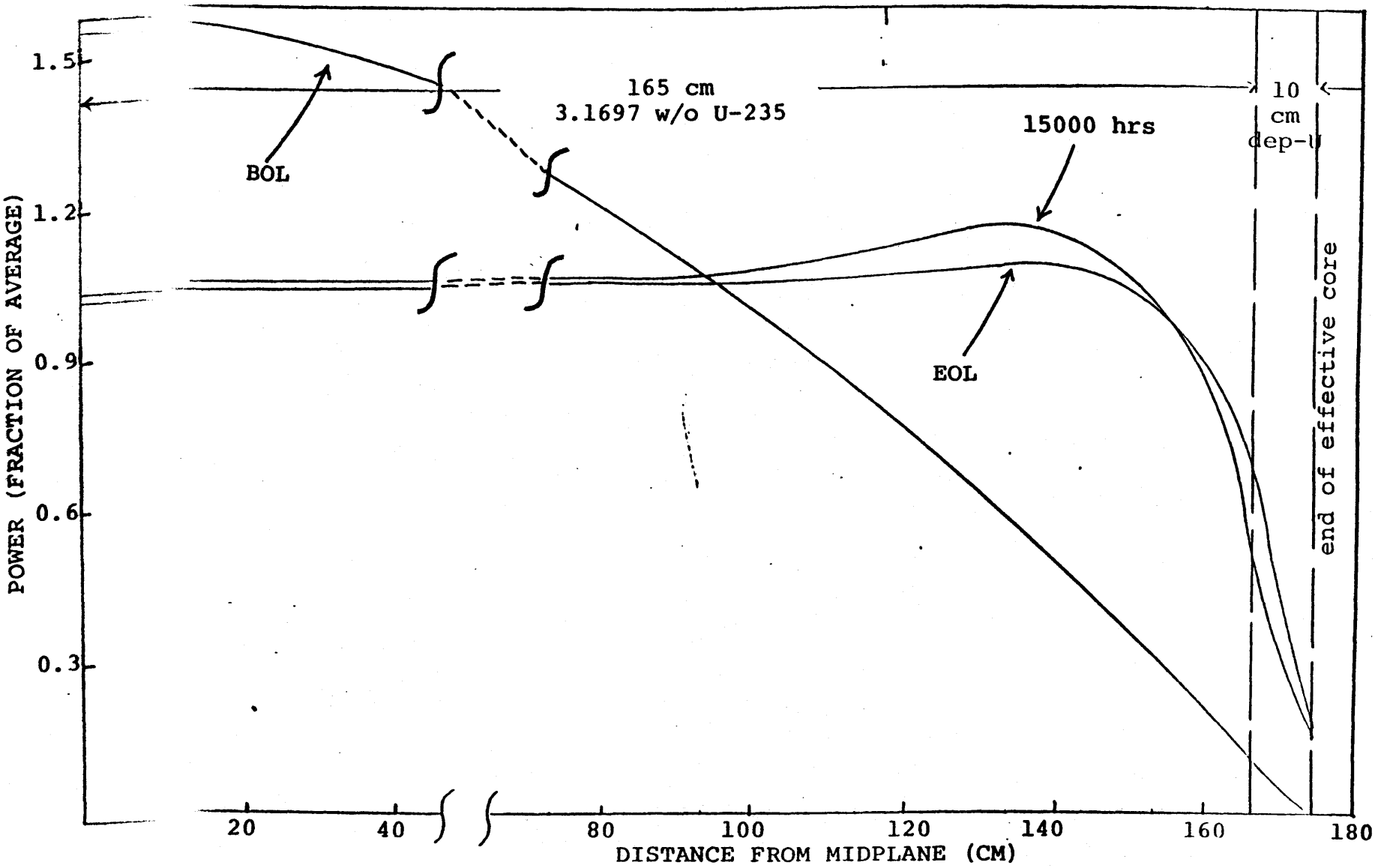

Figure 3.10 Axial Power Profiles for the Blanketed Case

been employed to reduce this power peaking while retaining some of the other advantages of the blanketed case.

3.4.3 Case 3 depletion

In the BOL studies of axial enrichment zoning, case 3 was found to yield a near-optimum power profile. PDQ-7 depletion results for this case are described in this section. The configuration of this case was shown in Figure 3.1.

Table 3.3 shows the variation of ρ_{eff} , ρ_L , k_{eff} and axial peak-to-average power with efph, obtained from PDQ-7 depletion analysis. A linear regression straight line fit was done on the reactivity as a function of efph data (shown in Figure 3.11). The correlation coefficient was 0.9987. The value of discharge efph (ρ=0 intercept) for a 3-batch core was calculated to be 25764.75 hours. This discharge time is 1.36% higher than that for the reference case. Also, the BOL peak-to-average power ratio is 19.3% less than the comparable ratio in the reference case, and 22.7% less than that in the blanketed case. However, the discharge time is 1.0% less than that in the blanketed case. Leakage is improved as compared to the reference case but this improvement is not as much as in the blanketed case. This comparison is shown in Figure 3.12. Axial power profiles at BOL and at selected burnups are shown in Figure 3.13. Note the tendency of the profile to burn into an end-peaked shape in the later stages of assembly exposure.

Table 3.3

Burnup results of Case 3: Axial Fuel Zoning
(128 cm 2.9 w/o, 37 cm 4.1 w/o and 10 cm 0.2 w/o)

Time (hours at full power)	ρ_{eff}	k_{eff}	ρ_L	Peak-to-Average Power Ratio
0	0.24561	1.32558	0.00340	1.212
125	0.21907	1.28053	0.00410	1.217
800	0.20950	1.26503	0.00415	1.189
1500	0.20270	1.25423	0.00453	1.235
3000	0.18680	1.22971	0.00532	1.302
4500	0.16962	1.20426	0.00589	1.311
6000	0.15178	1.17894	0.00654	1.329
7500	0.13354	1.15411	0.00704	1.315
9000	0.11485	1.12976	0.00767	1.321
10500	0.09579	1.10594	0.00808	1.295
12000	0.07615	1.08243	0.00874	1.302
13500	0.05604	1.05936	0.00904	1.268
15000	0.03503	1.03630	0.00984	1.297
16500	0.01349	1.01367	0.01004	1.250
18000	-0.00878	0.99130	0.01125	1.321
19500	-0.03122	0.96973	0.01157	1.295
21000	-0.05277	0.94988	0.01212	1.298
22500	-0.07397	0.93112	0.01217	1.252
24000	-0.09493	0.91330	0.01273	1.254
25500	-0.11566	0.89633	0.01280	1.211
27000	-0.13632	0.88004	0.01330	1.206
28500	-0.15686	0.86441	0.01352	1.179
30000	-0.17723	0.84945	0.01388	1.164

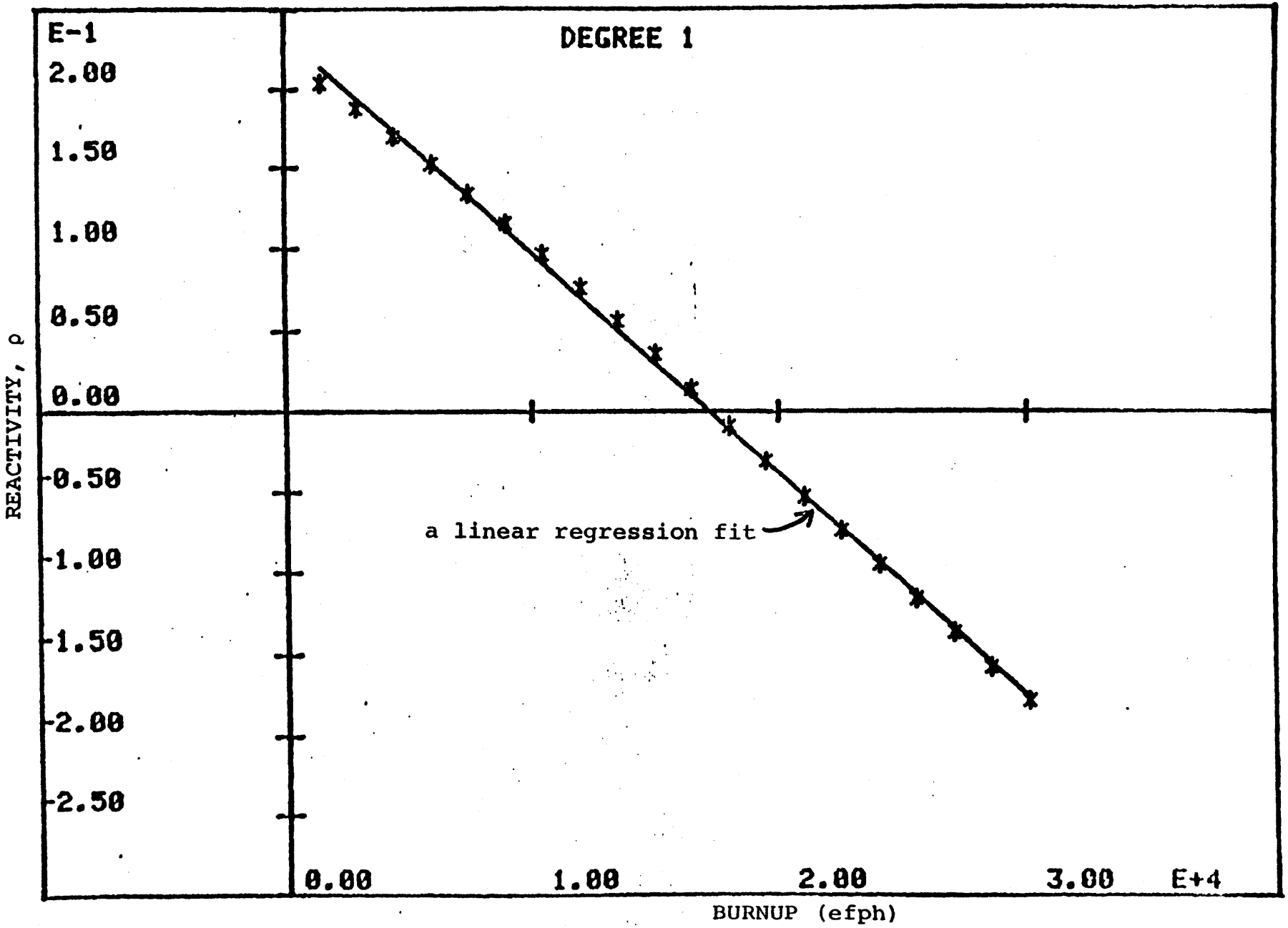

Figure 3.11 Reactivity as a Function of Burnup for Case 3

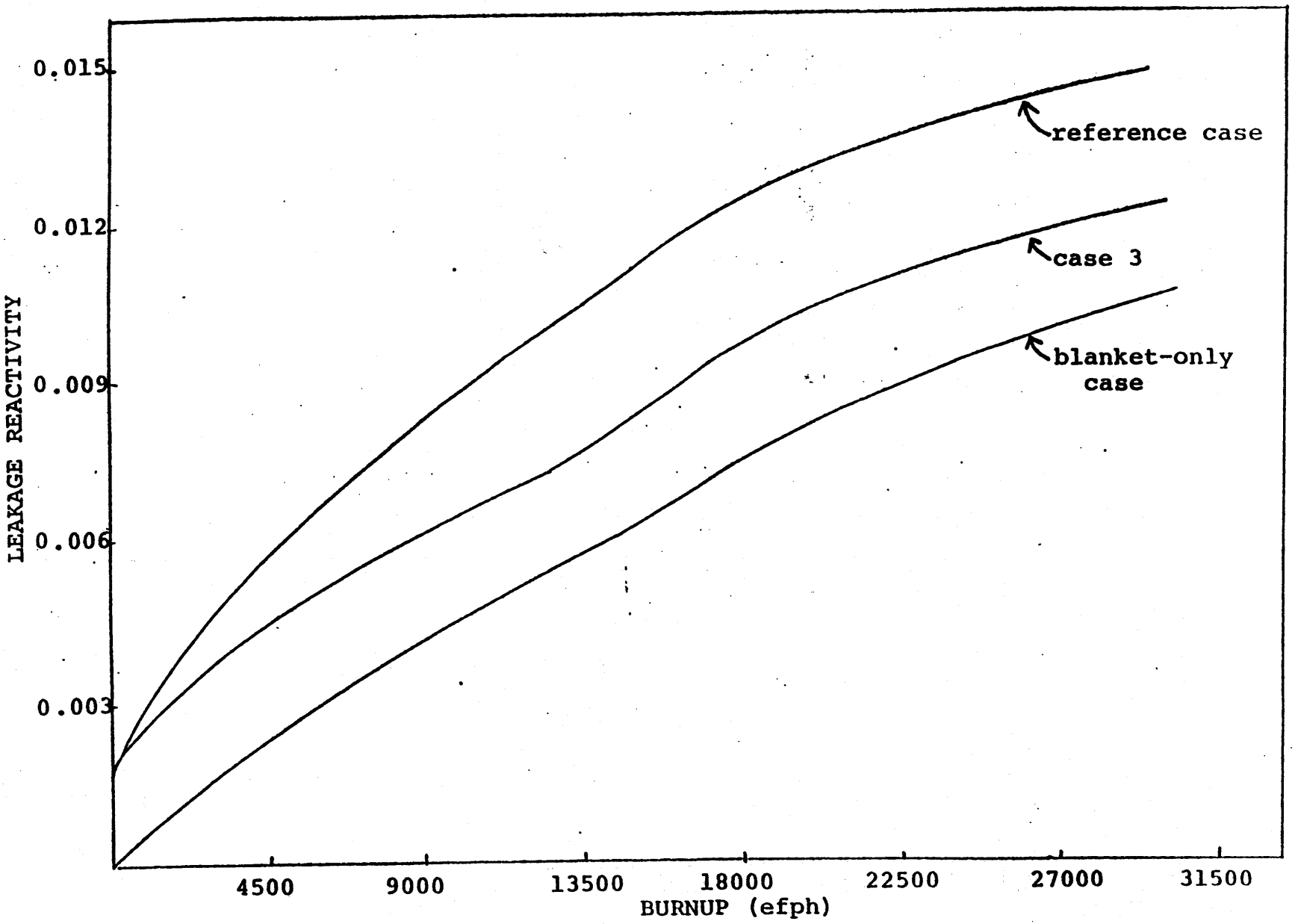

Figure 3.12 Leakage Reactivity, ρ_L , vs. Burnup for Various Cases

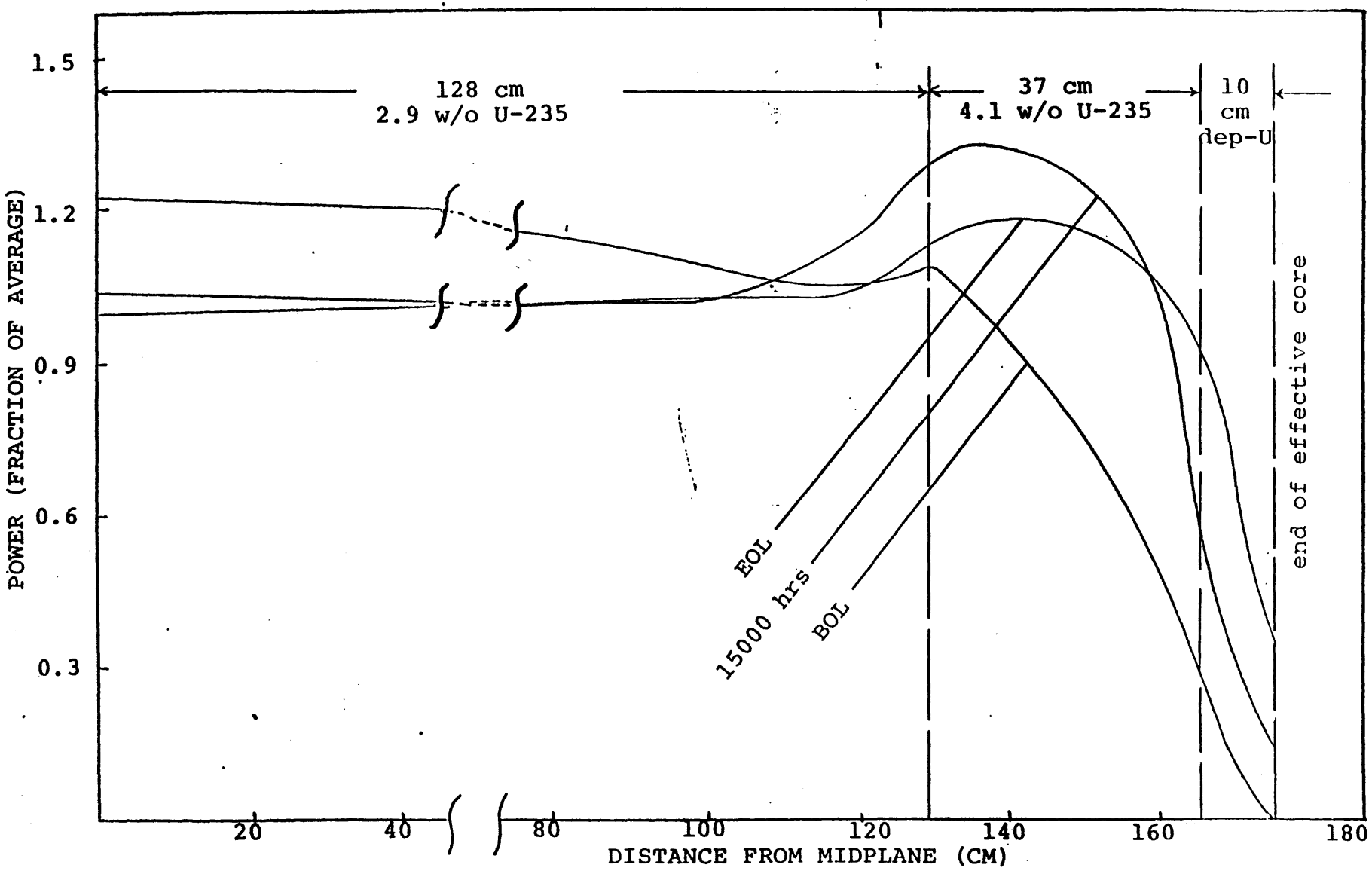

Figure 3.13 Axial Power Profiles for Case 3

3.5 Chapter Summary

In this chapter three modified PWR assembly designs were analyzed in a program of studies designed to approach an optimum power profile (investigated in Chapter 2). Static diffusion calculations showed that an axially enrichment zoned and blanketed configuration, case 3, gave a beginning-of-cycle power profile which was nearly optimum.

PDQ-7 depletion analyses of the reference case (the model used to describe a typical PWR assembly) and a blanketed case (using 10 cm of depleted uranium near the core's ends) were performed for comparison with subsequent modified designs.

Case 3 depletion results showed that the discharge time was 1.36% higher than that for the reference case. The BOL peak-to-average ratio for case 3 was found to be 19.3% and 22.7% less than that for the reference case and the blanketed case, respectively. However, the discharge time for case 3 is 1.0% less than that in the blanketed case. This leads to a search for additional modifications which can remedy this defect, while retaining the desirable features of reduced power peaking -- a task addressed in the following chapter.

CHAPTER 4

CASES WITH ANNULAR FUEL ZONES

4.1 Introduction

The BOL reactivity of an annular zone is not much lower than that in solid fuel of the same enrichment. Thus, initially, its presence near the blanket will help keep the central peaking factors low, while later on in life, because of its higher depletion rate, annular fuel will help in reducing the axial power peak near the ends of the assembly (which has been previously shown to occur and to cause higher axial leakage when axial enrichment zoning is employed -- see Chapter 3). Figure 4.1 illustrates this point; it shows the variation of the slope of $\rho(B)$ curves as a function of burnup, for annular and solid fuel of the same enrichment. The faster depletion of annular fuel is evident.

As mentioned earlier, LEOPARD was used for all cross section generation. This posed a problem as far as modeling annular fuel was concerned, since LEOPARD, being zero-dimensional, does not allow for an annulus to be specified in the fueled region. The best approximation, under the circumstances, was to specify a reduced fuel density corresponding to the size of the annulus. For example, to model a 10% by volume annular region, 90% of the usual (solid) fuel density was specified. Others have shown that in the 10-15% by volume range, the reduced density model yields a good approximation to Monte Carlo results (B-5).

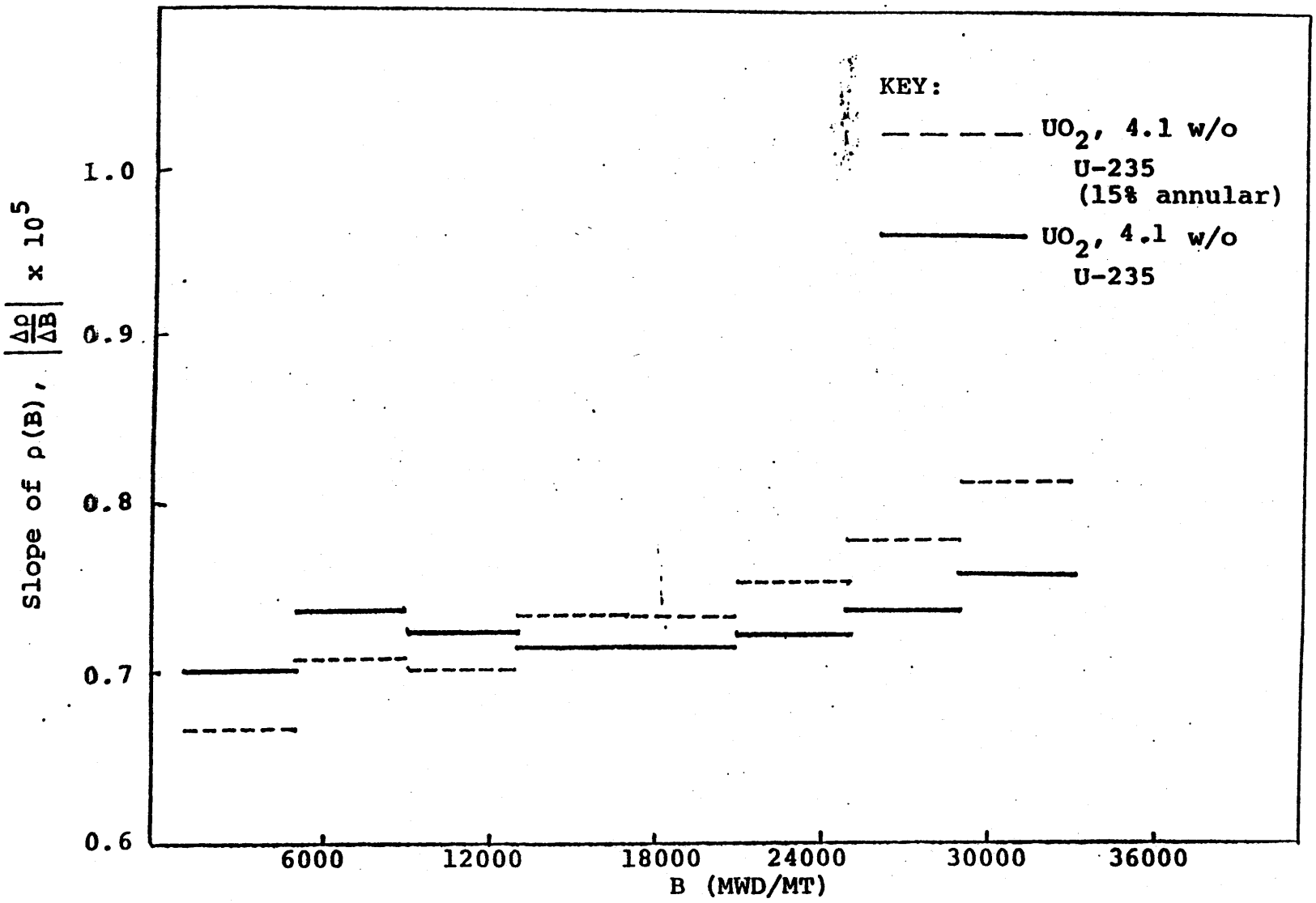

Figure 4.1 Slope of ρ(B) as a Function of Burnup, B

The annulus also provides other advantages: for example, additional volume for gaseous fission products. Furthermore, the absence of fuel at the center of the pellet reduces the peak and mean temperatures of the fuel. This decrease in temperature leads to a lower gaseous fission product release. These effects combine to cause significantly lower internal fuel rod pressure, which are very important in achieving higher burnups.

4.2 Configurations Examined

In the previous chapter, axial enrichment zoning was analyzed and compared with a blanket-only case. It was found through enrichment zoning that the problem of BOL power peaking in the blanketed case can be overcome, but the full advantages of blanketed cores (e.g., low leakage reactivity and higher burnup) were not retained. In this chapter axial enrichment zoning combined with the use of an annular fuel region is investigated in search of a modified assembly design which will have a low power peaking factor and a power profile which holds its shape over life.

Three configurations having the same region sizes, but different annulus size and enrichment, have been analyzed. First static diffusion theory calculations were used to identify a configuration which yields a near-optimum power profile. The cases analyzed are shown in Figure 4.2.

In the first case, a 15% annular region is used. Part (10%) of the U-235 removed due to the annulus has been

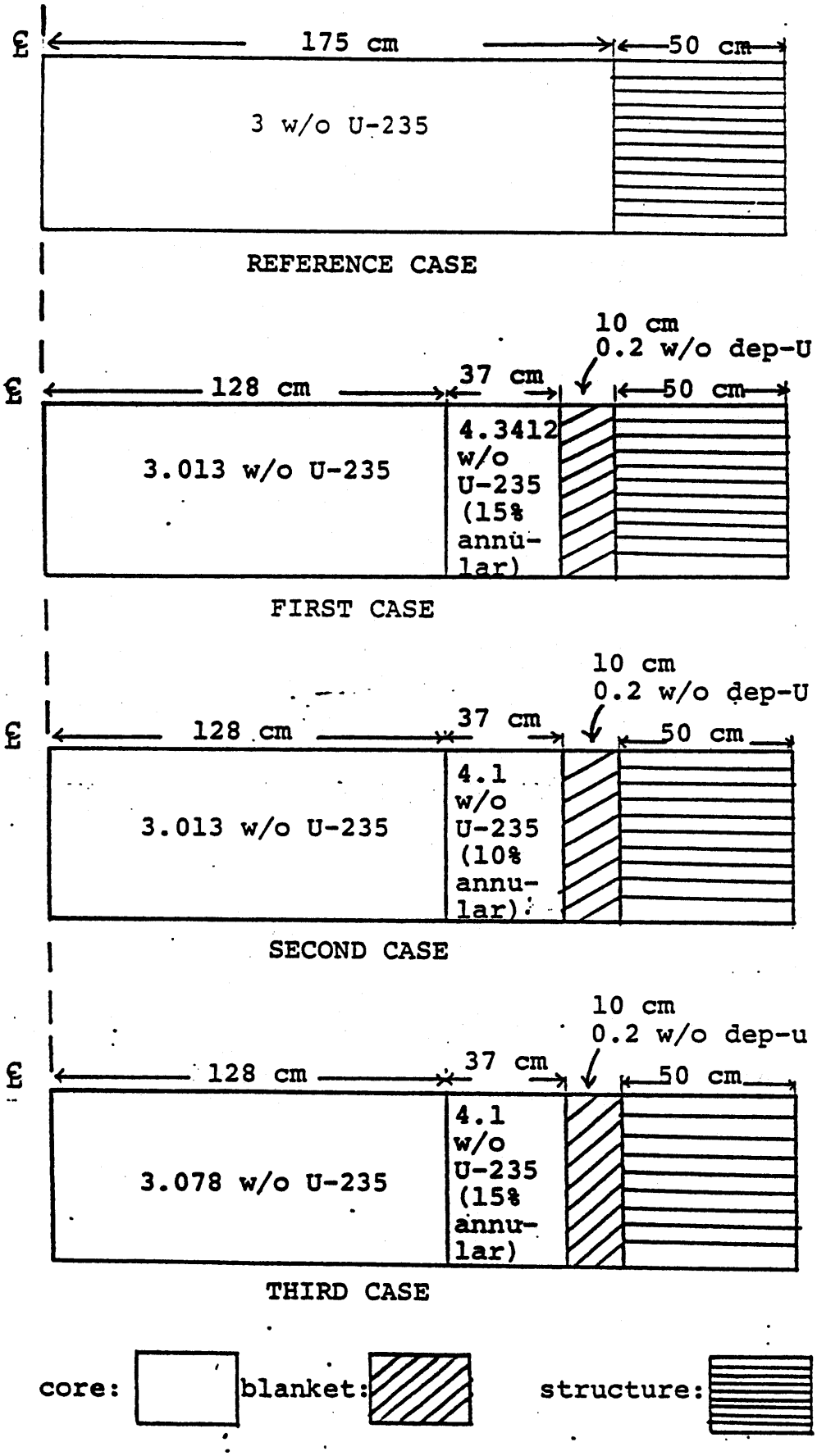

Figure 4.2 Cases Considered to Evaluate Annular Zoning for Power Profile Optimization

redistributed over the central region, so that the enrichment of this region is increased from 2.9% to 3.013%, and the rest (5%) of the U-235 has been redistributed in the annular region itself, which increased the enrichment of the annular region from 4.1% to 4.3412%.

In the second case a 10% annular region is used, and the removed U-235 has been redistributed over the central region alone; thus, the modified central region again has a 3.013% enrichment.

In the third case a 15% annular region is used and the enrichment of the central region is increased to 3.078%, once again to conserve the amount of ore utilized.

Static LEOPARD runs were used to generate two group sets of super-cell cross sections for the different enrichments involved. As previously noted, the annulus was modeled by using a reduced fuel density corresponding to the size of the annulus. These cross sections were used in the PDQ-7 code to obtain the power edit at each mesh point for all cases in question. The beginning-of-life power profiles of these runs are shown in Figures 4.3, 4.4 and 4.5.

Keeping in mind the results obtained in Chapter 3 for non-annular fuel, and the anticipated behavior of annular fuel, it can be inferred from these figures that the BOL power profile for the third case configuration is most promising, since it does not have peaking in the region of higher enrichment (annular region) and at the same time the central

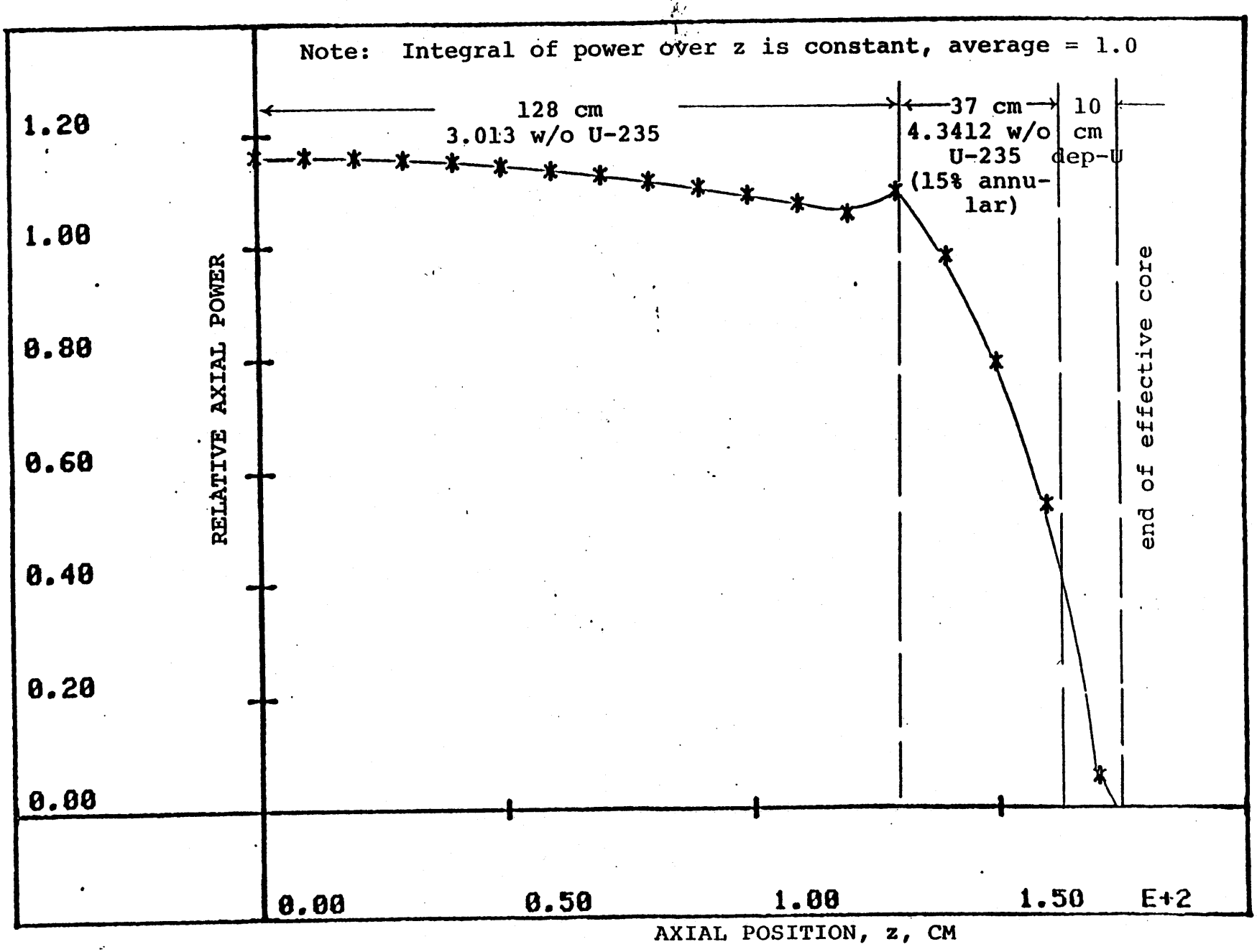

Figure 4.3 Axial Power Profile for the First Annular Zone Case

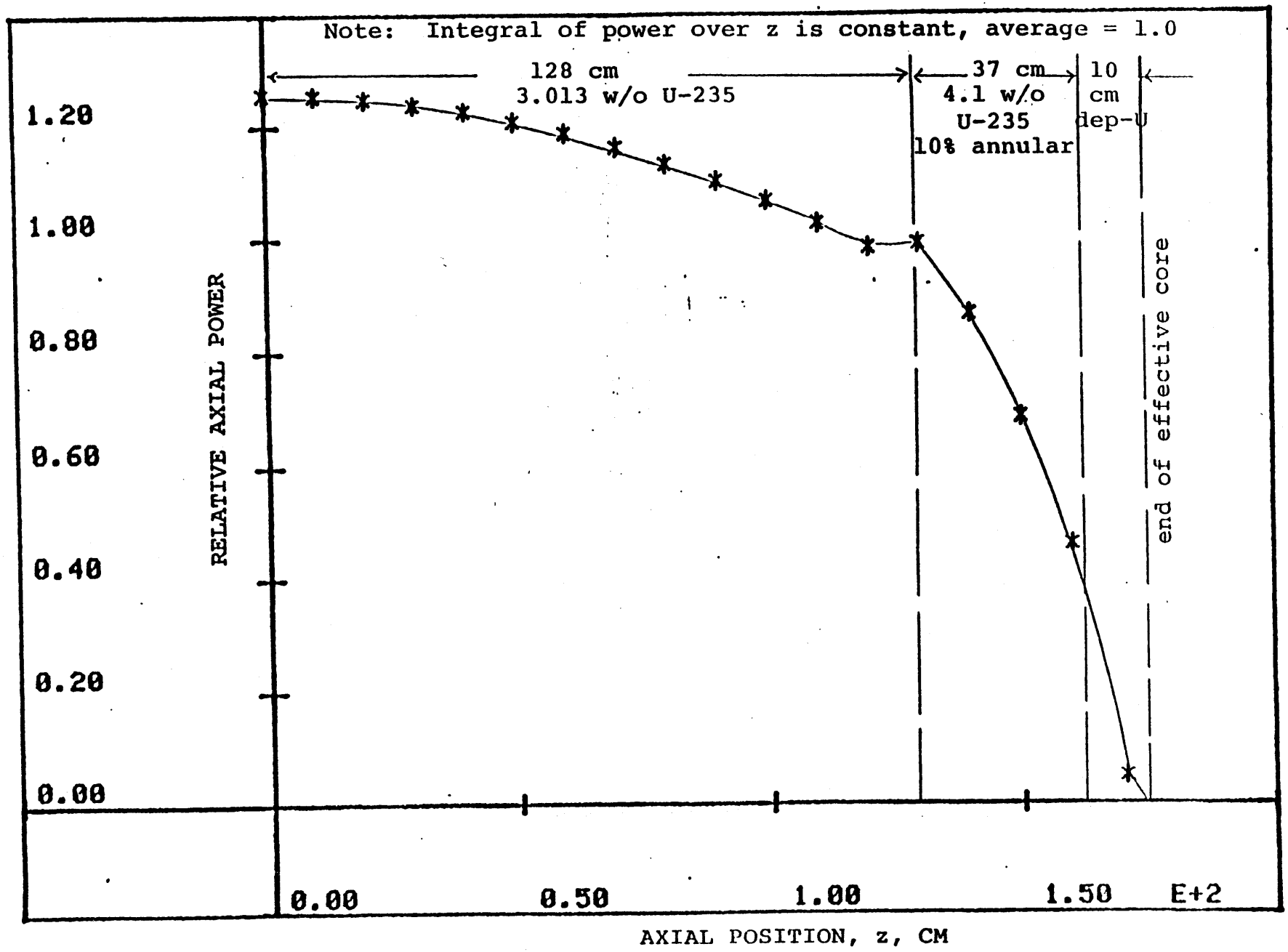

Figure 4.4 Axial Power Profile (BOL) for the Second Annular Zone Case

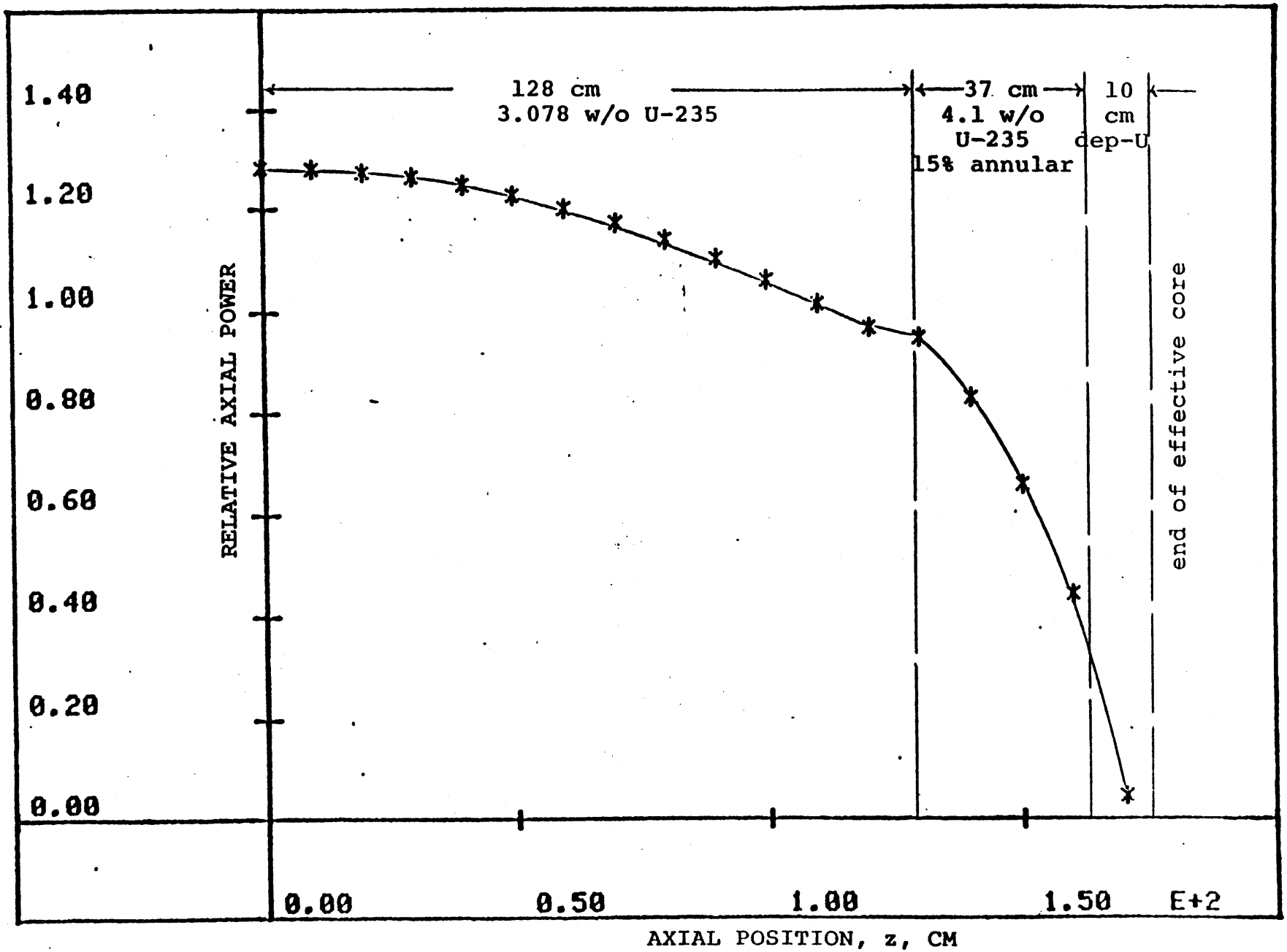

Figure 4.5 Axial Power Profile (BOL) for the Third Annular Zone Case

region peak is comparable to that of the other two cases. The advantages of the third case are analyzed in more detail in the next section using PDQ-7 depletion calculations.

4.3 Annular Zone Depletion

PDQ-7 depletion results for the annular zone case are described in this section. In this case 128 cm of 3.078 w/o U-235 occupied the central core region, 37 cm of the 15% annular region is next, while the last 10 cm of the core are comprised of a depleted uranium blanket (see Figure 4.2).

The depletion was carried out at constant total bundle power. Three time steps were used in the initial 1500 effective-full-power-hours (efph) and thereafter one time step per 1500 efph was used. The values of ρ_{eff} , k_{eff} , ρ_L and the axial peak-to-average power ratio, all as a function of efph, from the PDQ-7 depletion run are listed in Table 4.1.

A linear regression straight line fit (shown in Figure 4.6) to the (post-fission product saturation data) of reactivity as a function of efph gave a correlation coefficient of 0.998. The 3-batch reactivity-limited discharge efph (computed using the ρ=0 intercept) was 26122.5 hours. The power shapes at BOL and at different burnups are shown in Figure 4.7. Note that the power profile holds its shape quite well over life, especially after the first several thousand hours.

Table 4.1

Burnup Results for the Assembly Containing an Annular Zone

[128 cm @ 3.078 w/o U-235, 37 cm @ 4.1 w/o U-235 (15% annular) and 10 cm @ 0.2 w/o U-235]

Time (hours at full power)	ρ_{eff}	k_{eff}	ρ_L	Peak-to-Average Power Ratio
0	0.25117	1.33542	0.00341	1.254
125	0.22521	1.29067	0.00391	1.174
800	0.21691	1.27700	0.00381	1.202
1500	0.20998	1.26580	0.00415	1.139
3000	0.19421	1.24101	0.00489	1.152
4500	0.17710	1.21522	0.00537	1.161
6000	0.15929	1.18947	0.00593	1.178
7500	0.14101	1.16417	0.00634	1.164
9000	0.12225	1.13928	0.00681	1.160
10500	0.10306	1.11490	0.00717	1.141
12000	0.08324	1.09079	0.00758	1.131
13500	0.06282	1.06703	0.00793	1.112
15000	0.04155	1.04335	0.00832	1.094
16500	0.01955	1.01994	0.00881	1.091
18000	-0.00314	0.99690	0.00936	1.093
19500	-0.02674	0.97396	0.01005	1.105
21000	-0.05048	0.95194	0.01055	1.101
22500	-0.07273	0.93220	0.01050	1.076
24000	-0.09520	0.91307	0.01050	1.061
25500	-0.11705	0.89521	0.01100	1.093
27000	-0.13893	0.87802	0.01137	1.086
28500	-0.16073	0.86153	0.01157	1.096
30000	-0.18239	0.84574	0.01184	1.098

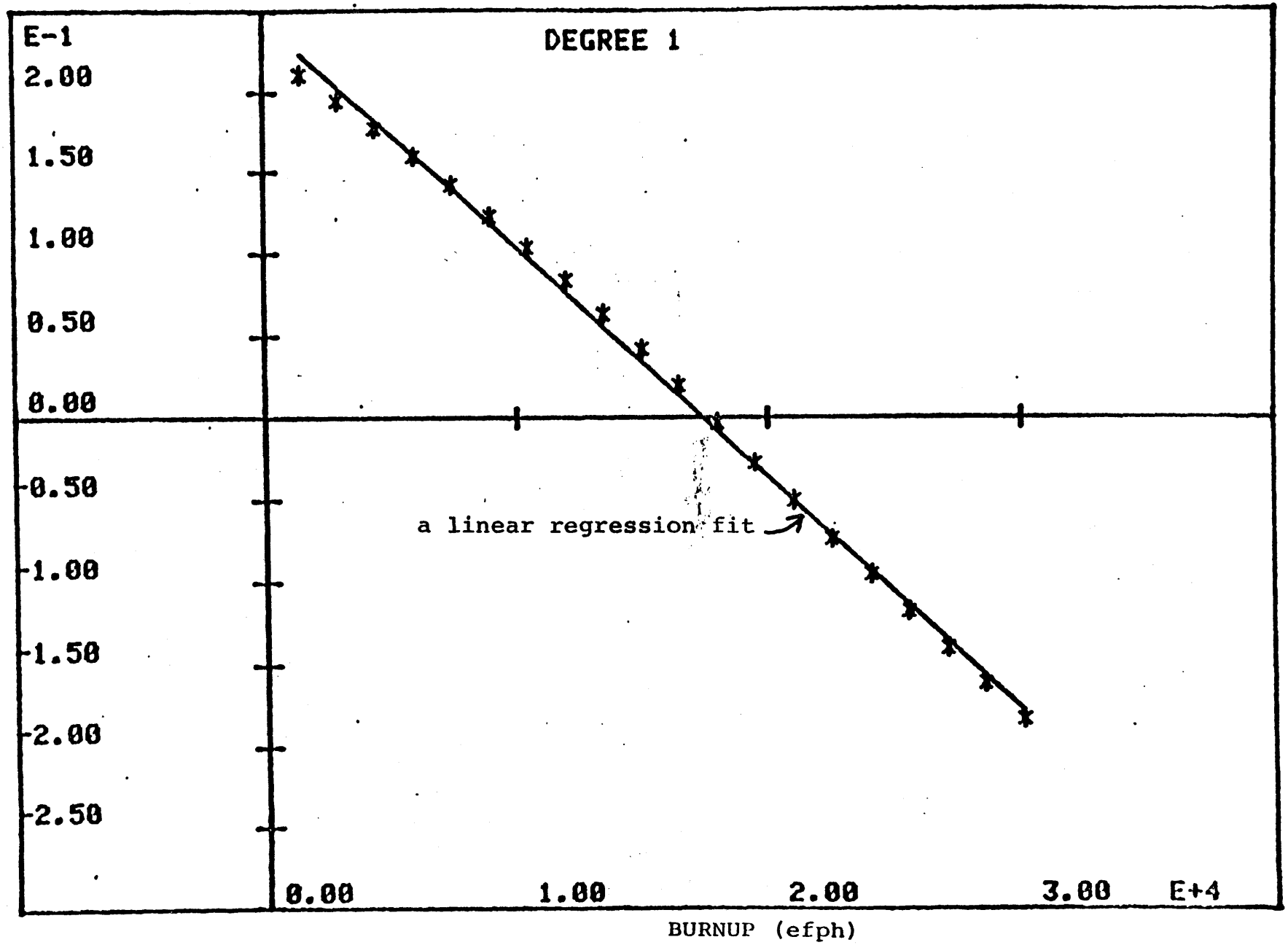

Figure 4.6 Reactivity as a Function of Burnup for the Zoned Annular Case

4.4 Comparison of Design Options

Table 4.2 shows the maximum/average power ratio at BOL for various test cases relative to the reference case. The blanket-only case has a higher axial peaking factor than the reference case at BOL. Cases with axial enrichment zones have much lower axial peaking factors than the reference case at BOL.

Table 4.3 shows the discharge time in hours at effective full power for the test cases relative to the reference case. Since the mass of natural uranium was kept the same for all cases, efph is a direct measure of uranium utilization. Case 3 (the design with axial enrichment zones) has a discharge time which is larger than the reference case, but less than that of the blanketed case. The annular zone case has a higher discharge time than the reference, and all the other, test cases.

The BOL k_{eff} for this annular case was 0.45% higher than that for the reference case. This is due to the redistribution of fuel from the ends to the central region (which has increased neutron importance) and to the reduced neutron leakage. Comparisons of the leakage reactivity for cases of interest are shown in Figure 4.8 and Figure 4.9. Note that the annularly-zoned case is always less leaky than the enrichment-zoned case, and while initially inferior to the blanket-only case, it burns into an equally good configuration..

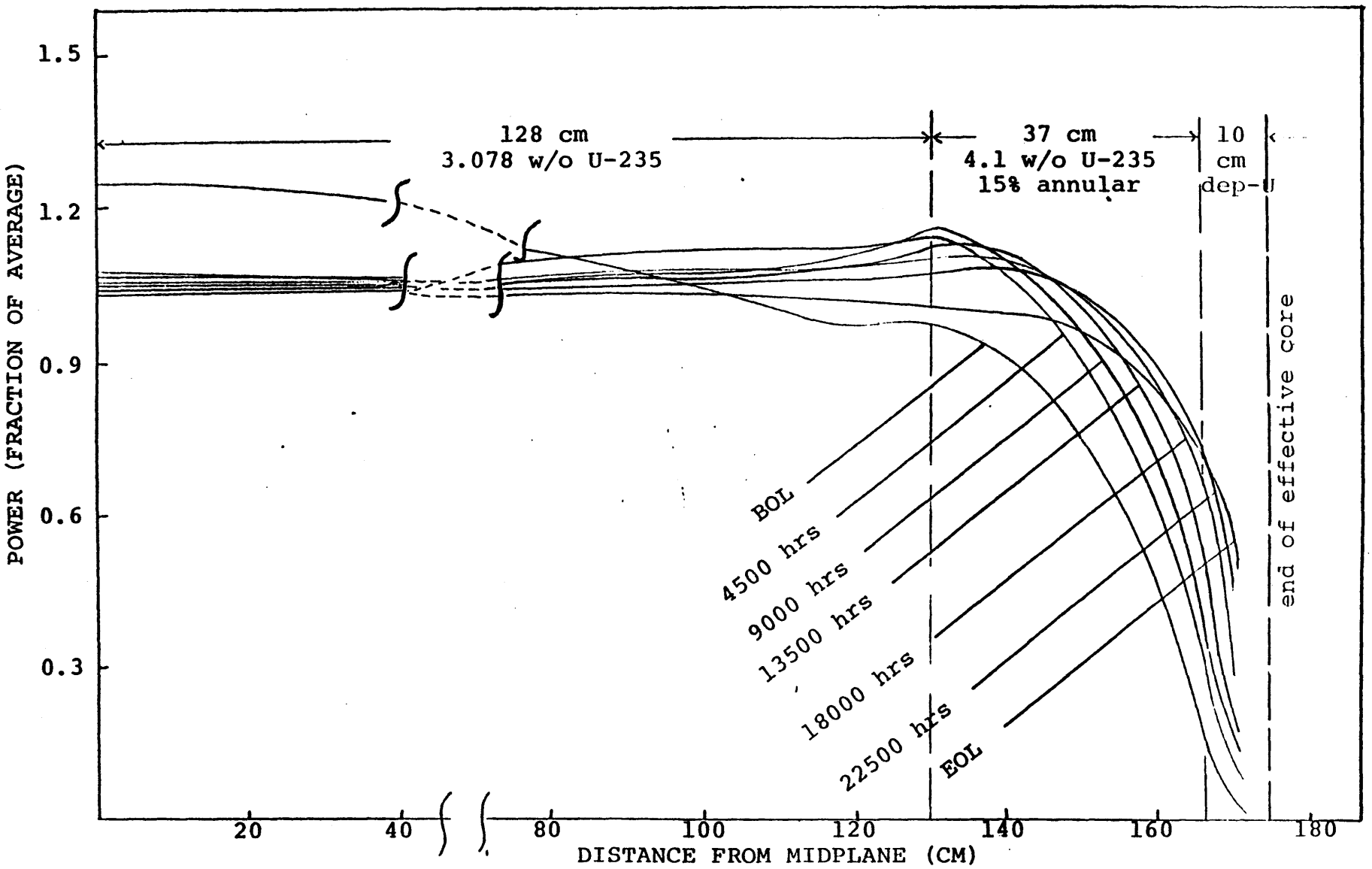

Figure 4.7 Axial Power Profiles for the Zoned Annular Case

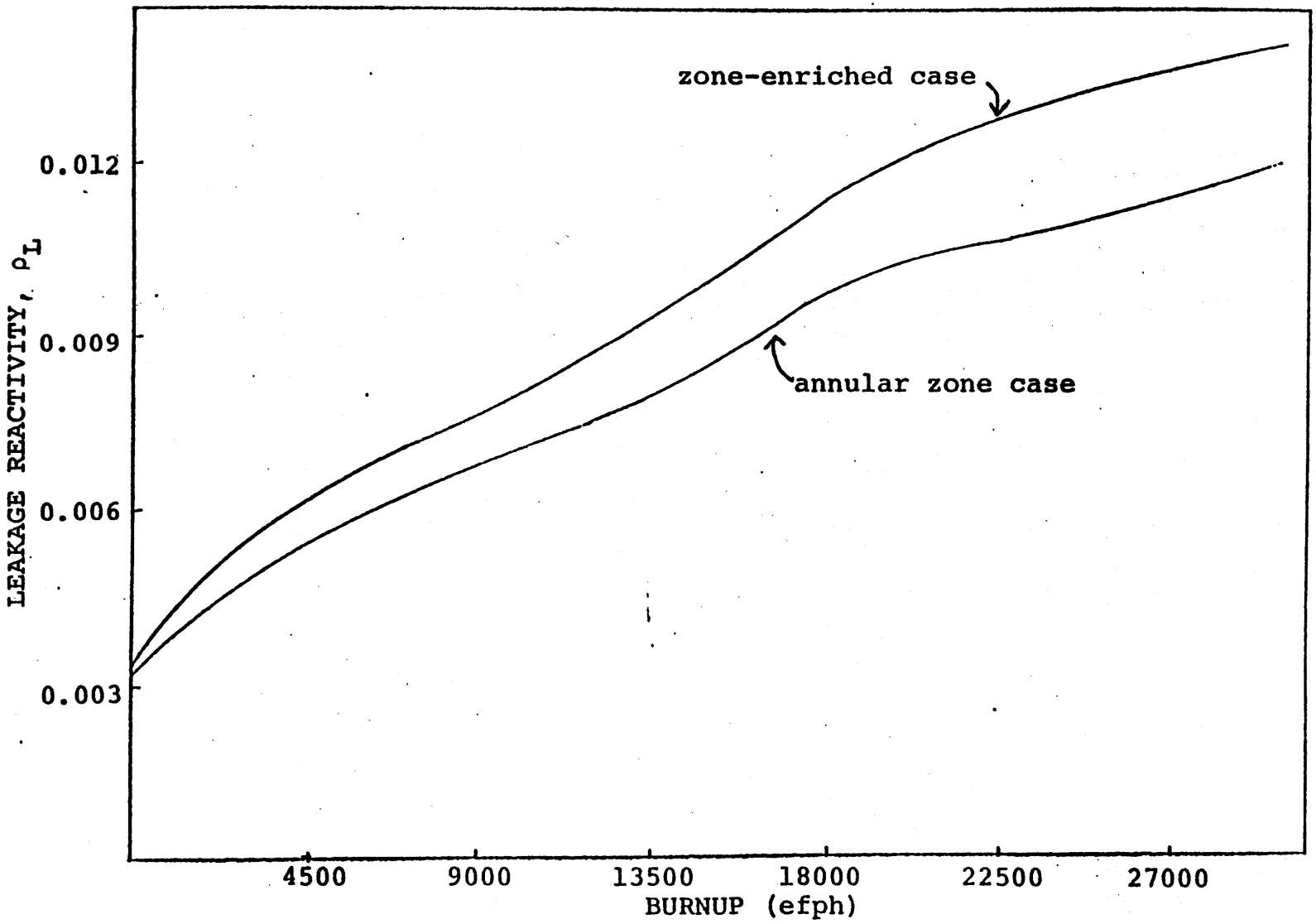

Figure 4.8 Leakage Reactivity, ρ_L , vs. Burnup for Zone-Enriched Case and Annular Case

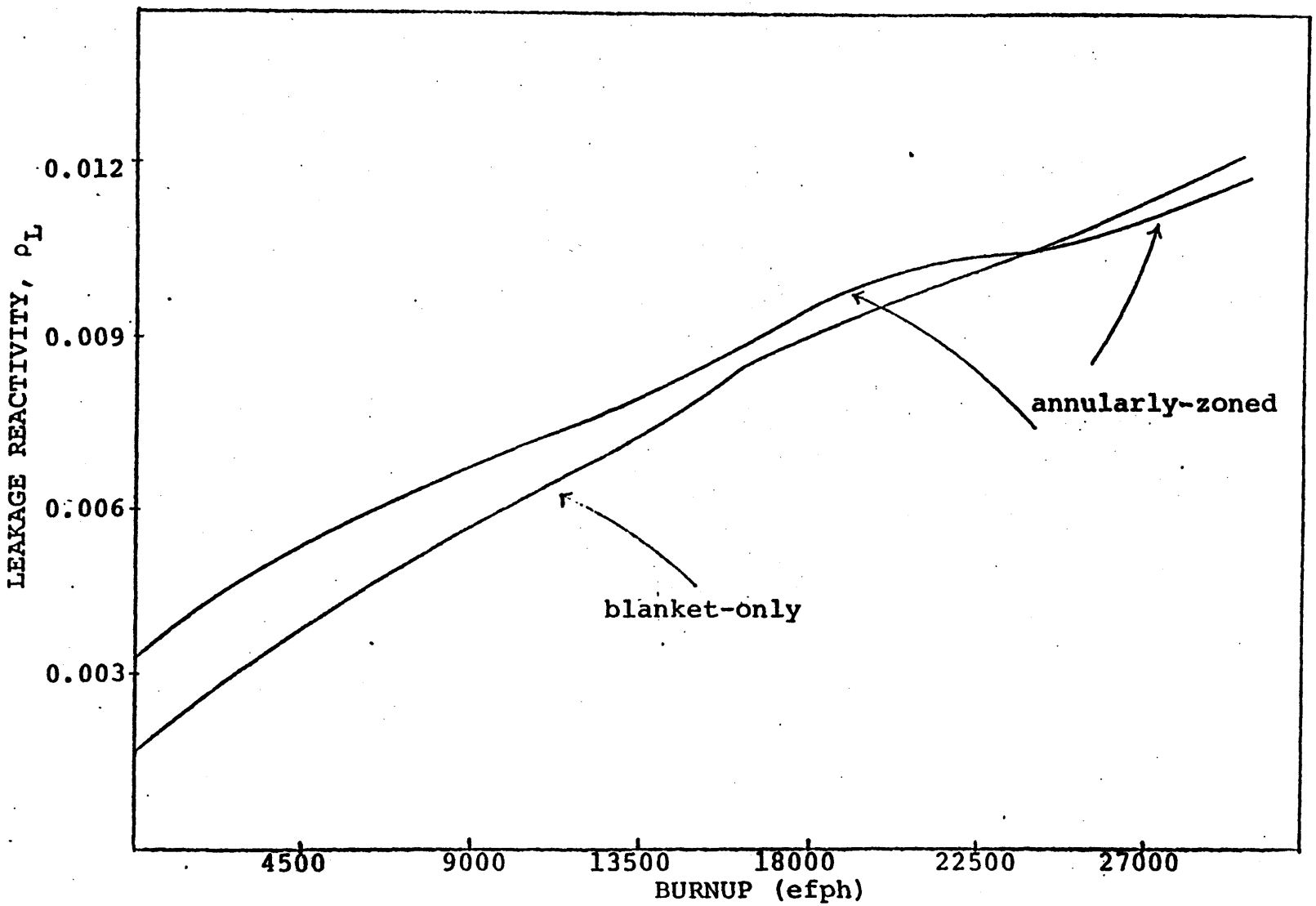

Figure 4.9 Leakage Reactivity, ρ_L , vs. Burnup (efph) for the Blanket-Only Case and the Annularly-Zoned Case

Table 4.2

Maximum/Average Power at BOL
for Various Test Cases Compared to the Reference Case

Case	Characteristics	Relative Maximum/ Average BOL Power*
1	3.0 w/o U-235, 175 cm, core (reference case)	1.000
2	3.1697 w/o U-235, 165 cm, core 0.2 w/o, 10 cm, blanket	1.044
3	2.9 w/o U-235, 128 cm, central zone 4.1 w/o, 37 cm, zone 2 0.2 w/o, 10 cm, blanket	0.807**
4	3.078 w/o U-235, 128 cm, central zone 4.1 w/o, 37 cm, 15% annular zone 0.2 w/o, 10 cm, blanket	0.835

* Maximum/average power divided by maximum/average power for the reference case.

** In case 3, power peaking at some subsequent times is more severe than BOL power peaking.

TABLE 4.3

Relative Discharge Time for Various Test Cases Compared to the Reference Case

Case	Characteristics	Relative Hours at Effective Full Power
1	3.0 w/o U-235, 175 cm, core (reference case)	1.000
2	3.1697 w/o U-235, 165 cm, core 0.2 w/o, 10 cm, blanket	1.024
3	2.9 w/o U-235, 128 cm, central zone 4.1 w/o, 37 cm, zone 2 0.2 w/o, 10 cm, blanket	1.014
4	3.078 w/o U-235, 128 cm, central zone 4.1 w/o, 37 cm, 15% annular zone 0.2 w/o, 10 cm, blanket	1.028

4.5 Chapter Summary

In this chapter, the combination of axial enrichment zoning with an annular fuel region was analyzed to reduce power peaking and to hold the power shape over life.

Static diffusion calculations were performed for three configurations having the same zone dimensions as case 3 (a case analyzed in the previous chapter), but different annulus size and, accordingly, different enrichments.

PDQ-7 depletion analyses, performed for the most promising configuration, showed that the discharge time is 2.8% higher than the reference case. This improvement is even more than in the blanket-only case. At the same time, the BOL power peaking (the limiting point in core life) is 16.5% less than that in the reference case and 20% less than that in the blanketed case. Furthermore, the power profile of this annular case holds its shape quite well over life.

CHAPTER 5

SUMMARY, CONCLUSIONS AND RECOMMENDATIONS

5.1 Introduction

It is desirable to extend uranium resources by optimizing current generation LWRs to use uranium as efficiently as possible on the once through fuel cycle, and preferably in ways compatible with recycle as well.

Increasing burnup and improving neutron economy are the principal means to reduce the consumption of uranium, and several approaches have been proposed to realize these goals (D-2). The objective of the present work was to investigate optimization of axial composition and power profiles, a strategy which improves thermal margins (thereby facilitating high burnup) and neutron economy (through the use of blankets). The focus has been on changes which do not involve large expenditures for their implementation and which could be retrofitted into current PWRs.

5.2 Background and Research Objectives

Some years ago the use of axial blankets was proposed to reduce leakage in BWRs. The benefits of this modification were subsequently demonstrated, and axial blankets have now been incorporated in newer BWR core designs. In PWRs, on the other hand, not much work has been done as far as axial power shaping is concerned. Many investigators, both at M.I.T. (F-1, K-1, S-1) and elsewhere (M-3, C-5, R-2) have shown that improvements in axial fuel design could result in ore saving in LWRs. For example, an analysis by Babcock and Wilcox (H-4)

indicated that 4% of the natural uranium feedstock can be saved by using a 9-inch natural uranium blanket on both ends of the core. However, a concurrent axial power peaking increase was found to occur, which reduces core thermal margins, and thereby forces a difficult tradeoff between economic and safety concerns.

Motivated by the above situation, the purpose of the present work was to find the optimum axial distribution of fuel enrichment with respect to uranium utilization, as a guide to design strategy, and upon this base to seek more benign ways to realize the target configuration.

This general goal of the present work had the following specific subtasks:

1. Determination of an optimum power shape through analytical methods.
2. Determination of reactivity and enrichment profiles which would give this optimum power shape.
3. Investigation of enrichment zones at beginning-of-cycle which will give this target power profile.
4. Verification of the suitability of candidate zoning arrangements over assembly burnup lifetime using the PDQ-7 depletion code, and finally,
5. Investigation of the use of an annular fuel region to remedy some of the shortcomings evidenced in the preceding stages.

5.3 Computational Methods Used

The present work relied mainly on the LEOPARD, CHIMP and PDQ-7 codes. LEOPARD was used to perform zero-dimensional depletion calculations to give spectrum-averaged cross sections at different time steps. These cross sections were processed by CHIMP to prepare microscopic and macroscopic tables for different fuel regions, to be used during PDQ-7 depletion analyses.

A small computer program was also developed to determine the optimum power profile using the so called "linear reactivity model" (S-1) and a fast neutron leakage kernel. The "group and one-half model" of neutron diffusion was used to determine continuously variable reactivity and enrichment profiles which have this optimum power shape. On the basis of this enrichment profile, simplified three zone axial enrichment profiles were developed and the resulting assembly designs were modeled on the PDQ-7 code for one-dimensional depletion analyses. Figure 5.1 shows the optimum axial power and enrichment profiles, and a simplified flat central zone/ cosine-ends arrangement which achieves the same (within 0.017%) enhancement in discharge burnup.

5.4 Results

A one-dimensional (axial) model of one half of a typical PWR fuel assembly was defined as a reference case. This assembly was based on the Maine Yankee Reactor. The reference

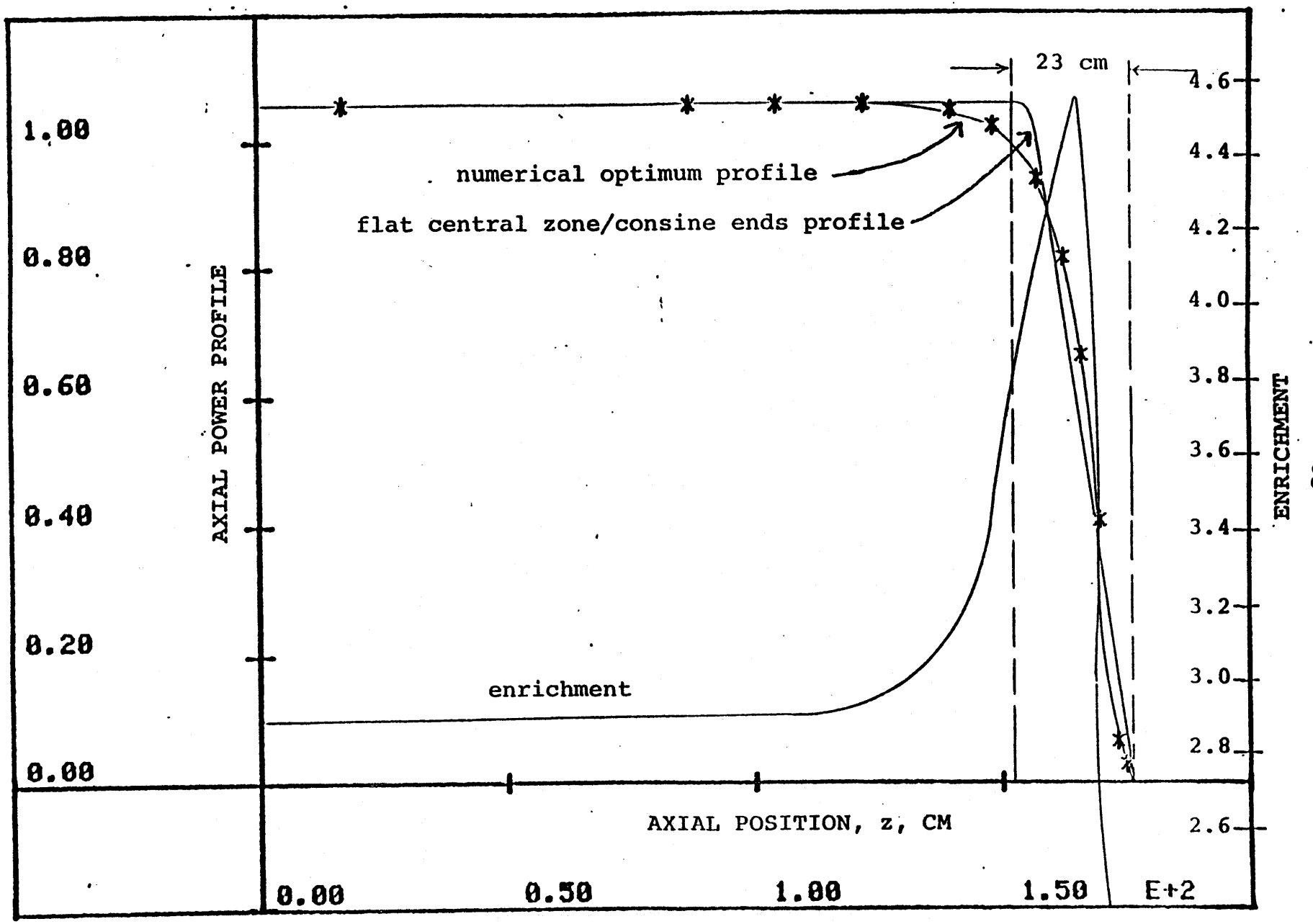

Figure 5.1 Optimum Axial Power and Enrichment Profiles, and Optimum Flat Central Zone/Cosine-Ends Profile

case configuration is shown in Figure 5.2 along with the configurations of the modified assembly designs investigated in the present work. The natural uranium consumption and total effective fuel length for each of the modified designs was kept the same as in the reference case to permit direct comparisons to be made.

The maximum/average power ratio at BOL and discharge time in hours at effective full power are tabulated for the various test cases relative to the reference case in Table 5.1. This table summarizes the main results obtained in this work.

Figure 5.3 shows the power evolution over life for the best configuration identified in the present work: a 3-zone core in which the outer zone is a depleted uranium blanket, and annular fuel pellets are used in the next zone which also has a higher enrichment than the large central region.

5.5 Conclusions

The following main conclusions can be drawn from the results of this study.

1. As few as three zones of enrichment (one of which is a depleted uranium blanket) can give results which are very close to an optimum solution.
2. An increase of 2.4% in discharge time (efph) can be achieved by using short (10 cm) axial blankets of depleted uranium. But this increase is at the expense of a 4.4% increased BOL power peaking.

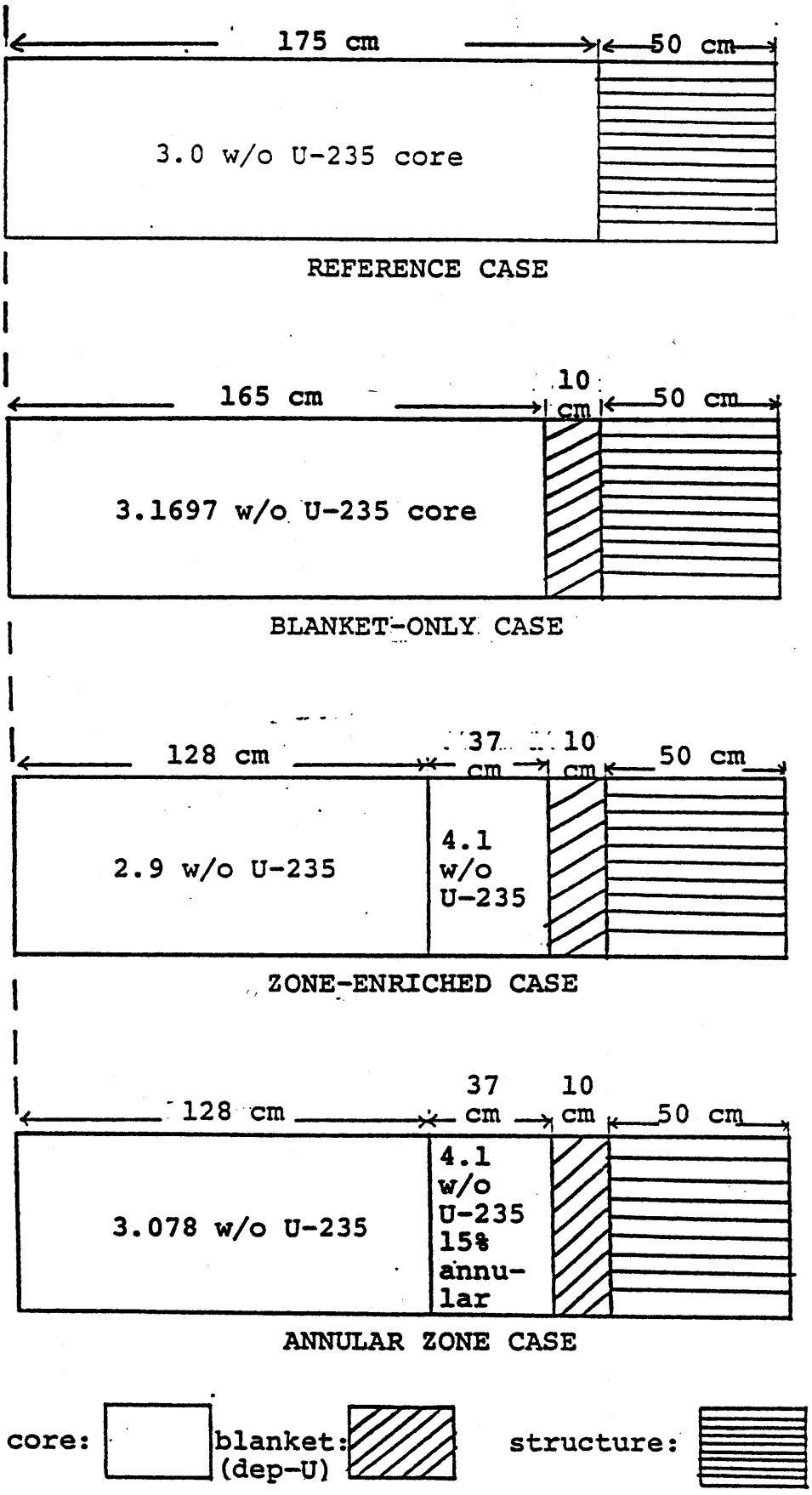

Figure 5.2 Assembly Designs Compared for Burnup Results

Table 5.1

Maximum/Average Power at BOL and Discharge Time
for Various Cases Relative to the Reference Case

Case	Characteristics	Relative Hours at Effective Full Power	Relative Maximum/ Average BOL Power
1	3.0 w/o U-235, 175 cm, core (reference case)	1.000	1.000
2	3.1697 w/o U-235, 165 cm, core 0.2 w/o, 10 cm blanket	1.024	1.044
3	2.9 w/o U-235, 128 cm, central zone 4.1 w/o, 37 cm, zone 2 0.2 w/o, 10 cm, blanket	1.014	0.807*
4	3.078 w/o U-235, 128 cm, central zone 4.1 w/o, 37 cm, 15% annular zone 0.2 w/o, 10 cm, blanket	1.028	0.835

* Power peaking is more severe in some subsequent time intervals than at the BOL in this particular case.

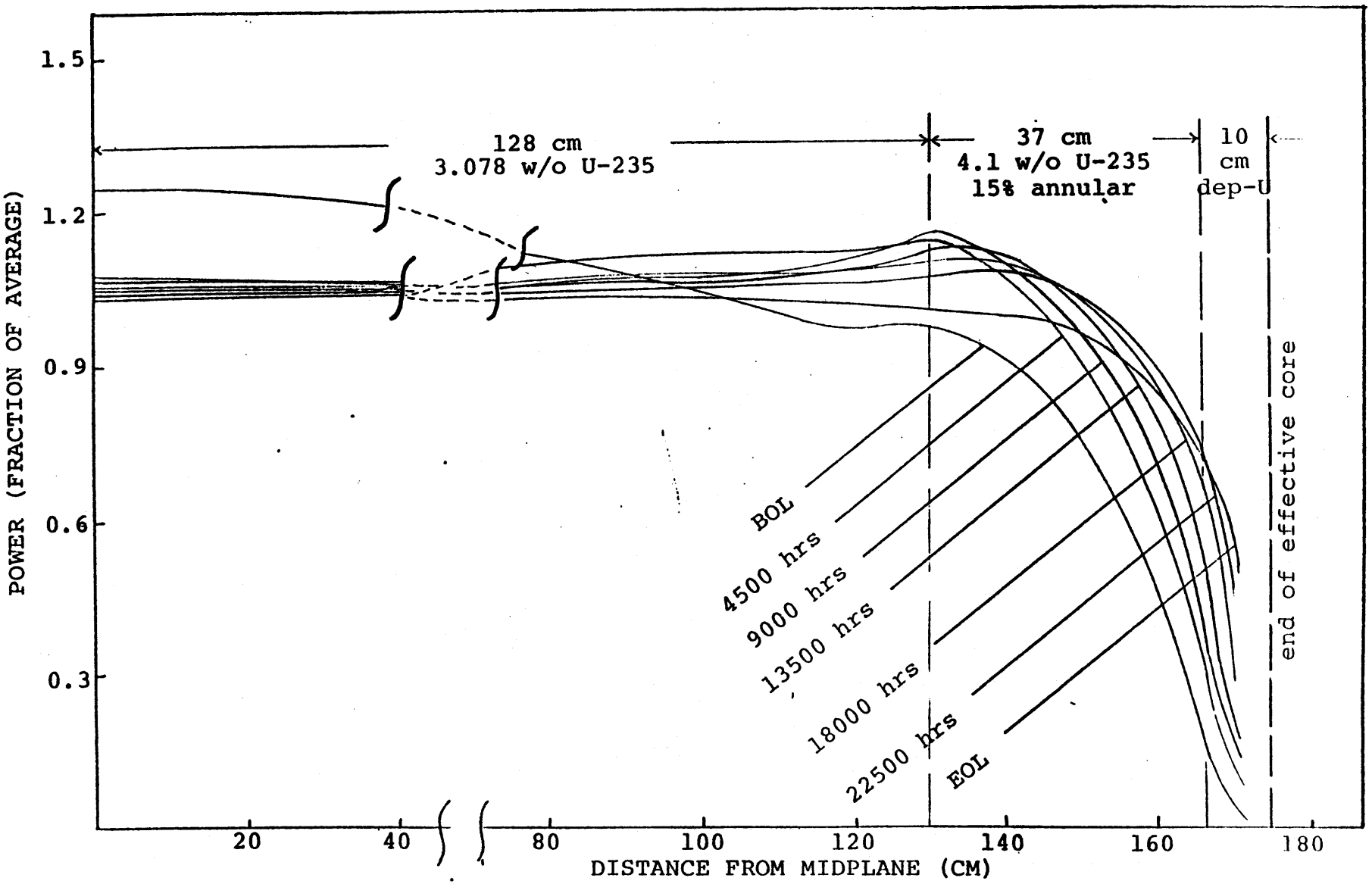

Figure 5.3 Power Evolution Over Life for the Best Configuration Identified

3. The problem of power peaking can be solved by using enrichment zones. The BOL peak-to-average power ratio for a representative axially-zoned case was found to be 19.3% and 22.7% less than that of the reference and blanketed cases, respectively. However, the discharge time for this case is 1.0% less than that in the blanketed case (but still 1.36% higher than the reference case). It also exhibits an undesirable tendency to burn into an end-peaked power profile late in life.
4. The use of annular fuel in the outer enrichment zone is an effective means of devising an assembly which holds a near-optimum power profile over its entire in-core residency.
5. The discharge time (hence uranium utilization) for the annularly-zoned case was found to be 2.8% higher than the reference case. This improvement is even more than that achieved by the blanket-only case. At the same time the BOL power peaking is 16.5% and 20.0% less than that in the reference and blanketed cases, respectively.

5.6 Recommendations for Future Work

The present work has identified an axial assembly design employing enrichment zoning, blankets and the use of annular fuel pellets over part of the core length, which has the attractive features of saving uranium and holding a

well-flattened power shape over its burnup lifetime. As such, it deserves further consideration as a PWR core design option. Based upon the results obtained here, follow-on work in several areas is suggested.

1. The economic tradeoff between increased fuel pin complexity and uranium savings should be quantified. Comparisons should be made to designs which employ zoned burnable poison to achieve power flattening, both for blanketed cores and for low-leakage fuel management schemes. BWR experience in the use of fuel having several axial composition zones should be taken into account. Full advantage of the lower power peaking should be taken, perhaps by shortening the core.
2. Additional case studies should be done, varying the dimensions and composition of the blanket and annular-enriched zones. The limited number of configurations studied here have not necessarily identified the overall best arrangement. More sophisticated analyses are also in order, which consider:
   a. The slightly asymmetric nature of the PWR core due to the decrease in coolant density as a function of axial distance from the assembly inlet, and to the different compositions of the inlet and outlet regions with respect to water, steel and control poison content.

b. Thermal-hydraulic design constraints under steady-state, transient and accident situations. (Appendix C documents some elementary considerations along these lines.)

3. **Finally, a full-fledged multi-cycle core burnup study should be carried out.**

APPENDIX A

OPTIMUM POWER AND CORRESPONDING ENRICHMENT PROFILES

A.1 Introduction

In Chapter 2, the linear reactivity model was applied to relate average assembly burnup, $\bar{B}$, with leakage reactivity, ρ_L , and power shape, f(z), as

$$\bar{B} = \frac{\bar{\rho}_o - \rho_L}{2bA \int_{-b}^{b} f^2(z)\,dz} \qquad (2.7)$$

The integral in the denominator is minimized when f(z) is uniform, but because of its higher leakage (i.e., ρ_L) this uniform power profile is not optimum with respect to $\bar{B}$. This leakage vs. power-squared trade-off leads to an optimum f(z). A simple computer program was written to optimize the axial power profile using burnup as an objective function. A flow chart of the iterative methodology has already been shown in Figure 2.1. The group and one-half model (see Chapter 2) was then used to find the reactivity profile corresponding to this optimum power profile.

A.2 Input/Output

In the subject program, the core is divided into 'N' evenly distributed mesh points in the axial direction. A flat power profile is used as the initial input guess. Other input values employed in the representative case examined in Chapter 2 were:

half core axial length (BL) = 175.26 cm

number of mesh points (N) = 100

migration length (XM) = 7.45 cm

initial reactivity (ρ_o) = 0.2

slope of reactivity vs. burnup (A) = 0.91 E-05

The approach followed in the program is rather straightforward. After making a local change in the flat power profile, the global effect on the burnup is computed for each mesh point. In the next step the profile is modified at each point according to the corresponding partial changes computed in the previous step, using an empirical algorithm. This process is repeated until no further increase in the discharge burnup is found.

The listing of the computer program and a sample output follow in Tables A.1, A.2 and A.3.

The optimum power profile determined in this manner was shown in Figure 2.2. The burnup for this optimum shape is 15.5% greater than the burnup associated with a cosine power shape, and 3.6% higher than the burnup generated by a flat power shape. Reactivity and enrichment profiles output by this program were plotted in Figure 2.3.

Table A.1

Program to Determine Axial Power Profile

```
C       ALGORITHM FOR  DETERMINATION OF OPTIMUM AXIAL POWER SHAPE          BLA00010
        DIMENSION FG(100),ALFA(100),FGG(100),FLUX(100),X(100),R(100)       BLA00020
        COMMON  XM,A,BL,RO,H,RL,CSI                                        BLA00030
        A=.91E-05                                                          BLA00040
        FACTOR=50.0                                                        BLA00050
        BL=175.26                                                          BLA00060
        N=100                                                              BLA00070
        RO=.20                                                             BLA00080
        XM=7.45                                                            BLA00090
        IT=0                                                               BLA00100
19      K=1                                                                BLA00110
        XN=N                                                               BLA00120
        H=BL/XN                                                            BLA00130
        DO 1 I=1,N                                                         BLA00140
 1      FG(I)=1.0                                                          BLA00150
        CALL FNORM(FG,N)                                                   BLA00160
        CALL BURNUP(FG,BO,N)                                               BLA00170
 2      DO3 I=1,N                                                          BLA00180
 3      FGG(I)=FG(I)                                                       BLA00190
        GAMA=.95                                                           BLA00200
        DO 5 I=1,N                                                         BLA00210
        FGG(I)=GAMA*FGG(I)                                                 BLA00220
        CALL FNORM(FGG,N)                                                  BLA00230
        CALL BURNUP(FGG,B,N)                                               BLA00240
        ALFA(I)=(B-BO)/(BO*(FGG(I)-FG(I))/FG(I))                           BLA00250
        FGG(I)=FGG(I)/GAMA                                                 BLA00260
 5      CONTINUE                                                           BLA00270
        DO 10 I=1,N                                                        BLA00280
 10     FG(I)=FG(I)*EXP(FACTOR*ALFA(I))                                    BLA00290
        CALL FNORM(FG,N)                                                   BLA00300
        CALL BURNUP(FG,B,N)                                                BLA00310
        WRITE(6,120)RL,CSI                                                 BLA00320
        WRITE(6,110)(FG(I),I=1,N),B,K                                      BLA00330
130     FORMAT(10(10E12.4/))                                               BLA00340
C       DELTAB=ABS((B-BO)/BO)                                              BLA00350
        IF(DELTAB.LT..1E-08.OR.K.GE.50)GO TO 15                            BLA00360
        K=K+1                                                              BLA00370
        BO=B                                                               BLA00380
        GO TO 2                                                            BLA00390
120     FORMAT('  RL=',E12.4,' CSI=',E12.4)                                BLA00400
110     FORMAT(10(10E12.4/),/' BURNUP=',E15.8,/'  NO. OF ITTERATION=',I4)  BLA00410
15      D=3.497                                                            BLA00420
        XLEMDA=1.0/(1.0-RO)                                                BLA00430
        SUM=0.0                                                            BLA00440
        DO 4 I=1,100                                                       BLA00450
4       SUM=SUM+FG(I)                                                      BLA00460
        DO 6 I=1,100                                                       BLA00470
6       FG(I)=.5*FG(I)/(SUM*1.7526)                                        BLA00480
        SUM1=0.0                                                           BLA00490
        DO 20 I=1,100                                                      BLA00500
       XI=I                                                                BLA00510
       SUM2=0.0                                                            BLA00520
       DO 30 J=1,200                                                       BLA00530
       XJ=J                                                                BLA00540
       Y=(XI-XJ+.5)*H+BL                                                   BLA00550
```

```
      IF(J.LE.100)K=101-J                                              BLA00560
      IF(J.GT.100)K=J-100                                              BLA00570
      SUM2=SUM2+EXP(-ABS(Y)/XM)*FG(K)                                  BLA00580
   30 CONTINUE                                                         BLA00590
      FLUX(I)=.5*XM*XLEMDA/D*SUM2*H                                    BLA00600
      SUM1=SUM1+FLUX(I)                                                BLA00610
   20 CONTINUE                                                         BLA00620
      XK=(1.0-RO)/(SUM1*H*2.0)                                         BLA00630
      DO 40 I=1,100                                                    BLA00640
      R(I)=1.0-XK*FLUX(I)/FG(I)                                        BLA00650
      X(I)=10.0*R(I)+1.0                                               BLA00660
   40 CONTINUE                                                         BLA00670
      WRITE(6,105)                                                     BLA00680
  105 FORMAT(' REGION  POWER-FACTORS    FLUX-SHAPE    REACTIVITY    EN  BLA00690
     1RICHMENT      ')                                                 BLA00700
      DO 50 I=1,100                                                    BLA00710
   50 WRITE(6,115)I,FG(I),FLUX(I),R(I),X(I)                            BLA00720
  115 FORMAT(2X,I5,4E14.4)                                             BLA00730
      SUM3=0.0                                                         BLA00740
      DO 60 I=1,100                                                    BLA00750
   60 SUM3=SUM3+FG(I)*R(I)                                             BLA00760
      RO=H*SUM3*2.0                                                    BLA00770
      WRITE(6,125)RO                                                   BLA00780
  125 FORMAT('      RO=',E12.4)                                        BLA00790
      STOP                                                             BLA00800
      END                                                              BLA00810
C     ------------------------------------------------------------     BLA00820
C     NORMALIZATION OF POWER  FACTORS                                  BLA00830
      SUBROUTINE FNORM(X,N)                                            BLA00840
      DIMENSION X(100)                                                 BLA00850
      SUM=0.0                                                          BLA00860
      DO 10 I=1,N                                                      BLA00870
   10 SUM=SUM+X(I)                                                     BLA00880
      DO 20 I=1,N                                                      BLA00890
   20 X(I)=0.5*X(I)/(SUM*1.7526)                                       BLA00900
      RETURN                                                           BLA00910
      END                                                              BLA00920
C     ------------------------------------------------------------     BLA00930
C     CALULATION OF BURN UP                                            BLA00940
      SUBROUTINE BURNUP(FG,B,N)                                        BLA00950
      DIMENSION FG(100)                                                BLA00960
      COMMON XM,A,BL,RO,H,RL,CSI                                       BLA00970
      RL=0.0                                                           BLA00980
      CSI=0.0                                                          BLA00990
      DO 10 I=1,N                                                      BLA01000
      XI=I                                                             BLA01010
      XN=N                                                             BLA01020
      CSI=CSI+FG(I)**2.                                                BLA01030
      RL=RL+FG(I)*(EXP((XI-XN)*H/XM)-EXP(H*((XI-1.)-XN)/XM))           BLA01040
   10 CONTINUE                                                         BLA01050
      RL=RL*XM                                                         BLA01060
      B=(RO-RL)/(A*CSI*4.*H*BL)                                        BLA01070
      RETURN                                                           BLA01080
      END                                                              BLA01090
```

Table A.2

Initial and Final Results for the Optimum Power Profile

RL= 0.1193E-01 CSI= 0.8289E-03

0.3000E-02	0.2982E-02	0.2971E-02	0.2999E-02	0.2982E-02	0.2971E-02	0.2999E-02	0.2982E-02	0.2971E-02	0.2999E-02
0.2982E-02	0.2971E-02	0.2999E-02	0.2982E-02	0.2971E-02	0.2999E-02	0.2982E-02	0.2971E-02	0.2999E-02	0.2982E-02
0.2971E-02	0.2999E-02	0.2982E-02	0.2971E-02	0.2999E-02	0.2982E-02	0.2971E-02	0.3000E-02	0.2982E-02	0.2971E-02
0.3000E-02	0.2982E-02	0.2971E-02	0.3000E-02	0.2982E-02	0.2971E-02	0.3000E-02	0.2982E-02	0.2971E-02	0.3000E-02
0.2982E-02	0.2971E-02	0.3000E-02	0.2982E-02	0.2971E-02	0.3000E-02	0.2982E-02	0.2971E-02	0.3000E-02	0.2982E-02
0.2971E-02	0.3000E-02	0.2982E-02	0.2971E-02	0.3000E-02	0.2982E-02	0.2971E-02	0.2999E-02	0.2982E-02	0.2971E-02
0.2999E-02	0.2982E-02	0.2971E-02	0.2999E-02	0.2981E-02	0.2971E-02	0.2998E-02	0.2980E-02	0.2970E-02	0.2996E-02
0.2978E-02	0.2967E-02	0.2993E-02	0.2974E-02	0.2961E-02	0.2986E-02	0.2966E-02	0.2951E-02	0.2973E-02	0.2948E-02
0.2930E-02	0.2945E-02	0.2915E-02	0.2887E-02	0.2891E-02	0.2846E-02	0.2802E-02	0.2783E-02	0.2713E-02	0.2637E-02
0.2578E-02	0.2462E-02	0.2332E-02	0.2207E-02	0.2023E-02	0.1818E-02	0.1611E-02	0.1358E-02	0.1099E-02	0.8514E-03

BURNUP= 0.20293629E+05
NO. OF ITTERATION= 1

RL= 0.8293E-02 CSI= 0.8426E-03

0.3022E-02	0.3022E-02	0.3024E-02	0.3020E-02	0.3026E-02	0.3023E-02	0.3020E-02	0.3020E-02	0.3022E-02	0.3022E-02
0.3023E-02	0.3018E-02	0.3021E-02	0.3023E-02	0.3020E-02	0.3025E-02	0.3013E-02	0.3028E-02	0.3018E-02	0.3023E-02
0.3025E-02	0.3016E-02	0.3027E-02	0.3018E-02	0.3025E-02	0.3019E-02	0.3023E-02	0.3019E-02	0.3021E-02	0.3020E-02
0.3021E-02	0.3019E-02	0.3021E-02	0.3022E-02	0.3020E-02	0.3020E-02	0.3019E-02	0.3019E-02	0.3021E-02	0.3019E-02
0.3021E-02	0.3021E-02	0.3022E-02	0.3021E-02	0.3024E-02	0.3019E-02	0.3022E-02	0.3021E-02	0.3021E-02	0.3023E-02
0.3021E-02	0.3021E-02	0.3021E-02	0.3021E-02	0.3024E-02	0.3019E-02	0.3023E-02	0.3021E-02	0.3019E-02	0.3021E-02
0.3023E-02	0.3018E-02	0.3022E-02	0.3023E-02	0.3019E-02	0.3023E-02	0.3022E-02	0.3019E-02	0.3021E-02	0.3019E-02
0.3020E-02	0.3011E-02	0.3020E-02	0.3011E-02	0.3012E-02	0.3009E-02	0.3007E-02	0.2999E-02	0.2996E-02	0.2987E-02
0.2977E-02	0.2969E-02	0.2959E-02	0.2931E-02	0.2915E-02	0.2892E-02	0.2855E-02	0.2810E-02	0.2748E-02	0.2679E-02
0.2586E-02	0.2466E-02	0.2321E-02	0.2133E-02	0.1893E-02	0.1579E-02	0.1167E-02	0.5906E-03	0.1879E-03	0.7795E-04

BURNUP= 0.20350344E+05
NO. OF ITTERATION= 50

Table A.3

Optimum Power, Reactivity and Enrichment Profiles Generated by the Program Listed in Table A.1

REGION	POWER-FACTORS	FLUX-SHAPE	REACTIVITY	EN RICHMENT
1	0.3022E-02	0.5977E-01	0.1897E+00	0.2897E+01
2	0.3022E-02	0.5977E-01	0.1897E+00	0.2897E+01
3	0.3024E-02	0.5977E-01	0.1902E+00	0.2902E+01
4	0.3020E-02	0.5977E-01	0.1891E+00	0.2891E+01
5	0.3027E-02	0.5977E-01	0.1910E+00	0.2910E+01
6	0.3023E-02	0.5976E-01	0.1900E+00	0.2900E+01
7	0.3020E-02	0.5976E-01	0.1893E+00	0.2893E+01
8	0.3020E-02	0.5976E-01	0.1893E+00	0.2893E+01
9	0.3022E-02	0.5976E-01	0.1898E+00	0.2898E+01
10	0.3022E-02	0.5976E-01	0.1898E+00	0.2898E+01
11	0.3024E-02	0.5976E-01	0.1904E+00	0.2904E+01
12	0.3018E-02	0.5975E-01	0.1888E+00	0.2888E+01
13	0.3021E-02	0.5976E-01	0.1896E+00	0.2896E+01
14	0.3024E-02	0.5975E-01	0.1904E+00	0.2904E+01
15	0.3020E-02	0.5975E-01	0.1893E+00	0.2893E+01
16	0.3025E-02	0.5975E-01	0.1907E+00	0.2907E+01
17	0.3013E-02	0.5975E-01	0.1875E+00	0.2875E+01
18	0.3029E-02	0.5976E-01	0.1917E+00	0.2917E+01
19	0.3018E-02	0.5975E-01	0.1888E+00	0.2888E+01
20	0.3023E-02	0.5976E-01	0.1901E+00	0.2901E+01
21	0.3025E-02	0.5975E-01	0.1907E+00	0.2907E+01
22	0.3016E-02	0.5975E-01	0.1883E+00	0.2883E+01
23	0.3027E-02	0.5975E-01	0.1912E+00	0.2912E+01
24	0.3018E-02	0.5975E-01	0.1889E+00	0.2889E+01
25	0.3025E-02	0.5975E-01	0.1907E+00	0.2907E+01
26	0.3019E-02	0.5975E-01	0.1892E+00	0.2892E+01
27	0.3023E-02	0.5974E-01	0.1903E+00	0.2903E+01
28	0.3019E-02	0.5974E-01	0.1893E+00	0.2893E+01
29	0.3021E-02	0.5974E-01	0.1898E+00	0.2898E+01
30	0.3020E-02	0.5974E-01	0.1896E+00	0.2896E+01
31	0.3021E-02	0.5974E-01	0.1899E+00	0.2899E+01
32	0.3019E-02	0.5974E-01	0.1893E+00	0.2893E+01
33	0.3021E-02	0.5974E-01	0.1899E+00	0.2899E+01
34	0.3022E-02	0.5973E-01	0.1901E+00	0.2901E+01
35	0.3020E-02	0.5973E-01	0.1896E+00	0.2896E+01
36	0.3020E-02	0.5973E-01	0.1897E+00	0.2897E+01
37	0.3019E-02	0.5973E-01	0.1894E+00	0.2894E+01
38	0.3019E-02	0.5973E-01	0.1894E+00	0.2894E+01
39	0.3021E-02	0.5973E-01	0.1899E+00	0.2899E+01
40	0.3019E-02	0.5974E-01	0.1893E+00	0.2893E+01
41	0.3021E-02	0.5974E-01	0.1898E+00	0.2898E+01
42	0.3021E-02	0.5974E-01	0.1898E+00	0.2898E+01
43	0.3022E-02	0.5975E-01	0.1900E+00	0.2900E+01
44	0.3021E-02	0.5975E-01	0.1897E+00	0.2897E+01
45	0.3024E-02	0.5975E-01	0.1905E+00	0.2905E+01
46	0.3019E-02	0.5975E-01	0.1892E+00	0.2892E+01
47	0.3022E-02	0.5975E-01	0.1899E+00	0.2899E+01
48	0.3021E-02	0.5975E-01	0.1897E+00	0.2897E+01
49	0.3021E-02	0.5975E-01	0.1897E+00	0.2897E+01
50	0.3024E-02	0.5975E-01	0.1904E+00	0.2904E+01
51	0.3021E-02	0.5975E-01	0.1897E+00	0.2897E+01
52	0.3021E-02	0.5975E-01	0.1897E+00	0.2897E+01
53	0.3021E-02	0.5975E-01	0.1897E+00	0.2897E+01
54	0.3021E-02	0.5974E-01	0.1897E+00	0.2897E+01

55	0.3024E-02	0.5974E-01	0.1906E+00	0.2906E+01
56	0.3019E-02	0.5974E-01	0.1893E+00	0.2893E+01
57	0.3023E-02	0.5974E-01	0.1904E+00	0.2904E+01
58	0.3021E-02	0.5973E-01	0.1899E+00	0.2899E+01
59	0.3019E-02	0.5973E-01	0.1895E+00	0.2895E+01
60	0.3021E-02	0.5972E-01	0.1900E+00	0.2900E+01
61	0.3024E-02	0.5971E-01	0.1909E+00	0.2909E+01
62	0.3019E-02	0.5971E-01	0.1895E+00	0.2895E+01
63	0.3022E-02	0.5970E-01	0.1907E+00	0.2907E+01
64	0.3023E-02	0.5968E-01	0.1911E+00	0.2911E+01
65	0.3019E-02	0.5966E-01	0.1903E+00	0.2903E+01
66	0.3023E-02	0.5964E-01	0.1917E+00	0.2917E+01
67	0.3022E-02	0.5961E-01	0.1918E+00	0.2918E+01
68	0.3019E-02	0.5958E-01	0.1915E+00	0.2915E+01
69	0.3021E-02	0.5953E-01	0.1926E+00	0.2926E+01
70	0.3019E-02	0.5948E-01	0.1929E+00	0.2929E+01
71	0.3020E-02	0.5941E-01	0.1941E+00	0.2941E+01
72	0.3011E-02	0.5933E-01	0.1928E+00	0.2928E+01
73	0.3020E-02	0.5923E-01	0.1965E+00	0.2965E+01
74	0.3011E-02	0.5910E-01	0.1958E+00	0.2958E+01
75	0.3012E-02	0.5896E-01	0.1981E+00	0.2981E+01
76	0.3009E-02	0.5878E-01	0.1997E+00	0.2997E+01
77	0.3007E-02	0.5856E-01	0.2022E+00	0.3022E+01
78	0.3006E-02	0.5829E-01	0.2038E+00	0.3038E+01
79	0.2996E-02	0.5797E-01	0.2071E+00	0.3071E+01
80	0.2988E-02	0.5759E-01	0.2104E+00	0.3104E+01
81	0.2977E-02	0.5712E-01	0.2139E+00	0.3139E+01
82	0.2969E-02	0.5656E-01	0.2196E+00	0.3196E+01
83	0.2959E-02	0.5589E-01	0.2260E+00	0.3260E+01
84	0.2931E-02	0.5509E-01	0.2301E+00	0.3301E+01
85	0.2915E-02	0.5413E-01	0.2391E+00	0.3391E+01
86	0.2891E-02	0.5300E-01	0.2491E+00	0.3491E+01
87	0.2855E-02	0.5165E-01	0.2589E+00	0.3589E+01
88	0.2810E-02	0.5005E-01	0.2701E+00	0.3701E+01
89	0.2748E-02	0.4819E-01	0.2816E+00	0.3816E+01
90	0.2679E-02	0.4602E-01	0.2962E+00	0.3962E+01
91	0.2586E-02	0.4352E-01	0.3105E+00	0.4105E+01
92	0.2466E-02	0.4065E-01	0.3246E+00	0.4246E+01
93	0.2321E-02	0.3742E-01	0.3394E+00	0.4394E+01
94	0.2134E-02	0.3381E-01	0.3507E+00	0.4507E+01
95	0.1893E-02	0.2988E-01	0.3534E+00	0.4534E+01
96	0.1560E-02	0.2569E-01	0.3330E+00	0.4336E+01
97	0.1167E-02	0.2143E-01	0.2476E+00	0.3476E+01
98	0.5906E-03	0.1739E-01	-0.2062E+00	-0.1062E+01
99	0.1880E-03	0.1388E-01	-0.2026E+01	-0.1926E+02
100	0.7795E-04	0.1101E-01	-0.4785E+01	-0.4686E+02

APPENDIX B

AN ANALYTICAL EXAMPLE

B.1 Introduction

The optimum enrichment profile (see Figure 2.3) shows that in the central region a uniform enrichment is needed, but in the rest of the assembly, near the periphery, a continuously varying distribution of fissile material is required. Thus an optimum shape can be achieved asymptotically as the number of core regions of different enrichment is increased. But, in fact, from the analytical example discussed here it will become clear that only a few zones of different enrichment can give a solution very close to the optimum solution.

It can be seen from Table 2.1 that the leakage generated by a cosine power shape is almost a factor of ten less than that associated with a uniform power shape. But, since the minimization of leakage, ρ_L , conflicts with the minimization of the axial power profile index, $\int_{-b}^{b} f^2(z)dz$, the pure cosine shape is not optimum with respect to burnup. Since the leakage effect is most prominent in the fuel regions within two or three migration lengths of the periphery, a flat power profile having a cosine shape only near the ends was examined, again using a small computer program. The important features of this example have already been shown in Table 2.2.

B.2 Input/Output

The following values were used as input for the test case examined:

half core axial length, AL + BL = 175.3 cm

AL = length of region with a cosine power shape

BL = length of region with a flat power shape

migration length, XM = 7.5 cm

initial reactivity (ρ_o) = 0.2

slope of reactivity vs. burnup, A = 0.91 E-5

A listing of the Fortran program and a sample output for this example follow in Tables B.1 and B.2. In this program the width of the cosine region is systematically varied from zero through the full core half-height. The last line of output identifies the maximum burnup case, which occurs at cosine width = 23 cm.

Table B.1

Program to Evaluate Flat Plus Cosine Shape Performance

```
C       OPTIMUM POWER PROFILE                                                  OPT00010
        A=.91E-05                                                              OPT00020
        RNOT=0.20                                                              OPT00030
        XM=7.45                                                                OPT00040
        PI=3.141592654                                                         OPT00050
        WRITE(6,110)                                                           OPT00060
        BMAX=0.0                                                               OPT00070
        DO 10 I=1,175                                                          OPT00080
        AL=I                                                                   OPT00090
        BL=175.3 0-AL                                                          OPT00100
        ALFA=0.5/(2.0*AL/PI+BL)                                                OPT00110
        DRL=(1./XM)**2+(PI/(2.0*AL))**2                                        OPT00120
        ERL=EXP(-AL/XM)                                                        OPT00130
        RL=0.5*ALFA/DRL*(PI/AL-2.0/XM*ERL)+XM*ALFA*ERL                         OPT00140
        CSI=ALFA**2*(AL+2.0*BL)                                                OPT00150
        B=(RNOT-RL)/(2.0*(AL+BL)*A*CSI)                                        OPT00160
        WRITE(6,120)AL,BL,RL,CSI,B                                             OPT00170
        IF(BMAX.GT.B)GO TO 10                                                  OPT00180
        BMAX=B                                                                 OPT00190
        AMAX=I                                                                 OPT00200
   10   CONTINUE                                                               OPT00210
        WRITE(6,130)BMAX,AMAX                                                  OPT00220
  110   FORMAT('      A        B          LEAKAGE REACTIVITY  CYCLE SCHEDULE  OPT00230
     1                              BURN UP  ')                               OPT00240
  120   FORMAT(2X,F5.1,5X,F5.1,5X,3(E15.8,5X))                                 OPT00250
  130   FORMAT(' MAXIMUM BURNUP=',E15.8,'   COSINE SHAPE=',F5.1)               OPT00260
        STOP                                                                   OPT00270
        END                                                                    OPT00280
```

Table B.2

Results of Flat Plus Cosine Computations

A	B	LEAKAGE REACTIVITY	CYCLE SCHEDULE	BURNUP
1.0	174.3	0.20294815E-01	0.28565966E-02	0.19722305E+05
2.0	173.3	0.19398648E-01	0.28602970E-02	0.19795016E+05
3.0	172.3	0.18560760E-01	0.28640032E-02	0.19861117E+05
4.0	171.3	0.17776705E-01	0.28677154E-02	0.19921121E+05
5.0	170.3	0.17042395E-01	0.28714342E-02	0.19975500E+05
6.0	169.3	0.16354091E-01	0.28751583E-02	0.20024672E+05
7.0	168.3	0.15708368E-01	0.28788892E-02	0.20069043E+05
8.0	167.3	0.15102081E-01	0.28826252E-02	0.20108973E+05
9.0	166.3	0.14532339E-01	0.28863673E-02	0.20144777E+05
10.0	165.3	0.13996497E-01	0.28901151E-02	0.20176781E+05
11.0	164.3	0.13492111E-01	0.28938693E-02	0.20205250E+05
12.0	163.3	0.13016950E-01	0.28976290E-02	0.20230441E+05
13.0	162.3	0.12568943E-01	0.29013949E-02	0.20252598E+05
14.0	161.3	0.12146190E-01	0.29051660E-02	0.20271922E+05
15.0	160.3	0.11746962E-01	0.29089430E-02	0.20288629E+05
16.0	159.3	0.11369623E-01	0.29127253E-02	0.20302902E+05
17.0	158.3	0.11012696E-01	0.29165144E-02	0.20314891E+05
18.0	157.3	0.10674808E-01	0.29203084E-02	0.20324770E+05
19.0	156.3	0.10354698E-01	0.29241082E-02	0.20332684E+05
20.0	155.3	0.10051195E-01	0.29279133E-02	0.20338750E+05
21.0	154.3	0.97631998E-02	0.29317241E-02	0.20343109E+05
22.0	153.3	0.94897337E-02	0.29355404E-02	0.20345871E+05
23.0	152.3	0.92298612E-02	0.29393623E-02	0.20347133E+05
24.0	151.3	0.89827217E-02	0.29431896E-02	0.20346996E+05
25.0	150.3	0.87475218E-02	0.29470222E-02	0.20345559E+05
26.0	149.3	0.85235164E-02	0.29508604E-02	0.20342895E+05
27.0	148.3	0.83100349E-02	0.29547040E-02	0.20339082E+05
28.0	147.3	0.81064329E-02	0.29585524E-02	0.20334199E+05
29.0	146.3	0.79121143E-02	0.29624065E-02	0.20328309E+05
30.0	145.3	0.77265315E-02	0.29662654E-02	0.20321480E+05
31.0	144.3	0.75491816E-02	0.29701299E-02	0.20313754E+05
32.0	143.3	0.73795803E-02	0.29739991E-02	0.20305211E+05
33.0	142.3	0.72172880E-02	0.29778737E-02	0.20295879E+05
34.0	141.3	0.70618875E-02	0.29817529E-02	0.20285812E+05
35.0	140.3	0.69129981E-02	0.29856374E-02	0.20275055E+05
36.0	139.3	0.67702569E-02	0.29895266E-02	0.20263641E+05
37.0	138.3	0.66333301E-02	0.29934209E-02	0.20251625E+05
38.0	137.3	0.65019019E-02	0.29973197E-02	0.20239027E+05
39.0	136.3	0.63756742E-02	0.30012236E-02	0.20225883E+05
40.0	135.3	0.62543787E-02	0.30051318E-02	0.20212230E+05
41.0	134.3	0.61377548E-02	0.30090453E-02	0.20198098E+05
42.0	133.3	0.60255565E-02	0.30129629E-02	0.20183508E+05
43.0	132.3	0.59175752E-02	0.30168851E-02	0.20168488E+05
44.0	131.3	0.58135800E-02	0.30208116E-02	0.20153070E+05
45.0	130.3	0.57133697E-02	0.30247432E-02	0.20137258E+05
46.0	129.3	0.56167841E-02	0.30286780E-02	0.20121098E+05
47.0	128.3	0.55236183E-02	0.30326182E-02	0.20104586E+05
48.0	127.3	0.54337196E-02	0.30365614E-02	0.20087762E+05
49.0	126.3	0.53469352E-02	0.30405102E-02	0.20070621E+05
50.0	125.3	0.52631125E-02	0.30444618E-02	0.20053199E+05
51.0	124.3	0.51821247E-02	0.30484183E-02	0.20035504E+05
52.0	123.3	0.51038265E-02	0.30523781E-02	0.20017555E+05
53.0	122.3	0.50281063E-02	0.30563427E-02	0.19999352E+05
54.0	121.3	0.49548373E-02	0.30603097E-02	0.19980934E+05

55.0	120.3	0.48839226E-02	0.30642815E-02	0.19962289E+05
56.0	119.3	0.48152506E-02	0.30682560E-02	0.19943449E+05
57.0	118.3	0.47487319E-02	0.30722341E-02	0.19924410E+05
58.0	117.3	0.46842694E-02	0.30762171E-02	0.19905187E+05
59.0	116.3	0.46217740E-02	0.30802020E-02	0.19885793E+05
60.0	115.3	0.45611709E-02	0.30841914E-02	0.19866234E+05
61.0	114.3	0.45023710E-02	0.30881825E-02	0.19846523E+05
62.0	113.3	0.44453107E-02	0.30921784E-02	0.19826668E+05
63.0	112.3	0.43899082E-02	0.30961758E-02	0.19806676E+05
64.0	111.3	0.43361075E-02	0.31001770E-02	0.19786555E+05
65.0	110.3	0.42838380E-02	0.31041808E-02	0.19766316E+05
66.0	109.3	0.42330511E-02	0.31081878E-02	0.19745953E+05
67.0	108.3	0.41836724E-02	0.31121967E-02	0.19725492E+05
68.0	107.3	0.41356571E-02	0.31162088E-02	0.19704926E+05
69.0	106.3	0.40889569E-02	0.31202228E-02	0.19684266E+05
70.0	105.3	0.40435158E-02	0.31242396E-02	0.19663523E+05
71.0	104.3	0.39992891E-02	0.31282580E-02	0.19642695E+05
72.0	103.3	0.39562359E-02	0.31322793E-02	0.19621785E+05
73.0	102.3	0.39143115E-02	0.31363019E-02	0.19600809E+05
74.0	101.3	0.38734772E-02	0.31403271E-02	0.19579758E+05
75.0	100.3	0.38336862E-02	0.31443532E-02	0.19558660E+05
76.0	99.3	0.37949090E-02	0.31483816E-02	0.19537496E+05
77.0	98.3	0.37571096E-02	0.31524110E-02	0.19516281E+05
78.0	97.3	0.37202532E-02	0.31564427E-02	0.19495016E+05
79.0	96.3	0.36843068E-02	0.31604744E-02	0.19473711E+05
80.0	95.3	0.36492406E-02	0.31645081E-02	0.19452359E+05
81.0	94.3	0.36150266E-02	0.31685424E-02	0.19430977E+05
82.0	93.3	0.35816359E-02	0.31725783E-02	0.19409562E+05
83.0	92.3	0.35490389E-02	0.31766139E-02	0.19388121E+05
84.0	91.3	0.35172158E-02	0.31806512E-02	0.19366645E+05
85.0	90.3	0.34861369E-02	0.31846878E-02	0.19345160E+05
86.0	89.3	0.34557811E-02	0.31887258E-02	0.19323645E+05
87.0	88.3	0.34261232E-02	0.31927628E-02	0.19302125E+05
88.0	87.3	0.33971434E-02	0.31968006E-02	0.19280586E+05
89.0	86.3	0.33688215E-02	0.32008379E-02	0.19259039E+05
90.0	85.3	0.33411379E-02	0.32048754E-02	0.19237488E+05
91.0	84.3	0.33140702E-02	0.32089117E-02	0.19215934E+05
92.0	83.3	0.32876011E-02	0.32129476E-02	0.19194379E+05
93.0	82.3	0.32617156E-02	0.32169824E-02	0.19172828E+05
94.0	81.3	0.32363953E-02	0.32210171E-02	0.19151277E+05
95.0	80.3	0.32116217E-02	0.32250525E-02	0.19129719E+05
96.0	79.3	0.31873812E-02	0.32290847E-02	0.19108187E+05
97.0	78.3	0.31636585E-02	0.32331140E-02	0.19086672E+05
98.0	77.3	0.31404404E-02	0.32371427E-02	0.19065168E+05
99.0	76.3	0.31177090E-02	0.32411686E-02	0.19043687E+05
100.0	75.3	0.30954545E-02	0.32451935E-02	0.19022215E+05
101.0	74.3	0.30736625E-02	0.32492147E-02	0.19000777E+05
102.0	73.3	0.30523206E-02	0.32532350E-02	0.18979352E+05
103.0	72.3	0.30314161E-02	0.32572511E-02	0.18957965E+05
104.0	71.3	0.30109391E-02	0.32612653E-02	0.18936594E+05
105.0	70.3	0.29908754E-02	0.32652759E-02	0.18915266E+05
106.0	69.3	0.29712187E-02	0.32692833E-02	0.18893965E+05
107.0	68.3	0.29519538E-02	0.32732869E-02	0.18872699E+05
108.0	67.3	0.29330729E-02	0.32772871E-02	0.18851473E+05
109.0	66.3	0.29145668E-02	0.32812823E-02	0.18830285E+05

110.0	65.3	0.28964253E-02	0.32852741E-02	0.18809137E+05
111.0	64.3	0.28786396E-02	0.32892609E-02	0.18788035E+05
112.0	63.3	0.28611999E-02	0.32932425E-02	0.18766980E+05
113.0	62.3	0.28441008E-02	0.32972200E-02	0.18745961E+05
114.0	61.3	0.28273307E-02	0.33011916E-02	0.18725008E+05
115.0	60.3	0.28108833E-02	0.33051581E-02	0.18704094E+05
116.0	59.3	0.27947503E-02	0.33091183E-02	0.18683234E+05
117.0	58.3	0.27789255E-02	0.33130730E-02	0.18662434E+05
118.0	57.3	0.27633996E-02	0.33170206E-02	0.18641691E+05
119.0	56.3	0.27481702E-02	0.33209620E-02	0.18621004E+05
120.0	55.3	0.27332236E-02	0.33248961E-02	0.18600383E+05
121.0	54.3	0.27185599E-02	0.33288235E-02	0.18579820E+05
122.0	53.3	0.27041691E-02	0.33327425E-02	0.18559324E+05
123.0	52.3	0.26900459E-02	0.33366543E-02	0.18538891E+05
124.0	51.3	0.26761843E-02	0.33405575E-02	0.18518531E+05
125.0	50.3	0.26625800E-02	0.33444527E-02	0.18498238E+05
126.0	49.3	0.26492251E-02	0.33483382E-02	0.18478023E+05
127.0	48.3	0.26361165E-02	0.33522155E-02	0.18457875E+05
128.0	47.3	0.26232474E-02	0.33560826E-02	0.18437809E+05
129.0	46.3	0.26106141E-02	0.33599404E-02	0.18417820E+05
130.0	45.3	0.25982116E-02	0.33637872E-02	0.18397914E+05
131.0	44.3	0.25860320E-02	0.33676226E-02	0.18378090E+05
132.0	43.3	0.25740743E-02	0.33714469E-02	0.18358359E+05
133.0	42.3	0.25623315E-02	0.33752571E-02	0.18338727E+05
134.0	41.3	0.25508031E-02	0.33790607E-02	0.18319148E+05
135.0	40.3	0.25394848E-02	0.33828553E-02	0.18299652E+05
136.0	39.3	0.25283671E-02	0.33866321E-02	0.18280273E+05
137.0	38.3	0.25174483E-02	0.33903918E-02	0.18261012E+05
138.0	37.3	0.25067271E-02	0.33941481E-02	0.18241793E+05
139.0	36.3	0.24961981E-02	0.33978857E-02	0.18222695E+05
140.0	35.3	0.24858569E-02	0.34016084E-02	0.18203707E+05
141.0	34.3	0.24757024E-02	0.34053233E-02	0.18184781E+05
142.0	33.3	0.24657287E-02	0.34090150E-02	0.18166004E+05
143.0	32.3	0.24559328E-02	0.34126940E-02	0.18147324E+05
144.0	31.3	0.24463106E-02	0.34163541E-02	0.18128766E+05
145.0	30.3	0.24368626E-02	0.34200018E-02	0.18110297E+05
146.0	29.3	0.24275822E-02	0.34236286E-02	0.18091957E+05
147.0	28.3	0.24184692E-02	0.34272440E-02	0.18073707E+05
148.0	27.3	0.24095168E-02	0.34308361E-02	0.18055605E+05
149.0	26.3	0.24007263E-02	0.34344140E-02	0.18037598E+05
150.0	25.3	0.23920906E-02	0.34379635E-02	0.18019762E+05
151.0	24.3	0.23836128E-02	0.34415021E-02	0.18002004E+05
152.0	23.3	0.23752882E-02	0.34450211E-02	0.17984375E+05
153.0	22.3	0.23671091E-02	0.34485119E-02	0.17966910E+05
154.0	21.3	0.23590801E-02	0.34519918E-02	0.17949531E+05
155.0	20.3	0.23511944E-02	0.34554407E-02	0.17932328E+05
156.0	19.3	0.23434514E-02	0.34588701E-02	0.17915254E+05
157.0	18.3	0.23358490E-02	0.34622797E-02	0.17898301E+05
158.0	17.3	0.23283849E-02	0.34656606E-02	0.17881512E+05
159.0	16.3	0.23210566E-02	0.34690213E-02	0.17864852E+05
160.0	15.3	0.23138623E-02	0.34723585E-02	0.17848328E+05
161.0	14.3	0.23067982E-02	0.34756635E-02	0.17831996E+05
162.0	13.3	0.22998648E-02	0.34789443E-02	0.17815805E+05
163.0	12.3	0.22930605E-02	0.34822032E-02	0.17799742E+05
164.0	11.3	0.22863813E-02	0.34854314E-02	0.17783855E+05
165.0	10.3	0.22798250E-02	0.34886284E-02	0.17768148E+05
166.0	9.3	0.22733917E-02	0.34917986E-02	0.17752594E+05
167.0	8.3	0.22670783E-02	0.34949339E-02	0.17737234E+05
168.0	7.3	0.22608875E-02	0.34980492E-02	0.17721996E+05
169.0	6.3	0.22548093E-02	0.35011224E-02	0.17706984E+05
170.0	5.3	0.22488497E-02	0.35041685E-02	0.17692125E+05
171.0	4.3	0.22430036E-02	0.35071815E-02	0.17677449E+05
172.0	3.3	0.22372711E-02	0.35101604E-02	0.17662957E+05
173.0	2.3	0.22316470E-02	0.35131038E-02	0.17648664E+05
174.0	1.3	0.22261364E-02	0.35160161E-02	0.17634535E+05
175.0	0.3	0.22207312E-02	0.35188831E-02	0.17620648E+05

MAXIMUM BURNUP= 0.20347133E+05 COSINE SHAPE= 23.0

APPENDIX C

OPTIMUM POWER PROFILES

C.1 Introduction

It was found that the optimum axial power shape with respect to uranium utilization has a large central region of uniform power density, with a roughly cosinusoidal shape near the ends of the assembly. In fact, this is also a favorable profile with respect to two key thermal-hydraulic criteria: fuel centerline temperature and departure from nucleate boiling ratio (DNBR). In the sections which follow it will be shown that optimum power profiles with respect to these parameters are closely approximated by a uniform axial power shape.

C.2 Optimum Power Profile with Respect to Fuel Centerline Temperature

The local fuel centerline temperature in a unit cell as a function of distance from the assembly inlet can be calculated using the following relation:

$$T(z) = T_o + \frac{1}{WC_p}\int_o^z q'(z)dz + Rq'(z) \qquad (C.1)$$

coolant temperature at z=0	ΔT of coolant up to z	ΔT between coolant and centerline

where

W = coolant flow rate

C_p = coolant heat capacity

R = thermal resistance, given by

$$R = \left[\frac{1}{2\pi hb} + \frac{1}{2\pi k_c} + \frac{\delta}{a+\varepsilon} + \frac{1}{2\pi h_g a} + \frac{1}{4\pi k_f} \right] \qquad (C.2)$$

in which

- h = heat transfer coefficient for coolant (c) or gap (g)
- b = outer fuel pin radius
- δ, ε = clad and gap thicknesses, respectively
- a = radius of fuel pellet
- k = thermal conductivity of clad (c) or fuel (f)

Differentiating Eq.(C.1) with respect to z, and applying Leibnitz's rule,

$$\frac{dT(z)}{dz} = \frac{1}{WC_p} q'(z) + R \frac{dq'(z)}{dz} \qquad (C.3)$$

For a uniform centerline temperature (i.e., for $\frac{dT(z)}{dz} = 0$), Eq.(C.3) reduces to

$$\frac{dq}{dz} = \frac{-q}{RWC_p} \qquad (C.4)$$

which has the solution

$$q = q_o e^{-z/RWC_p} \qquad (C.5)$$

For representative values (i.e., $WC_p \simeq \frac{2kw}{°F}$ and $R \simeq 7000\ °F\ \frac{cm}{kw}$), Eq.(C.5) gives

$$\frac{q}{q_o} = e^{-z/14000} \simeq 1 - \frac{z}{14000} \qquad (C.6)$$

Since the maximum value of z is roughly 400 cm, the optimum profile is nearly constant.

C.3 Optimum Power Profile with Respect to DNBR

The power profile will be optimum with respect to DNB if the ratio of heat flux to DNB heat flux is constant, i.e.,

$$\frac{q'(z)}{q'_{DNB}(z)} = A \qquad (C.7)$$

Consider a PWR core for which the axial DNB dependence can be roughly approximated by the relation:

$$q'_{DNB}(z) = 1.0 - \left[\frac{T(z)-T_o}{175}\right] \frac{kw}{cm} \qquad (C.8)$$

where T_o is the coolant inlet temperature and T(z) is the local coolant temperature, both in °F. These temperatures are related by:

$$\left[T(z)-T_o\right] = \frac{1}{WC_p} \int_o^z q'(\ell)d\ell \qquad (C.9)$$

Using Eqs. (C.7), (C.8) and (C.9),

$$q'(z) = A - \frac{A}{175\ WC_p} \int_o^z q'(\ell)d\ell \qquad (C.10)$$

Differentiating with respect to z, and applying Leibnitz's rule,

$$\frac{dq'(z)}{dz} = \frac{-A}{175\ WC_p}\ q'(z) \qquad (C.11)$$

and so

$$q'(z) = q'_o\ e^{-Az/175\ WC_p} \qquad (C.12)$$

From Eq.(C.10),

$$A = q'_o \qquad (C.13)$$

For representative values ($WC_p = \frac{2kw}{°F}$, $\int_o^L q'(z)dz = 100$ kw), integration of Eq.(C.12) gives $q_o = 0.31\ \frac{kw}{cm}$. Thus, Eq.(C.12) becomes

$$\frac{q'(z)}{q'_o} = e^{-7/1100} \qquad (C.14)$$

Eq.(C.14), while more inlet-peaked than Eq.(C.6), is again rather compatible with a uniform power profile. The power decrease near the core periphery in the optimum profile with respect to uranium utilization is also favorable with respect to the optimum DNBR profile — at least as regards the outlet end of the assembly. When additional

realism is introduced in terms of axially varying coolant density and with control rods banked at the exit of the core, an inlet-peaked shape even more favorable to DNBR would be anticipated in a uniformly zoned core of the type examined in Chapters 3 and 4.

C.4 Discussion and Conclusions

The optimum power profile with respect to fuel centerline temperature is quite compatible with that for maximum uranium utilization -- they are in fact identical (uniform) except for the latter's roughly cosinusoidal decrease in the last few migration lengths near the core periphery. It should also be noted that Eq.(C.1) also applies to other temperatures (average fuel temperature, cladding temperature) if appropriate values of the thermal resistance, R, are employed (merely retain only the series resistances which intervene in Eq.(C.2)). Hence, a nearly uniform profile is best under many constraints: stored energy, adiabatic post-LOCA clad temperature, etc. As one moves toward lower resistance, the optimum profile becomes more inlet-peaked, as is evident from Eq.(C.5). Thus, it may be of some interest to investigate asymmetric zoning, in which the higher-enrichment zone at the bottom of the core is not identical in length or enrichment to its counterpart at the top of the core.

Finally, it should be recognized that other criteria must be addressed in the search for an optimum axial

power profile: two which come to mind are stability against xenon oscillations (a category in which uniform profiles are inferior to buckled profiles) and amenability to post-LOCA reflood cooling, for which no simple objective function is evident. Hence, a complete licensing assessment on the order of that in Reference (M-1) should eventually be carried out on the axially-zoned-enrichment, partially-annular core concept.

REFERENCES

A-1 A.I.F., "Reprocessing-Recycle Economics," Atomic Industrial Forum, Washington, D.C., 1977.

A-2 Adamsam, E.G., et al., "Computer Methods for Utility Reactor Physics Analysis," Reactor and Fuel Processing Technology, 12(2):225-241, Spring 1969.

A-3 Amster, H. and Suarez, R., "The Calculation of Thermal Constants Averaged Over A Wigner-Wilkins Flux Spectrum: Description of the SOFOCATE Code," WAPD-TM-39, January, 1957.

A-4 Adams, C.H., "Current Trends in Methods for Neutron Diffusion Calculations," Nucl. Sci. Eng., 64:552, 1977.

B-1 Barry, R.F., "LEOPARD - A Spectrum Dependent Non-Spatial Depletion Code," WCAP-3269-26, September 1973.

B-2 Bohl, H., Gelbard, E., and Ryan, G., "MUFT-4-Fast Neutron Spectrum Code for the IBM-704," WAPD-TM-72, July 1957.

B-3 Breen, R.J., et al., "HARMONY: System for Nuclear Reactor Depletion Computation," WAPD-TM-478, January 1965.

B-4 Breen, R.J., et al., "A One-Group Model for Thermal Activation Calculations," Nucl. Sci. Eng., 9:91, 1961.

B-5 Badruzzaman, A., "Economic Implications of Annular Fuel in PWRs," Trans. Am. Nucl. Soc., 34:384, June 1980.

C-1 Clark, M., and Hansen, K.F., "Numerical Methods of Reactor Analysis," Academic Press, 1964.

C-2 Combustion Engineering Inc., "Improvements in Once Through Fuel Cycles: Progress Report for the Period April 1 - June 30, 1978," SPE-Th-37, 1978.

C-3 Cacciapouti, R.J., and Sarja, A.C., "CHIMP-II, A Computer Program for Handling Input Manipulation and Preparation for PWR Reload Core Analysis, YAEC-1107," May 1976.

C-4 Cadwell, W.R., "PDQ-7 Reference Manual," Bettis Atomic Power Laboratory, WAPD-TM-678, 1967.

C-5 Crowther, R.L., et al., "BWR Fuel Management Improvements for Once Through Fuel Cycles," Trans. Am. Nucl. Soc., 33:369, 1979.

C-6 Correa, F., Driscoll, M.J., and Lanning, D.D., "An Evaluation of Tight-Pitch PWR Cores," MIT-EL 79-022, August 1979.

D-1 Driscoll, M.J., Fujita, E.K., and Lanning, D.D., "Improvements of PWRs on the Once-Through Fuel Cycle," Trans. Am. Nucl. Soc., 30, 280, 1978.

D-2 Driscoll, M.J., "Nuclear Fuel Management (22.35) - Class Notes," M.I.T., Spring 1980.

F-1 Fujita, E.K., Driscoll, M.J. and Lanning, D.D., "Design and Fuel Management of PWR Cores to Optimize the Once-Through Fuel Cycle," MITNE-215, August 1978.

G-1 Graves, H.W., "Nuclear Fuel Management," John Wiley and Sons, New York, 1979.

G-2 Garel, K.C. and Driscoll, M.J., "Fuel Cycle Optimization of Thorium and Uranium Fueled PWR Systems," MITNE-204, October 1977.

H-1 Honeck, H.C., "THERMOS - A Thermalization Transport Theory Code for Reactor Lattice Calculations," BNL-5826, 1961.

H-2 Hageman, L.A. and Pfeifer, C.J., "The Utilization of the Neutron Diffusion Program PDQ-5," WAPD-TM-395, January 1965.

H-3 Haling, R.K., "Operating Strategy for Maintaining an Optimum Power Distribution Throughout Life," Nucleonics, 23, No. 5, 1965.

H-4 Hannah, M.A., "Axial Blanket Fuel Design and Demonstration," DOE/ET/34020-1 BAW-1643-1, November 1980.

I-1 INFCE, Report of the International Nuclear Fuel Cycle Evaluation, IAEA, Vienna, 1980.

K-1 Kamal, A., "The Effects of Axial Power Shaping on Ore Utilization in Pressurized Water Reactors," S.M. Thesis, M.I.T. Department of Nuclear Engineering, January 1980.

K-2 Khabaza, I.M., "Numerical Analysis," Pergamon Press, Oxford, England, 1966.

K-3 Kamal, A., Private Communication, M.I.T. Department of Nuclear Engineering, Cambridge, Mass.

M-1 Matzie, R.A., "Licensing Assessment of PWR Extended Burnup Fuel Cycles," Final Report, CEND-381, March 1981.

M-2 Macnabb, W.V., "Two Near-Term Alternatives for Improved Nuclear Fuel Utilization," Trans. Am. Nucl. Soc., 33: 398, November 1979.

M-3 Matzie, R.A., et al., "Uranium Resource Utilization Improvements in the Once-Through PWR Fuel Cycle," CEND-380, April 1980.

M-4 Mildrum, C.M. and Henderson, W.B., "Evaluation of Annular Fuel Economic Benefits for PWRs," Trans. Am. Nucl. Soc., 33:806, November 1979.

M-5 Mildrum, C.M., "Economic Evaluation of Annular Fuel for PWRs," Trans. Am. Nucl. Soc., 35:78, November 1980.

N-1 "Nuclear Proliferation and Civilian Nuclear Power," Report of the Nonproliferation Alternative System Assessment Program (NASAP), DOE/NE-0001, June 1980.

R-1 Robbins, T., "Preliminary Evaluation of a Variable Lattice Fuel Assembly and Reactor Design Concept," ORNL/Sub-79/13576/1, February 1979.

R-2 Rampolla, D.S., et al., "Fuel Utilization Potential in Light Water Reactors with Once-Through Fuel Irradiation," WAPD-TM-1371, 1978.

S-1 Sefcik, J.A., Driscoll, M.J. and Lanning, D.D., "Analysis of Strategies for Improving Uranium Utilization in PWRs," MITNE-234, January 1981.

S-2 Sider, F.M., "An Improved Once-Through Fuel Cycle for Pressurized Water Reactors," TIS-6529, Combustion Engineering Power Systems, Windsor, Conn., June 1980.

S-3 Strawbridge, L.E., and Barry, R.F., "Criticality Calculations for Uniform Water-Moderated Lattices," Nuc. Sci. Eng., 23:58, 1965.

T-1 Till, C.E., and Chang, Y.I., "Once-Through Fuel Cycles," 18th Annual ASME Symposium, Nonproliferation: "Reality and Illusion of a Plutonium Free Economy", Albuquerque, New Mexico (March 1978)

U-1. Umegaki, K., et al., "Application of Improved Core Designs to Conventional BWR", Trans. Am. Nuc-. Soc., 33 (1979).